LAPPEENRANTA UNIVERSITY OF TECHNOLOGY
LUT School of Engineering Science
Degree program in Chemical Engineering
Master's Thesis

Tuomas Suikkanen

ANALYTICS FOR THE MODIFIED KRAFT PULPS

Examiners: Associate Professor Satu-Pia Reinikainen, LUT
Senior Technologist, Ph.D., Matti Ristolainen, UPM

ABSTRACT

Lappeenranta University of technology
LUT School of Engineering Science
Degree Program in Chemical Engineering

Tuomas Suikkanen

Analytics for the modified kraft pulps
2015

Master's Thesis
Pages 85, figures 64, tables 11, appendices 6

Examiners: Associate Professor Satu-Pia Reinikainen

Ph.D. Matti Ristolainen

Keywords: Modified cellulose, pulp modification, fiber analysis, FTIR-ATR

The aim of this thesis is to develop a suitable quantitative analytical method for the degree of substitution (DS) determination for modified kraft pulp fibers. Modification in this context refers to attachment of molecules into pulp fiber surface by covalent bonding or adsorption. The literature part consists of a short review of the modification routes and compounds that can be used for the fiber modification to achieve certain properties for the end product. In addition, the most suitable direct and indirect analytical methods were reviewed. From these methods the most promising ones were selected for the experimental part.

The experimental part focuses mainly on developing quantitative method for the modified pulp fiber DS determination with Fourier transform infrared-Attenuated total reflectance (FTIR-ATR) device. Any documented quantitative method for the pulp fiber surface analysis with FTIR-ATR could not be found from the literature. Other methods like the elemental analysis, thermogravimetric analysis (TGA) and light microscope were used to produce supporting information about the modification. The cellulose acetate and cellulose betainate were used as modified fibers in the FTIR-ATR method development.

The results showed that with FTIR-ATR it is possible to achieve quantitative information about the DS of the modified kraft and sulfite fibers. Due to lack of suitable samples the complete calibration could not be performed with that method. The heterogeneity of the solid samples and the poor sensitivity against impurities was found out to be the major drawbacks of the developed method. However, with a further testing the developed method could be possibly used for repetitive analysis of the modified pulp fibers in the pulp industry.

TIIVISTELMÄ

Lappeenrannan teknillinen yliopisto
LUT School of Engineering Science
Kemiantekniikan koulutusohjelma

Tuomas Suikkanen

Muokatun kraft-sellun analytiikka
2015

Diplomityö
Sivuja 85, kuvia 64, taulukoita 11, liitteitä 6

Tarkastajat: Dosentti Satu-Pia Reinikainen

FT Matti Ristolainen

Hakusanat: Muokattu selluloosa, sellun muokkaus, kuitujen analysointi, FTIR-ATR

Tämän diplomityön tavoitteena on kehittää sopiva analyyttinen menetelmä muokatun kraft-sellukuidun substituutioasteen (DS) kvantitatiivista määrittämistä varten. Muokkauksella tarkoitetaan tässä yhteydessä joko kovalenttisesti tai adsorption avulla tapahtuvaa molekyylin kiinnittymistä sellukuidun pinnalle. Työn kirjallisuusosuudessa käsitellään lyhyesti eri muokkaustapoja ja yhdisteitä joiden avulla voidaan saavuttaa haluttuja ominaisuuksia sellusta valmistetuille lopputuotteille. Lisäksi kirjallisuusosuudessa käydään läpi käyttötarkoitukseen soveltuvimpia suoria ja epäsuoria analyysimenetelmiä. Analyysimenetelmistä kaikkein lupaavimpia testattiin työn kokeellisessa osassa.

Diplomityön kokeellisessa osassa keskityttiin kehittämään muokatulle sellulle kvantitatiivista menetelmää DS:n määrittämiseksi Fourier-muunnos infrapuna-vaimennettu kokonaisheijastus (FTIR-ATR) spektrometrillä. Kirjallisuuskatsauksessa ei löytynyt yhtään dokumentoitua tutkimusta, jossa FTIR-ATR menetelmää olisi käytetty muokatun sellukuidun kvantitatiiviseen tutkimukseen. Muiden analyysimenetelmien, kuten alkuaineanalyysin, termogravimetrisen analyysin (TGA) ja valomikroskopian avulla pyrittiin tuottamaan lisätietoa muokkauksesta. Kvantitatiivisen FTIR-ATR menetelmän kehitykseen käytetyt muokatut sellukuidut olivat selluloosa-asetaattia ja selluloosa betainaattia.

Saatujen tulosten perusteella muokattujen sulfiitti- ja kraft sellukuitujen DS:n kvantitatiivinen määrittäminen on mahdollista FTIR-ATR menetelmällä. Vähäinen kalibrointipisteiden määrä vaikeutti tarkan analyysimenetelmän tekemistä. Kehitetyn menetelmän suurimpina ongelmina olivat kiinteiden näytteiden heterogeenisyys sekä mahdollisten epäpuhtauksien tunnistaminen. Jatkotutkimusten avulla kehitettyä menetelmää on kuitenkin mahdollista käyttää muokattujen sellukuitujen jatkuvaan analysointiin selluteollisuudessa.

FOREWORDS

This thesis was made in the UPM Northern European Research Center (NERC) during the summer and fall in 2015. For starters I'd like to thank my supervisors, Satu-Pia and Matti, for the great support and some extraordinary ideas. Those ideas allowed me to look for the answers where I otherwise would have not searched.

A great thanks goes also for Ilkka Kilpeläinen and Tia Kakko from the University of Helsinki and Pia Willberg-Keyriläinen from VTT for providing the samples for my thesis. I also want to express my gratitude for all the UPM personnel who helped me during my work.

Last but not the least, I'd like to thank my beloved girlfriend Eliisa Soljasalo for supporting me during the writing process and providing me something else to think about.

Tuomas Suikkanen

Lappeenranta 20.11.2015

TABLE OF CONTENTS

APPENDICES

SYMBOLS

A	Absorbance
a	Absorption coefficient
b	Slope of the linear regression (sensitivity)
c	Concentration
σ	Standard deviation of reference samples
H	Signal height of the analyte
h	Peak to peak value of the noise
I	Intensity of the transmitted radiation
I_0	Intensity of the source
I_d	Reflectance from the sample
I_s	Reflectance from the sample surface
l	Optical path length
n	Number of reference samples
$\bar{n}$	Average of reference samples
S_e	Absorption capacity
S/N	Signal to noise ratio
T	Transmittance
U	Expanded uncertainty
U_r	Relative expanded uncertainty
W_1	Weight of cellulose graft copolymer
w_1	Wet sample weight
W_0	Initial weight of cellulose
w_0	Sample initial weight

ABBREVIATION

AAH	Acetic anhydride
AAS	Atomic absorption spectrometer
AFM	Atomic force microscopy
Ag NPs	Silver nanoparticles
AH	5-methyl-5-aminomethylhydantoin
AIBN	Azobisisobutylonitrile
BDDE	1,4-butanediol diglycidyl ether
BTCA	1,2,3,4-butanetetracarboxylic acid
CA	Cellulose acetate
CLS	Classical least squares
CMC	Carboxymethylcellulose
DMAEMA	2-(dimethylamino) ethyl methacrylate
DMDHEU	1, 3-dimethyol-4, 5-dihydroxyethylurea
DMeDHEU	1,3-dimethy-4, 5-dihydroxyimidazolidinone-2
DS	Degree of substitution
DVS	Divinylsulfone
EC	Ethylcellulose
EDANA	European disposables and nonwovens association
FTIR	Fourier transform infrared
GMA	Glycidyl methacrylate
GP	Guanidine polymer
HA	Hyaluronic acid
HEC	Hydroxyethylcellulose
HPMC	Hydroxypropyl methylcellulose
HPPA	3-(hydroxyphenylphosphinyl)-propanoic acid
ICP	Ion Coupled Plasma spectrometer
LOD	Limit of detection
LOQ	Limit of quantitation
MC	Methylcellulose

MFC	Microfibrillated cellulose
MMT	4-monomethoxytrityl
MPP	Methylphosphonatephosphate
MTMIO	3-methylol-2,2,5,5-tetramethylimidazolidin-4-one
NFC	Nanofibrillated cellulose
MDPA	N-methylol dimethyl phosphonopropionamide
ODPA	Octadecylphosphonic acid
PCA	Principal component analysis
PCR	Principal component regression
PEG	Polyethylene glycol
PLS	Partial least squares
PHGH	Polyhexamethylene guanidine hydrochloride
PHMB	Polyhexamethylen biguanide
Py-GC	Pyrolysis gas chromatography
RMSEC	Root mean squared error of calibration
SA	Succinic anhydride
SAF	Superabsorbent fiber
SAP	Superabsorbent polymer
SiF	1,1,2,2,-perfluorooctyltriethoxysilane
SiP	P,P-diphenyl-N-(3-(trimethoxysilyl)propyl) phosphinic amide
SiQ	3-(trimethoxysilyl)-propyldimethyloctadecyl ammonium chloride
SPH	3-trihydroxysilylpropyl-5,5-dimethylhydantoin
TGA	Thermogravimetric analysis
THPX	Tetrakis(hydroxymethyl)phosphonium salts
UH	University of Helsinki
WSC	Water soluble carbodiimide
β-CD	β-cyclodextrin

INTRODUCTION

The demand for renewable materials is growing globally due to negative environmental impact of the fossil based ones. Applications for renewable materials such as packaging materials, hygienic products, non-woven fabrics and tissue papers have rapidly increased their interest among consumers. The raw material in most of these applications is either bleached or unbleached wood based pulp, synthetic polymers or cotton. This thesis is focused on materials derived from bleached eucalyptus, birch, pine and spruce kraft pulps. The fibers from these pulps can be further modified to achieve new properties to the end product. The new properties for the end products can be for example a better water absorption, enhanced barrier properties, fire or antimicrobial resistance, or improved wet strength.

The aim of this master's thesis was to develop a suitable analytical methods for fiber modification in UPM. In the literature part the most promising pulp modifications for described properties are briefly summarized. The suitable direct and indirect analytical methods for pulp modification are also reviewed.

The experimental part is focused mainly on developing quantitative analysis procedure to determine DS of the modified pulp samples with FTIR-ATR spectroscopy. The literature review showed that some quantitative method have been used to determine degree of modification on modified pulp with KBr tablet method, but any documented quantitative analysis of modified pulp with FTIR-ATR could not be found. In addition, elemental analysis was demonstrated for the degree of substitution (DS) determination. Other indirect methods like thermogravimetric analysis (TGA) and light microscope were used to characterize modified pulp samples. TGA gave very variable results that were relatively hard to analyze. Nonetheless, a valuable observation was that even small change in DS can be detected with TGA. It was also find out that with light microscope it is possible to examine the distribution of attached compound on the fiber surface and degradation of fiber structure even with small DS.

The developed FTIR-ATR method showed promising results for quantitative DS determination. The method needs calibration samples which DS needs to be ensured with some other analytical technique such as NMR. In addition, the developed FTIR-ATR method needs further testing and validation which could not be conducted due to lack of suitable samples.

I THEORETICAL PART

1 MODIFICATION OF BLEACHED KRAFT PULPS

Bleached kraft pulp consist on two main component: cellulose and hemicellulose. Depending on cooking process and raw material that is used in the process the content of these two components may vary. Typical cellulose and hemicellulose composition in kraft pulps derived from different raw materials are shown in **Table 1**.

Table 1. Typical cellulose and hemicellulose composition of different wood species and pulps ([1]Sjöström & Westermark, 1999; [2]Sjöström, 1993; [3]Evtuguin & Pascoal Neto, 2007)

	Original amount (% of wood)	**Pine kraft**	**Birch kraft** (% of wood)	**Euca kraft**
Hemicellulose[1]				
Galactoglucomannan	5–8	-	-	-
(Galacto)glucomannan	10–15	4	-	-
Arabinoglucuronoxylan	7–10	5	-	-
Glucuronoxylan	15–30	-	16	10.6[3]
Glucomannan	2–5	-	1	0.4[3]
Cellulose[2]				
Hardwood	39–45	-	34	40[3]
Softwood	37–43	35	-	-

The chemical components enables certain chemical reactions and, therefore, pulp modification is possible to obtain. The possible reactions with cellulose and hemicelluloses are only examined in this thesis due to low lignin content of bleached pulps. Possible adsorption on the fibers is also taken into account.

1.1 Composition of bleached kraft pulp

The main component in bleached kraft pulp is cellulose and due to that the cellulose is also responsible for main reactions in pulp modifications. Cellulose is a natural polysaccharide which structure is based on *β*-(1, 4)-glycosidic bonded D–glucose monosaccharide units. As shown in **Figure 1** the main functional groups in D–glucose are two secondary hydroxyl groups in the positions of C–2, C–3 and one primary in position C–6 (Torres, *et al*. 2013). The hydroxyl groups forms intermolecular hydrogen bonds within cellulose backbone and intramolecular hydrogen bonds with other cellulose molecules. Intermolecular hydrogen bonds are formed between C–6 and C–2 OH groups and C–5 oxygen and C–3 hydroxyl group. Intramolecular hydrogen bond forms between C–3 and C–6 hydrogen bonds. Cellulose chains forms planar structure with the hydrogen bonds. These planar cellulose structures are bond together with weaker van der Waals interactions. (Ek, *et al*. 2009)

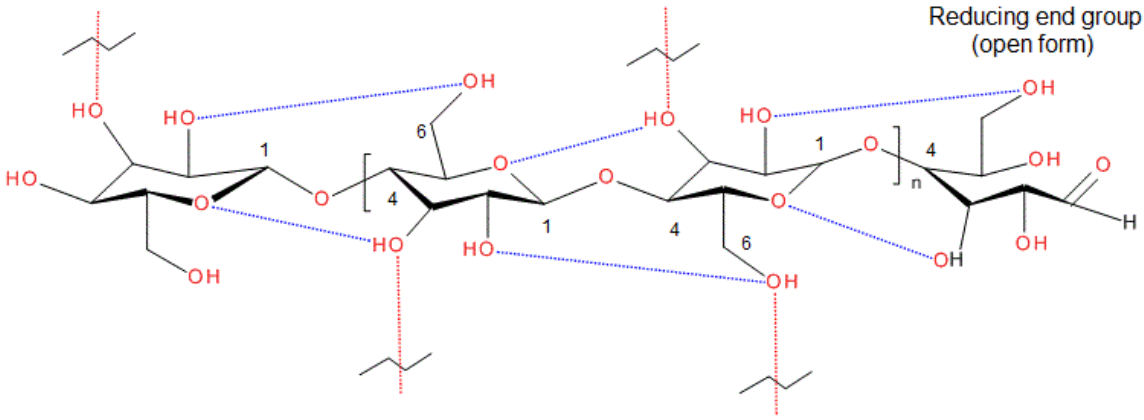

Figure 1. Chemical structure of cellulose. Intermolecular hydrogen bonds are shown in blue and intramolecular in red line.

Because of the specific web structure of hydrogen bonds and van der Waals interactions the cellulose fiber has both amorphous and crystalline regions. The cellulose has a four different crystalline structures and the native form described above is called cellulose I. Cellulose present in kraft pulp is mainly in form II and it is called regenerated cellulose because of the changes in intra- and intermolecular interactions due to alkaline pulping. The web of hydrogen bonds formed between cellulose fibers are responsible for many of the mechanical properties of kraft pulp such as viscosity, strength *et cetera*. In figure 1 is show also the open form of the reducing end of cellulose backbone. (Ek, *et al*. 2009; Sjöström, 1993)

During kraft process approximately 10 % of original cellulose content and major part of the hemicelluloses (30–70 %) is degraded (Sjöström & Westermark, 1999). During alkaline pulping so called peeling reaction causes the degradation of polysaccharides in lower temperatures (<130 °C) and in higher temperatures (160–180 °C) alkaline hydrolysis breaks down glycosidic bonds in polysaccharides (Casey, 1979). The bleaching of kraft pulp causes various hydroxyl groups to oxidise into carbonyl or carboxyl groups. The peeling reactions may also occur during oxygen–alkaline bleaching causing the formation of the acidic end products. The lignin content in bleached kraft pulp is usually reduced under level < 0.1 % of pulp dry mass. (Sjöström, 1993; Sjöström & Westermark, 1999)

According to Sjöström and Westermark (1999) the hemicellulose content in bleached softwood kraft pulp is usually around 18-19 % and hardwood around 30-32% of pulp dry mass (Sjöström & Westermark, 1999). The different amount of hemicellulose in softwood and hardwood kraft pulps can be explained with the raw material composition. Hemicelluloses that occur in softwood are more easily degraded during kraft process than

ones occurs in hardwood. This phenomenon can be explained with the closer examination of different hemicellulose structures in hardwood and softwood pulps. (Sjöström, 1993)

1.1.1 Hardwood kraft pulp

The most abundantly occurring hemicellulose in hardwoods such as birch or eucalyptus is glucuronoxylan. In **Figure 2** is shown how glucuronoxylan builds up from *β*-D-xylopyranose with linked acetyl groups and 4-*O*-methyl-α-D-glucopyranosyluronic acid groups. In the literature the xylose based hemicelluloses are usually referred as xylans. Xylan is relatively resistant against degradation in alkaline conditions during kraft cook. Most significant change in the xylan structure during alkaline cooking is the loss of glucuronic acid side groups. The main structure remains relatively stable during digestion. (Sjöström, 1993; Casey, 1979)

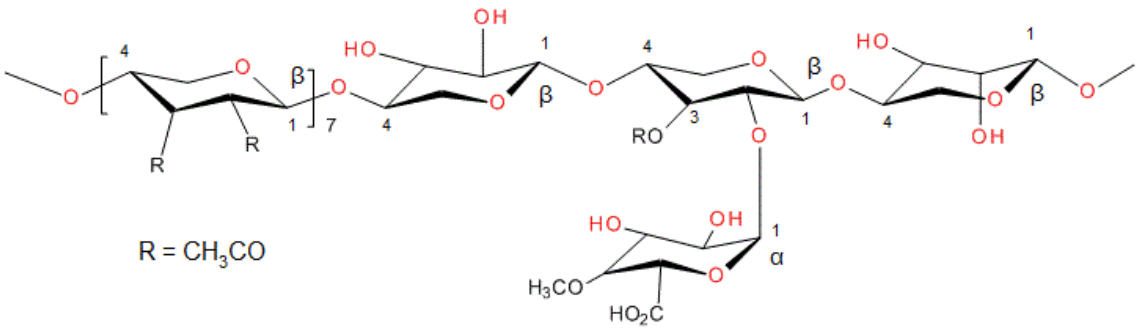

Figure 2. Chemical structure of glucuronoxylan (Sjöström, 1993).

In hardwood pulp the second most common hemicellulose is glucomannan. The main building blocks in glucomannan is *β*-D-glucopyranose and *β*-D-mannopyranose as shown in **Figure 3**. These two units are linked together by *β*-(1→4)-bonds. Glucomannan is effectively degraded between temperature region 100-130 °C during kraft cook (Kringstad & Lindström, 1984). Glucomannan starts to depolymerize during peeling reaction that attacks its reducing end. The peeling reaction cleaves monosaccharide units off the chain and these monosaccharides degrades further to different acidic compounds such as formic and acetic acid. In later stages of the cook peeling reaction ends when more stable carboxylic acid groups forms at the end of the polymer chain. (Sjöström, 1993)

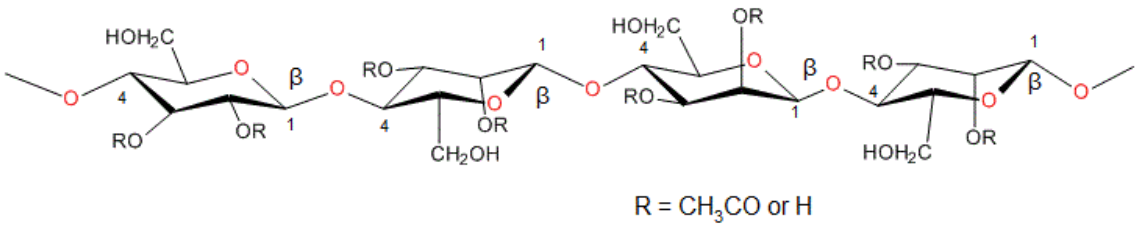

Figure 3. Chemical structure of glucomannan (Sjöström & Westermark, 1999).

1.1.2 Softwood kraft pulp

While hemicellulose occurring in hardwood kraft pulp consist mainly of xylan, galactoglucomannan (**Figure 4**) is the most commonly occurring hemicellulose in softwood such as pine or spruce based kraft pulp. Compared to glucomannan the main difference is (1→6)-bonded α-D-galactopyranose unit. Both galactoglucomannan and glucomannan have in C-2 and C-3 hydroxyl groups that are partially substituted with acetyl groups. During alkaline pulping these acetyl groups as well as the α-D-galactopyranose unit are very easily separated from the main polymer chain. (Sjöström, 1993; Sjöström & Westermark,1999)

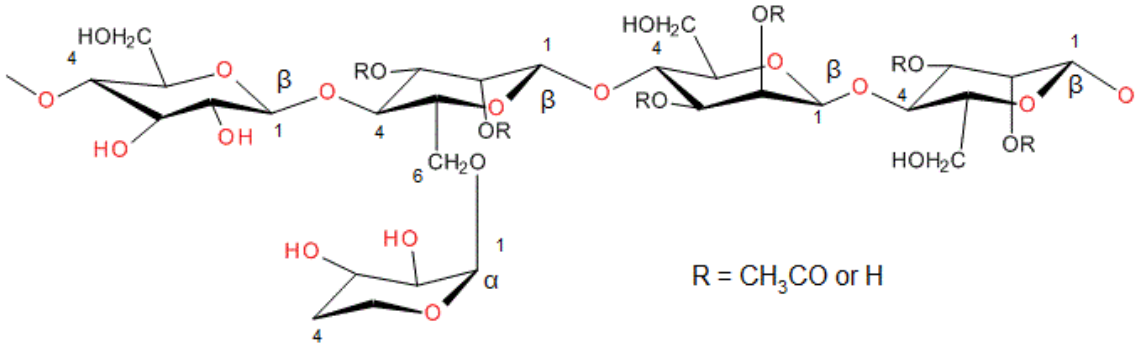

Figure 4. Chemical structure of galactoglucomannan (Sjöström, 1993)

The major xylan compound in softwoods is arabinoglucuronoxylan. As shown in the **Figure 5** the difference between arabinoglucuronoxylan and hardwood glucuronoxylan is the (1→3) linked α-L-arabinofuranose unit. This particular substituent is easily degraded during kraft cook and it only exists in very small quantities in bleached kraft pulp. Unlike in hardwood glucuronoxylan, acetyl groups are not present in softwood arabinoglucuronoxylan.

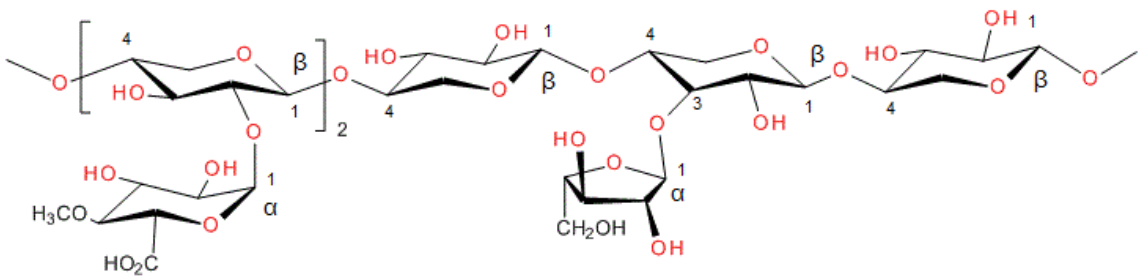

Figure 5. Chemical structure of arabinoglucuronoxylan (Sjöström, 1993).

Bleached softwood and hardwood kraft pulp may contain also some minor quantities of other polysaccharides such as starch and pectic substances (Sjöström, 1993). However, the quantities are so small that they does not have any significant effect on the reactivity of hemicelluloses and like lignin they are not further considered in this thesis.

1.2 Possible reactions with bleached kraft pulp

From the chemical aspect the reactivity of bleached kraft pulp is dependent on the functional groups present in the cellulose and hemicelluloses. While the cellulose is main component in kraft pulp also the most reactive functional groups can be found from cellulose fiber. Every D–glucose units in cellulose has three free hydroxyl groups that are able to react as primary and secondary alcohols. Due to that, the most common way to modify pulp fibers are esterification, etherification, cross-linking and graft polymerization. Other aspects such as fiber morphology, DS and intermolecular hydrogen bonds are also affecting the reactivity of pulp. (Debashis, *et al*. 2009; Sjöström, 1993; Tkacheva, *et al*. 2013)

Sjöström (1993) presents that the reactivity of hydroxyl groups in cellulose decreases in order C–6 < C–3 < C–2 in the case of etherification (Sjöström, 1993). The esterification reaction on the other hand happens more likely with the primary hydroxyl group C–6. In addition, the accessibility of the bulky substituents on the primary hydroxyl group is found to be easier than other hydroxyl groups. Part of the hydroxyl groups present in bleached pulp is oxidized to carboxyl and carbonyl groups during pulp bleaching. (Sjöström, 1993; Debashis, *et al*. 2009)

In cellulose the maximum degree of substitution is three due to amount of hydroxyl groups present in each D-glucose units. DS tells how many of possible functional groups are substituted in a particular molecule. DS does not tell which groups are substituted, only the amount of places occupied. DS works similarly with the hemicelluloses though usually DS refers only amount of groups attached on free hydroxyl groups.

In some applications cellulose is used in microfibrillated (MFC) or nanofibrillated (NFC) form. MFC and NFC are usually produced from bleached kraft pulp with mechanical and chemical treatment that shreds the pulp fibers into cellulose microfibrils and nanofibrils. MFC has some specific properties such as strength, hydrophilicity, high viscosity and high surface area compared to normal kraft pulp. The physical appearance of pure MFC is partly or fully transparent hydrogel. (Missoun *et al*. 2013)

The modification of bleached kraft pulp is also possible with the adsorption. The adsorption of various compounds into cellulose fibers is possible with electrostatic forces and weak chemical linkages such as hydrogen bonds and van der Waals forces (Fras *et al*. 2012). The cellulose modification with the adsorption is not as durable method as attachment of the functional groups with a covalent bonding.

1.2.1 Esterification

The esterification of cellulose and hemicelluloses present in pulp happens when the alcohol groups of polysaccharides react with acid. The simple esterification reaction of pulp containing polysaccharides is possible to carry out with inorganic acids such as nitric acid or sulfuric acid. Only commercially significant product from an inorganic esterification is cellulose nitrate. Various products such as cellulose acetate can be produced with an organic acid esterification. (Sjöström, 1993)

It is also possible to attach different side groups to the polysaccharides with an ester bond. For example the esterification of cellulose with different aromatic acids such as benzoic acid, phthalic acid and salicylic acid have also been investigated in pharmaceutical purposes. In addition, nitrogen containing cellulose ester compounds such as cellulose dialkyl diaminoacetate have been developed but only with a minor commercial significance. (Stinchfield, 1929; Sjöström, 1993; Talába, *et al*. 1996)

The studies made by Sun *et al.* (2000) showed that the esterification of hemicelluloses with different acyl chlorides was found to be the effective way to produce hemicellulose based esters. The hemicellulose used in the studies were extracted from rye straw and the predominant hemicellulose present was xylose. The acyl chloride esterified hemicellulose showed increased hydrophobicity.

1.2.2 Etherification

Commercially significant cellulose ethers such as methylcellulose (MC) ethylcellulose (EC) and carboxymethylcellulose (CMC) are produced by treating alkali cellulose with suitable reagent such as alkyl or aryl halides/sulfates, alkene oxides or sodium chloroacetate. From these three compounds CMC has the widest range of the applications. CMC can be used as a rheology modifier and stabilizer in food, pharmaceuticals, paint and in cosmetic products. (Sjöström, 1993; Ek *et al*. 2009)

New interest in the cellulose modification via the etherification is a regioselective functionalization using protective groups. This enables the etherification of certain hydroxyl groups in the cellulose chain. Schaller and Heinz (2005) have examined the effect of triphenylmethyl (trityl) and 4-monomethoxytrityl (MMT) protection during the synthesis of hydroxyalkyl ethers of cellulose. The studies show that with the protective group such as trityl or MMT it is possible to achieve selective substitution of hydroxyalkyl ether in the cellulose chain. (Schaller & Heinze, 2005)

The etherification reactions may also occur in hemicelluloses while they have the functional hydroxyl groups which can form an ether bond. For example Peng *et al.* (2010) have investigated the etherification of xylan rich hemicelluloses with maleic anhydride in ionic liquid. The research show that the etherification of xylan rich hemicellulose was possible and the 0.75 was the highest achieved DS. The end product could be used as a base material for the graft polymerization. (Peng *et al*. 2010)

1.2.3 Cross-linking

The cross-linking of cellulose and cellulose derivatives have been studied decades to obtain new cellulose based end products. In the case of cellulose the cross-linking means forming the ether or ester bonds between two cellulose molecules in the presence of suitable reagent, cross-linking agent. In practice, the ester cross-linking of cellulose is less used because of the ester cross-links are unstable in the alkali conditions. The cross-linking of cellulose molecules effects on the intermolecular structure of cellulose due to some of the hydrogen bonds are replaced with covalent ether bonds. First cross-linkers used with cellulose was aldehydes like formaldehyde. In the **Equation 1.1** is demonstrated the cross-link reaction of formaldehyde and cellulose according to Sjöström (1993). More developed and often used cross linking technique is the use of formaldehyde precondensates with some amides such as urea or carbamates. This treatment technique have been used in the textile industry to obtain crease resistance and dimensional stability to the fabrics. (Sjöström, 1993)

$$2\ \mathrm{Cell-OH} + \mathrm{HCHO} \xrightarrow{\mathrm{H^+}} \mathrm{Cell-O-CH_2-O-Cell} \qquad (1.1)$$

The cellulose derivatives such as CMC in sodium form, hydroxypropyl methylcellulose (HPMC), ethyl cellulose (EC) and hydroxyethylcellulose (HEC) have been used to develop biodegradable superabsorbent polymer (SAP). SAPs have a wide range of industrial applications in the hygienic products such as diapers and feminine pads. The cross-linking agents used with cellulose derivatives are numerous. At least epichlorohydrin, aldehydes and aldehyde-based reagents, carbodiimides and multifunctional carboxylic acids such as citric acid have been reported to function well as the cross-linking agent with cellulose and its derivatives. (Sannino *et al*. 2009; Sannino *et al*. 2005; Demitri *et al*. 2008; de Cuadro *et al*. 2015)

The cross-linking reactions are usually catalyzed to obtain the wanted reaction time and temperature. Some commonly used catalysts in the cross-linking reactions are metal salts and oxides such as magnesium chloride, titanium oxide and aluminum sulfate, the combination of the metal salts, acid and ammonium chloride, sulfate or nitrate salts.

Magnesium chloride may be considered as the most used catalyst together with certain acids in the cross-linking of cellulosic materials. (Korpela, 2008)

1.2.4 Graft polymerization

Apart from the traditional modifying techniques like the etherification or esterification more developed technique in the cellulose modification is so called graft copolymerization or briefly grafting. The grafting is usually carried out in a heterogeneous system such as grafting vinyl monomers onto cellulose. Several different grafting methods have been applied like radical, ionic, ring opening and condensation or addition polymerization. The cellulose grafting is mostly conducted via the radical polymerization. (Sjöström, 1993; Neira *et al*., 2008)

The mechanism of the radical copolymerization can be divided in three phases: an initiation, propagation and termination. The initiation reaction needs free radicals that can be produced by a radiation, Fenton's reagent, ceric ammonium nitrate, various persulfates or azobisisobutylonitrile (AIBN). Fenton's reaction steps are shown in the **Equations 1.2-1.5** (Haber & Weiss, 1934):

$$Fe^{2+} + H_2O_2 \rightarrow {}^{\bullet}OH + OH^{-} + Fe^{3+} \quad (1.2)$$

$${}^{\bullet}OH + Fe^{2+} \rightarrow OH^{-} + Fe^{3+} \quad (1.3)$$

$${}^{\bullet}OH + H_2O_2 \rightarrow H_2O + {}^{\bullet}OOH \quad (1.4)$$

$${}^{\bullet}OOH + H_2O_2 \rightarrow {}^{\bullet}OH + O_2 + H_2O_2 \quad (1.5)$$

These hydroxyl radicals formed during reaction (Eq.1.2) are able to abstract a hydrogen atom from the hydroxyl group present in cellulose. In consequence the secondary cellulose radical is formed (Eq.1.6). These cellulose radicals initiate the grafting and the proposed mechanism is shown in the **Equations 1.6-1.11** (Gürdag & Sarmad, 2013):

$${}^{\bullet}OH + Cell - OH \rightarrow H_2O + Cell - O^{\bullet} \quad (1.6)$$

$${}^{\bullet}OH + M \rightarrow OH - M^{\bullet} \xrightarrow{nM} OH - M^{\bullet}_{n+1} \quad (1.7)$$

$$OH - (M_{n+1})^{\bullet} + Cell - OH \rightarrow OH - (M_{n+1}) - H + Cell - O^{\bullet} \quad (1.8)$$

$$Cell - O^{\bullet} + M \rightarrow Cell - O - M^{\bullet} \xrightarrow{nM} Cell - O - M^{\bullet}_{n+1} \quad (1.9)$$

$$Cell - O - M^{\bullet}_{n+1} + OH - M^{\bullet}_{n+1} \rightarrow Cell - O - M_{2n+2} \text{ (graft copolymer)} \quad (1.10)$$

$$Cell - O - M^{\bullet}_{n+1} + Fe^{3+} \rightarrow Fe^{2+} + Cell - O - M_{n+1} \text{ (graft copolymer)} \quad (1.11)$$

The propagation reaction (Eq.1.9) shows how the secondary cellulose radical polymerizes with a monomer such as vinyl. Equations 1.7 and 1.8 show the possible side reaction where the monomer forms an unwanted homopolymer. In the Equations 1.10 and 1.11 are two possible termination reactions. In the Equation 1.11 the propagation is terminated too soon and it has a negative effect on the grafting. In the case of the Fenton reagent the molar ratio of H_2O_2 and Fe (II) affects highly on the grafting yield. (Gürdag & Sarmad, 2013)

The polymerization is called “grafting from” polymerization when the polymerization is initiated from the hydroxyl group in the cellulose backbone and the polymer monomers grow on the surface of cellulose. If the polymerization is initiated from the monomers so that they grow into polymers with an initiator head which attaches to the cellulose surface, the polymerization reaction is called “grafting to” polymerization. (Gürdag & Sarmad, 2013)

Researchers have been studied for decades the grafting of cellulose and cellulose derivatives with different monomers to produce new cellulose based materials. Several materials such as acrylic acid, acrylamide, 2-acrylamidomethylpropane sulfonic acid, methyl methacrylate, styrene, acrylonitrile, butadiene, isobutyl vinyl ether, and vinyl acetate have been grafted with cellulose to achieve better moisture absorbency or adhesion. Cellulose fibers that are grafted with certain monomer to produce the superabsorbent material is called superabsorbent fibers, SAFs. (Chang & Cheng, 2002; Gürdag & Sarmad, 2013; Cooke, 2006)

The characterization of the grafted copolymers can be carried out with various techniques. The basic characterization such as a grafting percentage (GP %) can be determined by volumetric or gravimetric measurements. An elemental analysis is also a good method to determine GP % if monomer contains for example nitrogen that does not naturally occur in cellulose. (Gürdag & Sarmad, 2013)

GP % stands for the weight increase during the graft polymerization. Gürdag &Sarmad (2013) have proposed following **Equation 1.12** for calculating GP %:

$$GP\ \% = \frac{W_1 - W_0}{W_0} \times 100 \qquad (1.12)$$

Where W_1 Weight of cellulose graft copolymer

W_0 Initial weight of cellulose

GP % calculated from the Equation 1.12 is only for the crude estimation of the grafting percent because usually the weighted polymer contains some residues of the non-reacted cellulose. The non-reacted cellulose would need to be separated for more accurate values.

1.2.5 Adsorption

The modification of the cellulose fibers is also possible other ways than by the covalent bonding. The adsorption is one option to attach for example modified polysaccharides or surfactants with charge into cellulose fiber. The cellulose modification by the adsorption may enhance the mechanical properties of the end product and improve the beatability of pulp (Silva *et al*. 2010; Miletzky *et al*. 2015). Other interesting applications have been developed by adsorbing chitosan on cellulose. Fras *et al.* (2012) have studied antibacterial effect of chitosan adsorbed on cellulose viscose fibers and found out that chitosan modified cellulose viscose fibers had a significant antimicrobial resistance. This kind of modified cellulose would be promising material for sanitary products or medical textiles. (Fras *et al*. 2012)

Important factors that effects on the adsorption are temperature, available surface area of the adsorbent, pH, molecular weight, solvent, surface charge, time of the adsorption and functionalities both adsorbent and adsorbate (Fras *et al*. 2012; Shirazi *et al*. 2003; Xhanari *et al*. 2011). The adsorption can be either reversible or irreversible depending on the interactions between molecules. When large molecules, such as polysaccharides, are adsorbed on cellulose the exact mechanism remains unknown in most of the cases.

2 APPLICATIONS OF THE MODIFIED KRAFT PULP

The pulp modification is a promising way to create new properties for certain cellulose based materials. The literature part of this thesis is focusing on the possible use and analysis of the modified kraft pulp in tissue papers, hygienic products, packaging applications and in cellulose based non-woven materials. Wanted properties for the products mentioned above can be for example increased absorbency, antimicrobial properties, flame retardant, water and grease barrier and enhanced wet strength.

2.1 Tissue paper

Traditionally important factors in tissue papers have been mechanical properties such as wet- and tensile strength, softness and absorption capacity. The most common tissue paper grades are toilet papers, napkins, facial towel, freshen-up towel, kitchen paper and paper towels (Kiiskinen *et al*. 2012). New properties such as antibacterial or enhanced absorbance have been studied a lot during recent years (Wu *et al*. 2015; Fras *et al*. 2012). It has also been noticed that the cross-linking of wood cellulose with polycarboxylic acids like polymaleic acid (PMA) or 1,2,3,4-butanetetracarboxylic acid (BTCA) increases the wet-strength of paper (Yang *et al*. 1996). The structures of PMA and BTCA are shown in **Figures 6** and **7**, respectively. The wet-strength for various tissue and towel papers can also be enhanced by adsorbing glutaraldehyde-chitosan complexes into cellulose matrix (Wu *et al*. 2015).

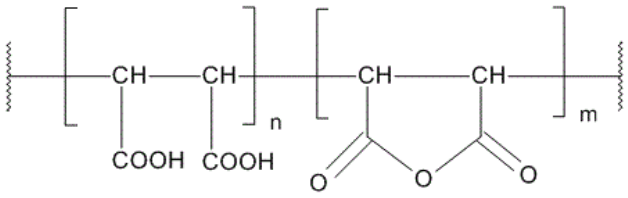

Figure 6. The structure of poly maleic acid (PMA)

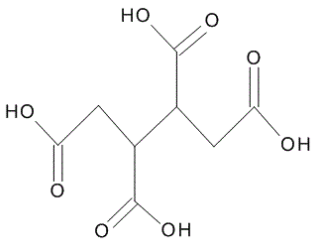

Figure 7. The structure of 1,2,3,4-butanetetracarboxylic acid (BTCA).

Korpela (2008) have studied the cross-linking effect on birch kraft pulp. In the study bleached birch kraft pulp was cross-linked with 1,3-dimethyol-4,5-dihydroxyethylurea (DMDHEU) and 1,3-dimethyl-4,5-dihydroxy-imidazolidinone-2 (DMeDHEU). The structures of DMDHEU and DMeDHEU are shown in **Figures 8** and **9**, respectively. The study showed that the cross-linking increased the tensile strength of paper and it may have positive effect on the wet strength of the end product. (Korpela, 2008)

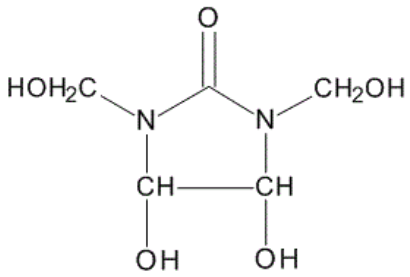

Figure 8. The structure of 1,3-dimethyol-4,5-dihydroxyethylurea (DMDHEU).

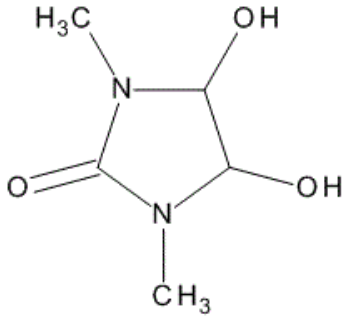

Figure 9. The structure of 1,3-dimethyl-4,5-dihydroxy-imidazolidinone-2 (DMeDHEU).

Various patents of the facial towels and freshen-up towels with the antimicrobial agent have been applied during past few years (Charest, 2012; Buder, 2012). In addition, many studies concerning the cellulose modification with the antibacterial molecules like triazine derivatives, chitosan and 2-(dimethylamino) ethyl methacrylate (DMAEMA) have been done recently (Fras *et al*. 2012; Roy *et al*. 2009; Hou *et al*. 2009). The structures of chitosan and DMAEMA are shown in **Figures 10** and **11**, respectively.

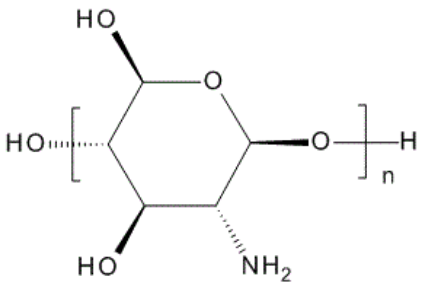

Figure 10. The structure of chitosan.

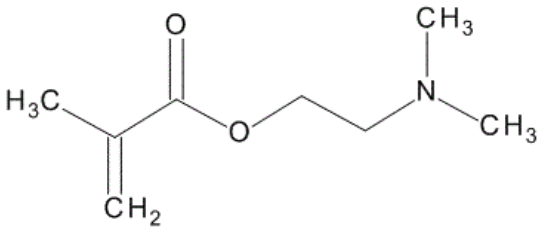

Figure 11. The structure of 2-(dimethylamino) ethyl methacrylate (DMAEMA).

Lund *et al.* have recently studied the effect of the cross-linking of Scandinavian softwood kraft pulp with diepoxide. In the study 1,4-butanediol diglycidyl ether (BDDE) was used as a cross-linking agent. The structure of BDDE is shown in **Figure 12**. The aim of the study was to develop a low density pulp with good strength and liquid distribution characteristics for the tissue and hygienic products. Usually low density pulp is used as a structural reinforcement for the SAP materials. The cross-linking resulted better strength properties, higher water retention and the cross-linked pulp was found to be soft to the touch. The softness can be a great benefit in the end product like the feminine pads. (Lund *et al*. 2011)

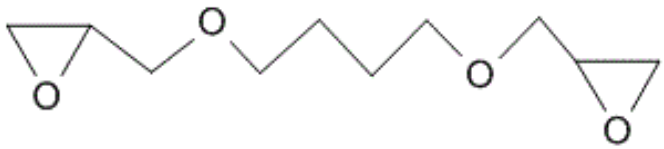

Figure 12. The structure of 1,4-butanediol diglycidyl ether (BDDE).

2.2 Hygienic products

The demand of the disposable cellulose based hygienic products such as the diapers, feminine pads and incontinence products have been increased lately. Numerous patents for new kind of hygiene products have been applied especially in China and Japan in the 21st century (Kiiskinen *et al*. 2012). Important factors for new products are absorption, which usually is achieved with SAPs or SAFs, and antibacterial property (Sannino *et al*. 2009).

The commonly used SAPs are made from acrylic compounds such as polyacrylate or polyacrylamide but the environmental trends have been driven the research towards the renewable materials such as the cellulose, starch and chitin derivatives. According to Zohuurian-Mehr and Kabiri (2008) the graft copolymerization of vinyl monomer into polysaccharide backbone and direct cross-linking of polysaccharides are the two predominant ways to produce renewable SAPs.

The example of the renewable cellulose based SAPs is CMC and HEC cross-linked with citric acid demonstrated by Demitri *et al.* (2008). Citric acid as the cross-linker is found out

to be non-toxic, relatively cheap and widely available chemical which makes it commercially significant. Other biodegradable cellulose derived SAP demonstrated by Sannino *et al.* (2005) has been developed from the mixture of hyaluronic acid (HA), CMC and HEC cross-linked with non-toxic and water soluble carbodiimide; 1-ethyl-3-(3-dimethylaminopropyl)carbodiimide (WSC). The structure of WSC is shown in **Figure 13**. The cross-linked material showed an excellent swelling capacity for distilled water, over 400 g_{water}/g_{SAP}. Other cross-linker used before for biodegradable SAP production is divinylsulfone (DVS).

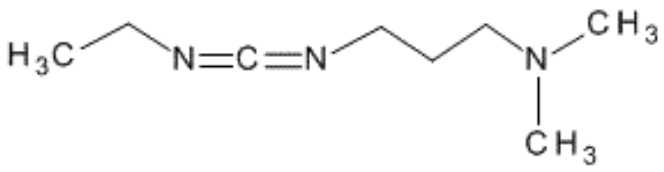

Figure 13. The structure of water soluble carbodiimide 1-ethyl-3-(3-dimethylaminopropyl) carbodiimide (WSC).

The antibacterial activity in the hygienic products can be enhanced similar way as in tissue papers discussed above. A semi-durable antibacterial treatment for cotton fabric have been demonstrated in a study made by Kou *et al.* (2006). Cotton was treated with 5-methyl-5-aminomethylhydantoin (AH) with the cross-linking agent butanetetracarboxylic acid (BTCA). Another promising way to produce antimicrobial cellulose material for the hygienic product purpose is the esterification with ethylenediaminetetraacetic acid, EDTA (Luo, *et al*. 2013). Cotton fibers grafted with the mixture of glycidyl methacrylate (GMA) and β-cyclodextrin (β-CD) and treated with chlorohexidin diacetate have also found to be the suitable antibacterial material for the hygienic purposes (Abdel-Halim *et al*. 2010). The structures of EDTA, GMA and β-CD are shown in **Figures 14-16**, respectively.

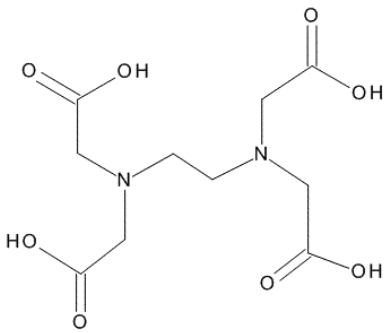

Figure 14. The structure of ethylenediaminetetraacetic acid (EDTA).

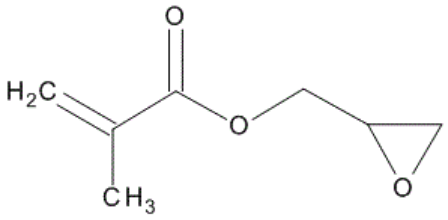

Figure 15. The structure of glycidyl methacrylate (GMA).

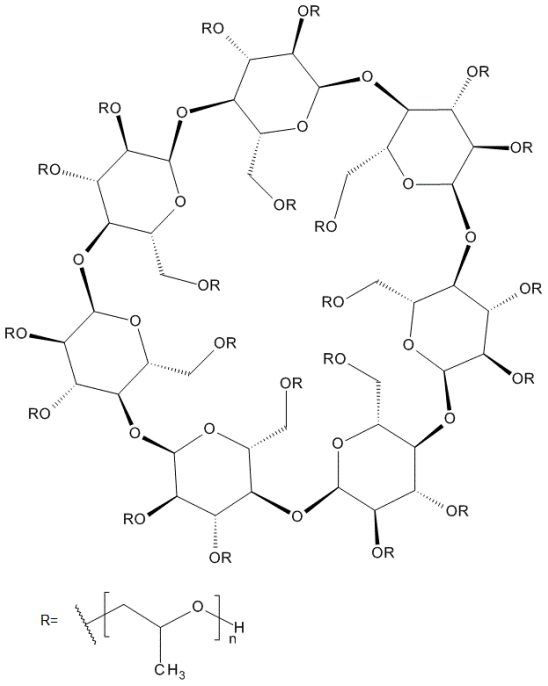

Figure 16. The structure of β-cyclodextrin (β-CD).

The antimicrobial properties can be efficiently adapt to the raw material of the hygienic products such as bleached pulp itself. Guan *et al.* (2007) have studied the grafting of the softwood sulfite pulp with guanidine polymer, GMA modified polyhexamethylene guanidine hydrochloride (PHGH). The structure of PHGH is shown in **Figure 17**. The study showed that even 1 w-% of grafted PHGH on the pulp surface inhibited 99% of bacterial growth of *Escherichia coli*.

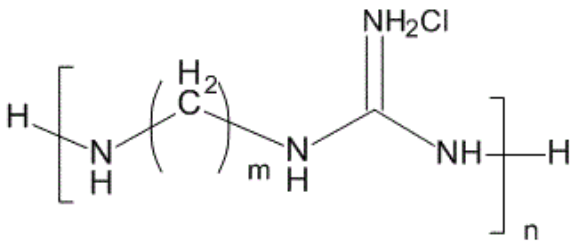

Figure 17. The structure of polyhexamethylene guanidine hydrochloride (PHGH).

2.3 Cellulose based non-woven fabrics

The cellulose based non-woven materials are used for example in different filter applications, medical textiles and hygienic products. Certain properties like the flame retardancy and antimicrobial resistance are wanted properties in the non-woven end products such as fire resistant textiles, air filters, medical textiles and respirator masks. (Le Blan *et al*. 2007.) Followed non-wovens are cellulose based in this thesis if not stated otherwise.

The anti-flammable properties of the non-wovens have been developed with various techniques. The coating of the non-woven material with the flame retardant agent is one possible way, although the coatings usually will be washed off relatively easy. Other and more stable way to improve anti-flammable properties of the non-woven is to modify cellulose with the proper flame retardant. Phosphorous or nitrogen containing flame retardant agents like tetrakis(hydroxymethyl)phosphonium salts (THPX), urea, different melamines and 3-(hydroxyphenylphosphinyl)-propanoic acid (HPPA) have been found to improve the anti-flammability of the non-wovens. Commercially available Pyrovatex® treatment for the cellulose material is based on the cross-linking of N-methylol dimethyl phosphonopropionamide (MDPA) to the cellulose fiber with amino resin cross-linking agent. Another commercial flame retardant for the cellulose based material is Fyroltex®. Fyroltex is based on the cross-linking of oligomeric methylphosphonatephosphate (MPP) to the cellulose backbone with BTCA or citric acid. (Weil & Levchik, 2008; Zheng *et al*. 2015) The structures of THPX, HPPA, MDPA and MPP are shown in **Figures 18-21**, respectively.

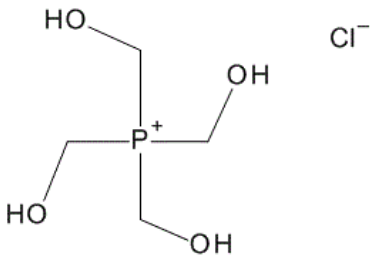

Figure 18. The structure of tetrakis(hydroxymethyl)phosphonium salts (THPX).

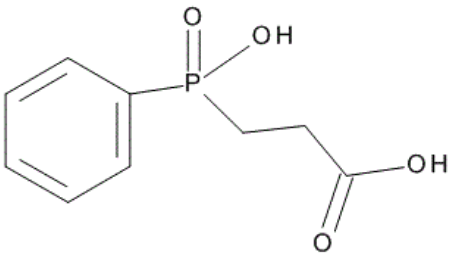

Figure 19. The structure of 3-(hydroxyphenylphosphinyl)-propanoic acid (HPPA).

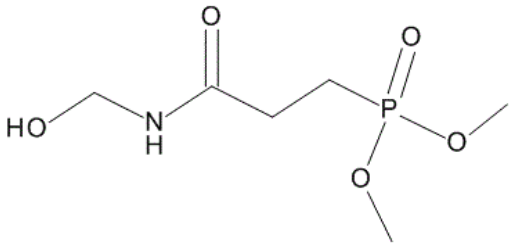

Figure 20. The structure of N-methylol dimethyl phosphonopropionamide (MDPA).

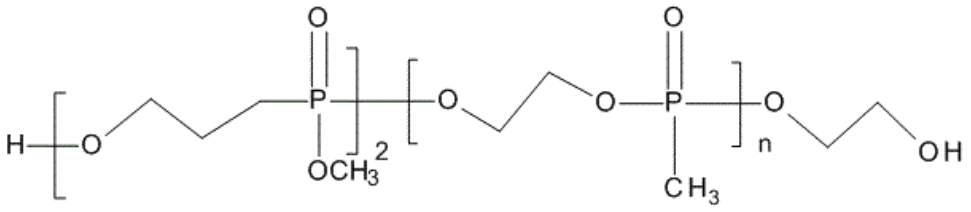

Figure 21. The structure of oligomeric methylphosphonatephosphate (MPP).

The enhanced antimicrobial activity of the non-woven materials may be implemented same way as in the hygiene products: with the proper antibacterial agent. The antiviral properties are also necessary since the non-wovens are used as a base material in different respirator masks. Catel-Ferreira *et al.* found out that the filter material of catechin polyphenol (**Figure 22**) grafted non-woven had a significant antiviral properties against airborne viruses (Catel-Ferreira, *et al*. 2015). Another study made by Seong *et al.* showed that the chito-oligosaccharides are environmental friendly way to enhance the antibacterial activity in the non-wovens (Seong, *et al*. 1999). The adsorption of metallic salts such as $CuSO_4$ and $ZnSO_4$ after succinic anhydride (SA) pretreatment into the non-woven material have also reported to decrease the bacterial activity on the fabric (Nakashima *et al*. 2001). Silver nanoparticles (Ag NPs) and silver salts such as $AgNO_3$ and AgCl have been used as the antibacterial finishing agents in the cellulose based fabrics and non-wovens. The adsorption of silver can be enhanced by grafting some acidic compound onto the fiber surface. An extensive review of different methods and applications of modifying cellulosic fibers with the silver compounds have been published recently (Simoncic & Klemcic, 2015). Emam *et al.* (2014) have investigated the antimicrobial effect of the copper (I) oxide for the surface modification of Lyocell fibers. Lyocell have been used in many hygiene and medical applications like bandages, wound dressings, diapers *et cetera*.

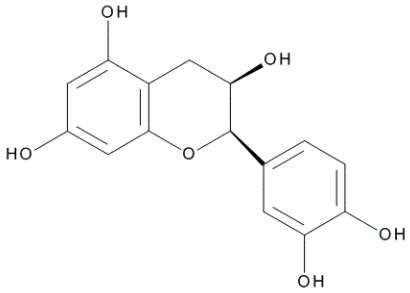

Figure 22. The structure of catechin polyphenol.

Some commercially available antimicrobial wound dressing material have been developed by adsorbing polyhexamethylen biguanide (PHMB) into cellulose fibers (Ristic *et al*. 2011). Various N-halamine compounds such as 3-methylol-2,2,5,5-tetramethyl-imidazolidin-4-one (MTMIO) and 3-trihydroxysilylpropyl-5,5-dimethylhydantoin (SPH) have been grafted into cellulose to produce the antibacterial material for the medical textiles (Sun & Worley, 2006). The structures of MTMIO and SPH are shown in **Figures 23** and **24**, respectively.

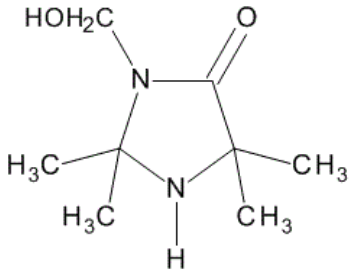

Figure 23. The structure of 3-methylol-2,2,5,5-tetramethyl-imidazolidin-4-one (MTMIO).

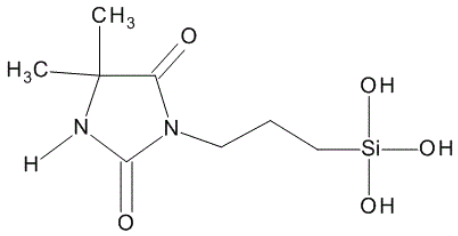

Figure 24. The structure of 3-trihydroxysilylpropyl-5,5-dimethylhydantoin (SPH).

The multifunctional polymer mixture of 1,1,2,2,-perfluorooctyltriethoxysilane (SiF), 3-(trimethoxysilyl)-propyldimethyloctadecyl ammonium chloride (SiQ) and P,P-diphenyl-N-(3-(trimethoxysilyl)propyl) phosphinic amide (SiP) have been grafted on the cotton fabric by a sol-gel method to produce a water and oil repellent, antibacterial and flame-retardant textiles. Vasiljevic *et al.* (2014) showed that more than one property is possible to achieve by the multifunctional mixture of the above mentioned compounds. The structures of SiF, SiQ and SiP are shown in **Figures 25-27**, respectively.

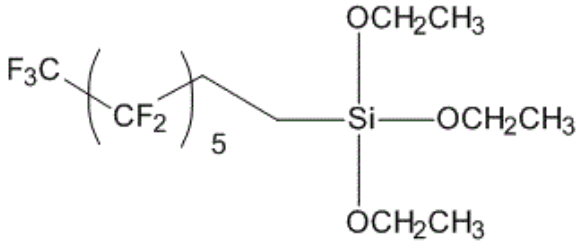

Figure 25. The structure of 1,1,2,2,-perfluorooctyltriethoxysilane (SiF).

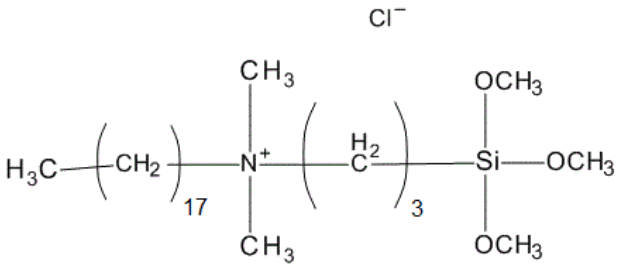

Figure 26. The structure of 3-(trimethoxysilyl)-propyldimethyloctadecyl ammonium chloride (SiQ).

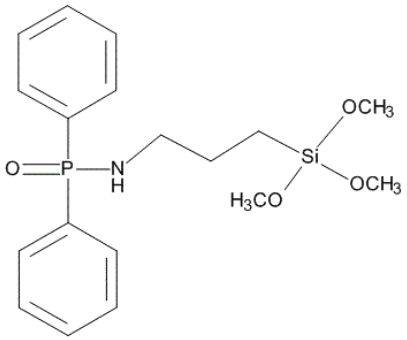

Figure 27. The structure of P,P-diphenyl-N-(3-(trimethoxysilyl)propyl) phosphinic amide (SiP).

2.4 Packaging applications

For the packaging applications, the modified cellulosic materials can offer new barriers for different purposes. Especially the chemically modified MFC have drawn attention in the barrier applications due to the easy modification. An example of the modified MFC as a barrier material is acetylated MFC film prepared by Rodionova *et al.* (2011). The study show that a film prepared from acetic anhydride acetylated MFC had excellent oxygen barrier properties and increased hydrophobic character.

Vaca-Garcia *et al.* (1998) have esterified cellulose with fatty acids with different carbon chain length in the presence of acetic anhydride (AAH). The structure of AAH is shown in **Figure 28**. The study showed that fatty acids with longer carbon chain produces more

hydrophobic surface. Vartiainen *et al.* (2014) has found out that fatty acid esters of cellulose have the excellent grease and moisture barrier properties because of their hydrophobic nature. The coatings made from fatty acid esterified hemicelluloses have also found to improve the grease barrier properties of papers.

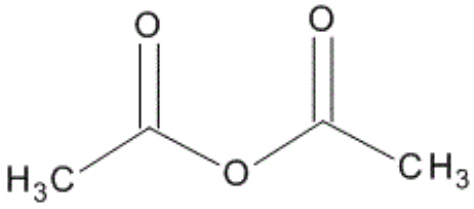

Figure 28. The structure of acetic anhydride (AAH).

The different modifications and achieved properties of cellulose have been listed on **Table 2**. These cellulose modifications should be possible also for bleached kraft pulp, due to composition of pulp. As presented above, the hydroxyl, carbonyl and carboxyl groups are the main routes to modify the kraft pulp. The hemicelluloses present in different pulps have also an impact on the pulp reactivity.

Table 2. The summary of the different modifications and achieved properties for cellulose

Method & chemistry	Antimicrobial	Flame retardancy	Absorption	Other	End product	Reference
Cross linking						
BDDE+softwood pulp				Softness	Tissue papers	Lund *et al*. 2011
DVS+CMC/HEC			X		SAP	Sannino *et al*. 2005
WSC + CMC/HEC			X		SAP	Sannino *et al*. 2005
Epichlorohydrin			X		SAP	Sannino *et al*. 2009
BTCA/AH +cotton	X				Textiles	Kou *et al*. 2006
CMC+citric acid			X		SAP	Demitri *et al*. 2008
HEC+citric acid			X		SAP	Demitri *et al*. 2008
PMA+kraft paper				Wet strength	Tissue papers	Yang *et al*. 1996
BTCA+kraft paper				Wet strength	Tissue papers	Yang *et al*. 1996
DMDHEU+birch pulp				Tensile strength	Tissue papers	Korpela, 2008
DMeDHEU+birch pulp				Tensile strength	Tissue papers	Korpela, 2008
MPP/citric acid+cotton		X			Textiles+non-wovens	Weil & Levchik, 2008
MDPA+cellulose		X			Textiles+non-wovens	Weil & Levchik, 2008
THPX+cotton		X			Textiles	Weil & Levchik, 2008
Graft polymerization						
MTMIO	X				Medical textiles	Sun & Worley, 2006
SPH	X				Medical textiles	Sun & Worley, 2006
Acrylic acid			X		SAP	Zohuurian-Mehr & Kabiri, 2008
β-CD/GMA	X				Medical textiles	Abdel-Halim *et al*. 2010
Vinyl acetate			X		SAP	Gürdag & Sarmad, 2013
DMAEMA	X				Medical textiles	Roy *et al*. 2009
Catechin polyphenol	X				Non-wovens	Catel-Ferreira *et al*. 2015
GMA+PHGH	X				Tissue papers	Guan *et al*. 2007
SiF+SiP+SiQ	X	X		Water & greaseproof	Non-woven textiles	Vasiljevic et al. 2014

Table 2. Continues

Method & chemistry	Antimicrobial	Flame retardancy	Other	End product	Reference
Esterification					
EDTA	X			Bandages, wound dressing	Luo *et al*. 2013
HPPA		X		Textiles, non-wovens	Zheng *et al*. 2015
Fatty acids+AAH			Grease barrier	Packaging applications	Vaca-Garcia *et al*. 1998
MFC+AAH			O_2&H_2O Barrier	Packaging applications	Rodionova *et al*. 2011
Adsorption					
PHMB	X			Medical textiles	Ristic *et al*. 2011
Cu-D-Gluconate	X			Non-woven	Emam *et al*. 2014
Chitosan	X			Medical textiles	Fras *et al*. 2012
Chito-Oligosaccharides	X			Medical textiles	Seong *et al*. 1999
Glutaraldehyde-Chitosan	X		Wet strength	Tissue & towel paper, packaging	Wu *et al*. 2015
CuSO4+SA	X			Non-wovens, hygienic products	Nakashima *et al*. 2001
ZnSO4+SA	X			Non-wovens, hygienic products	Nakashima *et al*. 2001
Ag NP	X			Textiles, non-wovens	Simoncic & Klemcic, 2015
AgCl	X			Textiles, non-wovens	Simoncic & Klemcic, 2015
$AgNO_3$	X			Textiles, non-wovens	Simoncic & Klemcic, 2015

3 ANALYTICAL METHODS OF MODIFIED KRAFT PULP

Various analytical methods have been developed for the pulp fiber analysis. These methods are commonly divided into the direct and indirect methods. The analyses can be either destructive or non-destructive. The most promising method for the quantitative and easily repetitive analysis of the fiber surface would be the direct and non-destructive method.

3.1 Direct methods

The direct analytical methods give information directly from the component chemical structure. The most widely used structural analysis techniques of the pulp fibers are Fourier transform infrared spectroscopy (FTIR), ultraviolet/visible spectroscopy (UV/Vis), Raman spectroscopy, nucleomagnetic resonance (NMR) techniques, electron spectroscopy for chemical analysis (ESCA) and secondary ion mass spectroscopy (SIMS) (Stenius & Vuorinen, 1999). Pyrolysis gas chromatography (Py-GC) may also be used in some cases to determine the concentration of the substituted compound. In addition to these, some titration methods can be used to analyze certain functional groups on the fiber surface.

From these techniques FTIR and UV/Vis are relatively easy to use, non-destructive, fast and accurate methods for the characterization of the chemical structure from the dry pulp samples. In industrial point of view, these two techniques would be the most promising ones for repetitive analyses. The FTIR and UV/Vis techniques do not provide the direct information about the location where the substituent have attached. For more detailed information of the substitution more specific techniques like NMR, ESCA or SIMS are needed.

3.1.1 Fourier transform infrared spectrometer (FTIR)

FTIR is a useful tool for the characterization of the modified pulp fibers and attached side groups on the cellulose or hemicellulose chain. The operational principle in FTIR is based on the infrared absorption of certain chemical bonds with the specific infrared region frequencies due to the vibrations and stretching of the functional groups. The intensity of the absorbance or transmittance peak corresponds to the amount of certain bonds in the molecule structure. (Gremlich, 2012.) The typical wavenumbers of the different functional groups are listed in **Appendix I**. Gürdag & Sarmad (2013) have also gathered an extensive list of the characteristic frequencies for numerous modified cellulosic compounds.

In FTIR, the Lambert-Beer's law expresses the intensity of the IR radiation traversing through sample, and it is shown in the **Equation 3.1**.

$$I = I_0 \times 10^{-acl} \tag{3.1}$$

Where I Intensity of the transmitted radiation

I_0 Intensity of the source

a Absorption coefficient

c Concentration

l Optical path length

By extending Lambert-Beer's law the transmittance can be converted from the transmittance to the absorbance with the following equation:

$$T = \frac{I}{I_0} = 10^{-acl} A = -\log_{10} T = acl \tag{3.2}$$

Where T Transmittance

A Absorbance

The wavenumber range in the modern mid-range FTIR equipment usually varies from 200 to 4000 cm^{-1}. The needed amount of the sample is very small with FTIR, usually around 1 mg. (Gremlich, 2012). The schematic picture of the working principle of the FTIR equipment is shown in the **Figure 29**.

Even though FTIR is very useful technique to analyze the fiber modifications, the quantitative analysis is completely dependent on the sample preparation and calibration (Leclerc, 2000). These techniques are discussed further in the chapter 3.3. The basic idea is that the infrared radiation from the radiation source is split and recombined with two mirrors and the recombined beam is directed through the sample. The beam from the sample is gathered into the detector where the intensity is measured. This signal is then transformed by Fourier Transform into IR spectra.

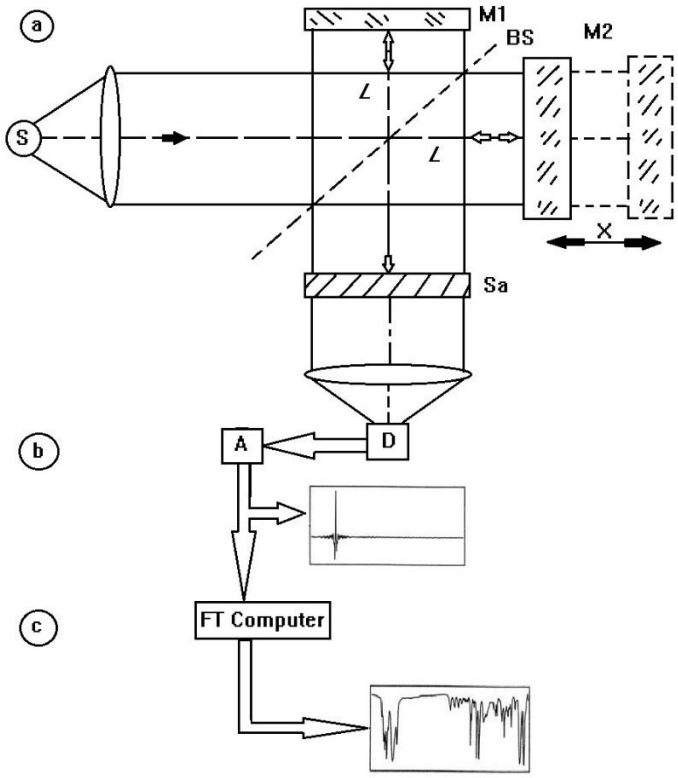

Figure 29. The schematic diagram of the FTIR equipment by Gremlich (2012). In a) Michelson interferometer b) Signal registered by the detector (interferogram) c) Spectrum obtained via Fourier Transform of the interferogram by the computer. S = Radiation source, Sa = Sample cell, D = Detector, A = Amplifier, M1 = Fixed mirror, M2 = movable mirror, BS = Beam Splitter, x = Mirror displacement.

As stated before, most of the cellulose modifications are conducted by forming the covalent bonds with the hydroxyl groups present in the cellulose or hemicellulose backbone. Therefore the peak intensities at certain wavenumbers that are specific for the hydroxyl groups may be used to estimate the amount of the reacted groups. The generality of the modification reactions with the hydroxyl groups are either esterification or etherification reactions and the specific wavenumbers of the ether and ester bonds are also objects of interest. The attachment point of the molecule may be determined by studying the response from the differently oriented OH groups in cellulose. The characteristic frequencies for the typical functional groups in cellulose are listed in **Table 3**.

Table 3. The characteristic frequencies of the functional groups in cellulose (Hinterstoisser & Salmén, 2000; Kondo, 1997; Gürdag & Sarmad, 2013; Fan *et al.* 2012; Noureddine*, et al.* 2011; Socrates, 2001)

Characteristic frequency (cm^{-1})	**Assignment**
3580	free OH (2)
3555	free OH (6)
3410-3460	O(2)H...O(6) intramolecular H-bonds
3340-3375	O(3)H...O(5) intramolecular H-bonds
3230-3310	O(6)H...O(3) intermolecular H-bonds
2920	Symmetrical CH_2 stretching
2883	Asymmetrical CH_2 stretching
1724	C=O stretching vibration
1623	OH Bending of absorbed water
1420	CH_2 Symmetric bend
1340	OH def. vibration
1316	CH_2 Wagging
1205	C-O-C stretching on pyranose ring
1175-1160	Asymm. C-O-C bridge stretch
1108	Nonsymmetrical in-phase ring
1046	C-C, C-OH and C-H ring vibration
1020	C-C, C-OH and C-H ring vibration
896	Stretch C_1-O-C_4
711	CH_2 Rocking
662	C-OH out-of-plane bending

Kondo (1997) have studied how the hydrogen bonds in cellulose affect the frequency of the hydroxyl group in the FTIR technique. The study showed that only C-2 and C-6 bonded hydroxyl groups can appear in free form. The C-3 OH group is basically always hydrogen bonded. The major problem with the characterization of differently oriented hydroxyl groups from IR spectra is that they all occur very close each other. As a result of this, only one sum spectra can usually be detected in the wavenumber region 3700-3100 cm^{-1}. This makes detection of chance in the intensity values of certain hydroxyl group quite impossible. In addition, the absorbed water affects the peak intensity at the wavenumber area 3700-3100 cm^{-1} so, therefore, that wavenumber region should be avoided in the quantitative analysis.

For FTIR there are two predominant sampling methods: attenuated total reflectance (ATR) and diffuse reflectance infrared Fourier transform spectroscopy (DRIFTS). In the ATR method the radiation is directed through a highly reflective material such as diamond, zinc sulfide or germanium to the sample. The frequencies at which the sample absorbs the infrared radiation the evanescent wave is attenuated. By measuring the attenuated absorbance it is possible to get the structural information about the measured sample. The DRIFTS sampling method varies from ATR so that the sample itself is diluted in a highly reflecting matrix that does not absorb the infrared radiation such as powdered potassium

bromide or chloride. The absorbance can be calculated from the intensity difference between the ingoing and outgoing radiation. (Leclerc, 2000) The ATR and DRIFTS sampling methods have been illustrated in **Figure 30**.

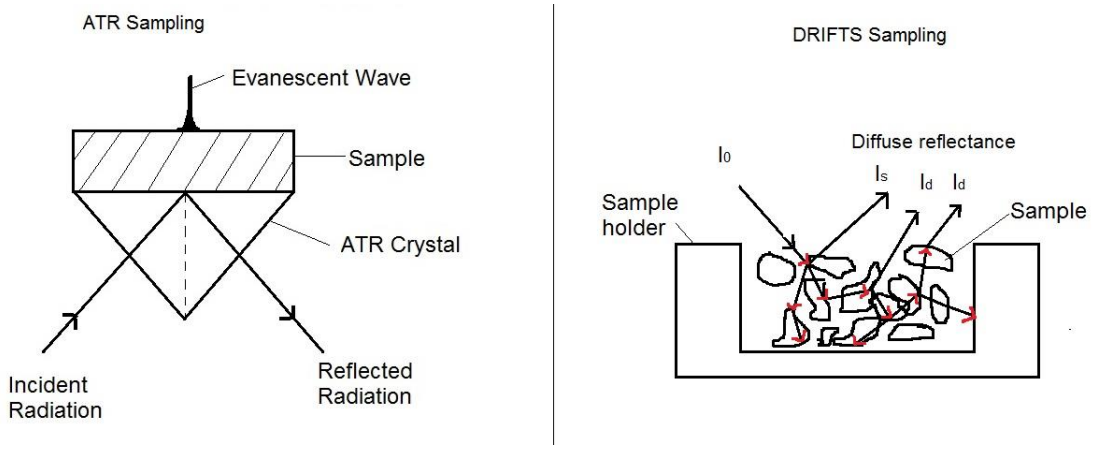

Figure 30. The illustrated figures of the ATR and DRIFTS sampling techniques in FTIR. I_0 = ingoing intensity of ir, I_s = reflectance from sample surface and I_d = reflectance from sample. Outgoing intensity = I_d+I_s. (Leclerc, 2000; Stenius & Vuorinen, 1999)

The disadvantage with the DRIFTS technique is possible water that is absorbed into the sample matrix. Water absorbs the IR radiation and thus it causes error to the signal. ATR is more resistant to water, it has better resolution and it needs minimal sample preparation. Therefore, it is the predominant sampling method with the modified cellulosic fibers.

The quantitative determination for the amount of the substituted species is possible with the assistance of some other analytical method such as the elemental analysis. If the substituted side group contains for example nitrogen or sulfur that does not occur naturally in cellulose, it is possible to find correlation between certain peak intensity and for example nitrogen content. O'Connor *et al.* (1957) have studied the quantitative analysis of cellulose and modified cellulose with FTIR. They found out that it is possible to find linear correlation between the peak intensities and the degree of modification of cyanoethylated, acetylated and tosylated cellulose. With the assistance of some other analytical method it is possible to create the calibration curve between the peak intensity and the degree of modification. This enables easy and non-destructive method for determining the degree of the substitution by FTIR.

The one of the downsides in the quantitative analysis of fibers with FTIR is the sample preparation. The linear correlation between the peak intensity and the concentration of certain substituent depends on the optical path length as stated in Equation 3.1. With DRIFTS technique the sample thickness can be obtained relatively constant by using the constant amount of the matrix material. The ATR technique on the other hand is more

problematic. The sample thickness may vary depending on the sample material and the infrared beam in ATR can only penetrate about 0.25 to 4 µm to the sample surface depending on the contact angle of the beam (Leclerc, 2000). This problem can be partially overcome by using so called peak ratio method. In this method the intensity ratio of two characteristic peaks are used instead of single peak intensity. These peaks should be selected so that the other peak represent the studied phenomena and the reference peak can be used to estimate the contact status of the sample. A good choice for the reference peak is the most intensive peak of the spectra. This peak should be adjusted to certain intensity to provide similar contact between all measurements (Shimadzu corporation, 2015). For example in the case of cellulose modification the carbonyl peak in 1700 cm^{-1} is often a good choice for the characteristic peak and the reference peak for cellulose based materials could be the most intensive peak around 1020-1030 cm^{-1} caused by C-C, C-OH, C-H and other vibrations.

3.1.2 Pyrolysis gas chromatography (Py-GC)

Apart from the non-destructive spectroscopic analysis methods, Py-GC is a destructive analytical method for the chemical composition of different polymeric materials.

Py-GC have been used in the pulp industry to determine the lignin and monosaccharide content in pulp. Py-GC may also be used to examine the grafting results of cellulose. Dorez *et al.* (2014) have used Py-GC to proof the grafting of octadecylphosphonic acid (ODPA) on flax fibers. Usually the grafted molecule can be identified by comparing Py-GC results of the pure component and grafted molecule. This way it is possible to find the characteristic pyrolysis product peaks for certain compounds.

Py-GC is based on the partial thermal degradation of the sample (<0.1 mg) on the inert atmosphere. The pyrolysis is conducted rapidly (<10 s) in the pyrolysis chamber and the products are channeled into the GC column. The products from the pyrolysis are separated according to their chemical nature and boiling point in column which is coated with silica or polyethylene glycol (PEG) and analyzed usually with mass spectrometer. (Stenius & Vuorinen, 1999)

3.1.3 UV/Vis spectrophotometry

The working principle of the UV/Vis spectrometry is similar to FTIR, the main difference is the operating wavenumber area. The typical operating wavenumber region of the UV/Vis apparatus is from 200 to 800 nm. The spectrometer measures the absorbance in the different frequencies similarly to FTIR and certain chromosphores absorbs at certain

frequencies. In addition, some transition metal ions and complexes causes the absorption in the visible region (400-700 nm). The UV/Vis spectrometry is commonly used with the liquid samples so that sample is mainly homogeneous and does not cause the scattering inside the sample. (Owen, 1996)

The analysis of the solid sample analysis with UV/Vis is also possible. The samples are prepared similarly than in DRIFTS technique; grinded and pressed into pellets. The quantitative analysis with the solid samples is challenging due to the solid sample can easily scatter the light beam if the sample is not prepared properly. The absorption peaks are wide with solid samples which makes the detailed characterization difficult. The calibration with solid samples is also relatively challenging though in some cases the internal reference may be used. (Stenius & Vuorinen, 1999; Owen, 1996)

The UV/Vis spectrometry has been used for lignin content analysis from the pulp and fiber samples. Lignin components such as coniferaldehyde gives the absorption peak in 350nm. Kallavus *et al.* developed semi quantitative methods to determine lignin content in lignocellulosic products with UV/Vis spectrometer (Kallavus, et al., 2015). Romi *et al.* (2005) characterized cyclodextrin grafted cotton with the UV/Vis apparatus in another study. However, it can be concluded that the short literature review showed the lack of the reported quantitative analyses of the modified cellulosic fibers with the UV/Vis technique.

3.2 Indirect methods

The indirect analysis methods can be used to characterize the chemical chance in the pulp fibers *e.g*. hydrophobicity or absorbency. The indirect methods gives supporting information for the direct analytical methods. Some methods like the elemental analysis may be used to determinate DS after the fiber modification or determine the amount of the adsorbed compound.

3.2.1 Thermogravimetric analysis (TGA)

The TGA is useful and simple tool to evaluate the change in the cellulose structure. The TGA device measures the weight loss as a function of the temperature. The TGA gives information about the physical and chemical phenomena that causes change in the sample weight such as the desorption, vaporization, dehydration and decomposition. With TGA it is possible to obtain valuable information about the thermal stability of the modified cellulosic materials. The thermogravimetric analyses can be carried out in normal atmosphere when oxygen can react with the compound or in a nitrogen atmosphere. (Coats & Redfern, 1963)

TGA have been used to examine the thermal degradation of the modified cellulose compounds especially in textile research. In addition, polymer grafted cellulose materials are often characterized with TGA. Especially the cellulose based textiles with the anti-flammable properties are usually characterized with TGA along with other flammability tests. The flame retardant compounds prevents the complete oxidation of textile and the formation of the volatile compounds that enhances the burning process. This shows as a higher weight residue at certain temperature when the thermogravimetric curves of the flame retardant cellulose and original cellulose fibers are compared. In addition, the temperature region where the fiber ignites can rise due to the anti-flammable treatment. (Katovic *et al*. 2012; Vasiljevic *et al*. 2014)

3.2.2 Microscopic methods

Different microscopic techniques have been used to visualize and characterize the modified pulp fibers. The light microscope can be used to visualize a fiber shape and orientation. In addition, some surface modifications can be detected with the light microscope. Emam *et al.* (2014) used the light microscope to visualize the adsorption of Cu-D-gluconate complexes into Lyocell fibers. The adsorbed copper complexes were easily detectable from the light microscopic images. The light microscope could also be used to visualize how the Cu-D-gluconate have been distributed on the surface of the fibers.

The light microscope have been commonly used in the pulp analysis for identifying wood cell origin or examine the fibrillation of the fibers. Different stains such as Graff C can be used to separate for example chemically and mechanically produced pulps. The different light microscopic techniques like a phase contrast and dark-field microscopy may be used to add more contrast to the transparent samples such as wood cells or fibrils. Fluorescence microscopy techniques have also been applied with the pulp fiber research. This technique could be useful tool to analyze the distribution of certain modifications in cellulose that responses to the ultraviolet light such as aromatic compounds. (Murphy, 2001) Other way to detect the cellulose modifications could be the staining of the modified groups with fluorescent dye. The research articles about this kind of research could not been found from the literature, however.

For better resolution image scanning electron microscope SEM is widely used for the surface visual characterization of the modified fibers. Many chemical modifications may be ensured from the SEM pictures. For more detailed image from the surface of modified fibers or cellulose based materials (films *etc*.) can be achieved with the atomic force microscopy (AFM).

3.2.3 Absorption of water and grease

The measurement of the water absorption capacity is important analysis method for all kind of cellulosic materials because the water absorption is vital property for many end products like the tissue papers and hygienic products. Standardized procedures have been developed to determine the absorption capacity of the different cellulose based materials such as the tissue papers, non-woven and SAP and SAF materials.

The water absorption capacity of the fluff pulp can be tested according to SCAN-C 33:80 test. The test was developed by Scandinavian pulp, paper and board testing committee and it is widely used among Scandinavian fluff pulp producers like UPM RaumaCell. The water absorption capacity of the tissue papers and tissue products can be tested with ISO 12625-8:2010 method.

Zohuurian-Mehr (2008) have described three test methods to determine the absorption capacity of SAP and SAF materials: tea bag, centrifuge and sieve methods. In the simplest tea bag method the SAP sample is placed on fine meshed tea bag made from acrylic or polyester gauze with sample initial weight of w_0 = 0.1-0.3g. The bag is dipped into water for one hour and excess water is removed by hanging. The wet sample is weighted (= w_1) and the absorption capacity S_e can be calculated from **Equation 3.3**:

$$S_e = \frac{w_1 - w_0}{w_0} \tag{3.3}$$

Other standardized tests for the petroleum based SAPs in the hygiene products are further described in standard ISO 17190 series. For the non-wovens, ISO 9073-6:2000 describes proper test method for the determination of the water absorption capacity. There is also available test method WSP 010.4 R3 (12) developed by European Disposables and Nonwovens Association (EDANA) for the oil and fatty liquid absorption of the non-woven material.

3.2.4 Elemental analysis

The elemental analysis can be used to determine the DS of the modified cellulose or it can be used as a tool for analyzing the amount of the adsorption of certain compound onto cellulose. One restriction for the DS determination is that the substituent have to contain the element that does not occur naturally in cellulose such as nitrogen or sulfur. The elemental analysis gives the amount of the elements, usually carbon, hydrogen, nitrogen, sulfur and oxygen, as a weight percentage. When the structure of the starting compound and product is known the DS can be calculated from elemental analysis data. The elemental analysis does not provide accurate data if the concentrations of the substituents are under limit of

detection (LOD) values. The heterogeneity and moisture content of the sample also affects highly on the outcome of the elemental analysis.

Other compounds such as metals can be analyzed with the atomic absorption spectrometer (AAS) directly from the solid samples. AAS can be used for example to determine how much metal is adsorbed onto cellulose. Other way to estimate the amount of the adsorbed metal ion is to measure the metal ion concentration in solution before and after the adsorption. Metal ions can be detected from liquid media with different techniques like UV/Vis, AAS or ion coupled plasma spectrometer (ICP).

3.3 Development of analytical methods

The development process of the quantitative analysis usually consist of following steps: Setting the goal for the analysis, a selection of a suitable pretreatment method, the test of selectivity and linearity of the method, the determination of limit of detection and the limit of quantitation (LOQ) and testing the method. If the testing shows appropriate results the method should be validated. (Thompson *et al*. 2002)

Various factors such as the baseline correction and other spectra treatment methods affects highly on the outcome of the FTIR analysis. The effect of these procedures is optimized and the standard procedures in the sample and spectra handling are be proposed. Some main aspects of the different calibration methods are also discussed.

The experimental part of the thesis is focused on developing the quantitative analysis method with FTIR for DS determination of the modified pulp samples. The DS is proportional to the concentration of the attached groups at the surface of the fiber and on that account, it should have linear correlation to the peak height ratios of characteristic peaks in FTIR.

3.3.1 Sample preparation

Depending on the sample, the proper preparation should be carried out before the analysis. For example removing the excess amount of the polymers or other impurities from the wet pulp sample by washing or extracting with the proper solvent might be necessary. The excess monomers from the grafting or other impurities might cause the false signals to FTIR spectrum. The proper washing is necessary also to remove the non-adsorbed species from the pulp.

The solid pulp sample with the minimal preparation for the FTIR-ATR technique is advantageous. However, the water content in the pulp should be minimized or set to constant level. The drying can be done in oven, in normal pressure or in vacuum. Commonly

used temperature range is 40–100 °C and time varies from couple of minutes to hours. The freeze drying or vacuum drying are also alternatives. After drying the temperature of the sample should be lowered to room temperature by placing it to a desiccator. In some cases the desiccator alone is an adequate drying method.

3.3.2 Selectivity and linearity

The FTIR analysis measures the amount of absorbed infrared light by different functional groups at certain frequencies. In the case of modified pulps it is essential to figure out whether the signal in the FTIR apparatus is caused by the covalently bonded side group of the pulp fibre or the unbounded reagent. This can be done by comparing the IR spectra of pure reagent and the modified pulp. The functional groups in covalently bonded side group gives a signal at different wavenumber than the unbounded reagent.

The characteristic frequencies needs to be identified to describe the wanted functional group. The peak height should have a linear correlation with the concentration, or in this case the DS, if the peak is caused by the attached functional group of the fibre. To identify the analytical working area the linearity should be tested with a sample group with different DS values. The correlation is linear only at certain concentration area.

The peak height measurements should have certain amount of the reference measurements to overcome the heterogeneity of the samples. The error for the reference samples can be estimated with the expanded uncertainty U for 95 % confidence interval given in **Equation 3.4**:

$$U = \frac{2\sigma}{\sqrt{n}} \tag{3.4}$$

Where σ Standard deviation of reference samples

n Number of reference samples

The relative expanded uncertainty U_r can be calculated from the Equation (3.5)

$$U_r = \frac{U}{\bar{n}} \times 100 \tag{3.5}$$

Where $\bar{n}$ Average of reference samples

3.3.3 Determination of detection limits and quantitation limits

The determination of LOQ and LOD are necessary to determine for the quantitative analysis. LOD refers to the smallest concentration value, or in this case DS value, that can be detected with the applied analytical method. LOQ refers to the smallest concentration

value when the quantitation with the statistical uncertainty level is possible. Various methods like visual evaluation, signal to noise ratio and determination of LOD and LOQ from standard deviation of response and slope are widely used and accepted. (Shrivastava & Gupta, 2011)

The signal to noise ratio is used very often with the chromatographic methods. The signal of the analyte is compared to the surrounding measurement noise. The highest intensity of the noise can be measure by using the peak-to-peak value which indicates the difference between the highest and lowest value of the noise. The signal to noise ratio of 3:1 is usually used for LOD and 10:1 is used for LOQ. This can be tested with sample series of increasing concentrations and evaluate where the signal exceeds the calculated value for signal height. The signal to noise can be calculated from the **Equation 3.6** by Shrivastava & Gupta 2011**:**

$$S/N = \frac{2H}{h} \tag{3.6}$$

Where H Signal height of the analyte

h Peak to peak value of the noise

LOD and LOQ can be determined from the regression line with the **Equation 3.7** (Shrivastava & Gupta, 2011):

$$LOD\ (LOQ) = \frac{F*SD}{b} \tag{3.7}$$

Where F Constant factor. 3.3 for LOD and 10 for LOQ

SD Standard deviation of the blank or ordinate intercept or residual standard deviation of the linear regression

b Slope of the linear regression (sensitivity)

This is a very useful way to determine LOD and LOQ from the regression line of the calibration curve and it can be applied with all methods. This method gives good estimation in the case where signal to noise ratio is difficult to determine due to lack of small concentration samples. The values for standard deviation can be obtained from the regression analysis. However, the accuracy of these values need to be tested if the method is to be validated.

3.3.4 Baseline correction

The baseline correction of the IR spectra is important to carry out for the quantitative analysis. The correction have significant effect especially in the single peak measurements. The baseline correction is usually done for absorbance spectra. The baseline can be corrected by either automatically or manually. The automatic correction might be good alternative in some cases but the manual correction enables similar correction for every spectra. The identical baseline correction is vital due to its direct effect on the obtained value. The basic idea is to determine the baseline for the spectra in a way that they are converted into the equal level. However, a simple linear baseline correction via certain wavelengths is recommended to ensure the systematic and robust result. Usually the baseline is curved in the fingerprint region of the spectrum (<1500 cm^{-1}) because of the higher penetration of IR light in lower wavenumbers. (Stuart, 2004)

3.3.5 Calibration

The calibration is an essential part for the quantitative analysis. The spectroscopic methods like FTIR have two main calibration routes: a univariate and multivariate calibration. For the multivariate calibrations different methods like classical least squares (CLS), partial least squares (PLS), principal component regression (PCR) and principal component analysis (PCA) are applied for the calibration. Problem with the quantitative analysis of the modified cellulose with FTIR is lack of calibration samples, and a prior knowledge of the heterogeneous organic substances that affect the spectra. For data of this kind, a large calibration set is needed to be able to utilize large wavelength areas. Thus the multivariate approach would require the additional information about the sample matrix and larger calibration set representing the variation. (Leclerc, 2000; Haaland & Thomas, 1988)

The univariate calibration with Lambert Beer's law is suitable method for relatively simple compounds that gives the clear peak at certain frequency area where it does not have overlapping peaks. The simple univariate calibration for FTIR needs isolated band in spectra. The calibration is based on the peak heights or areas that correlates with the compounds concentration in the measured sample. Even the small overlapping of the peaks causes easily error on the univariate calibration because it affects the total absorbance and peak height. Especially the modified pulp fibers gives complex IR spectra and in most cases the univariate calibration does not give the accurate results. In these cases the multivariate calibrations are required. (Leclerc, 2000)

The CLS is a suitable calibration method when the concentrations of more than one component affects the intensity of the examined peak. The CLS method can be used in the

same way as simple Beer's law method by measuring the single peak heights or areas but it can also be used for a certain region from the spectra. The CLS calibration gives a linear least-square regression model between the real and calculated concentration values. The CLS method is weak against detecting impurities in the sample and it is not suitable in the case where the examined peak tend to shift. For very complex spectra where the effect of other components are unknown PLS, PCR or PCA are more suitable methods for multivariate calibration in pulp analysis with FTIR. These methods can be used to detect the presence of impurities and they are more resistant to the peak shifting. (Leclerc, 2000)

II EXPERIMENTAL PART

4 MATERIALS AND METHODS

The chapter describes materials and analytical methods used in the experimental part. The direct chemical structure analysis of the samples is mainly based on FTIR studies that are verified with NMR. Other analytical methods such as TGA, elemental analysis and light microscope were used to produce supporting information about the pulp modification. The availability of the modified pulp samples was limited. Therefore, the complete development process could not be accomplished

4.1 Materials

The modified pulp samples were kindly provided by Technical Research Center of Finland (VTT), and University of Helsinki (UH). In addition, the pulp samples from the UPM's commercial pulp grades were also tested. The modified pulp samples from the University of Helsinki included chlorobetainyl chloride modified cellulose betainate which structure is shown in the **Figure 31**.

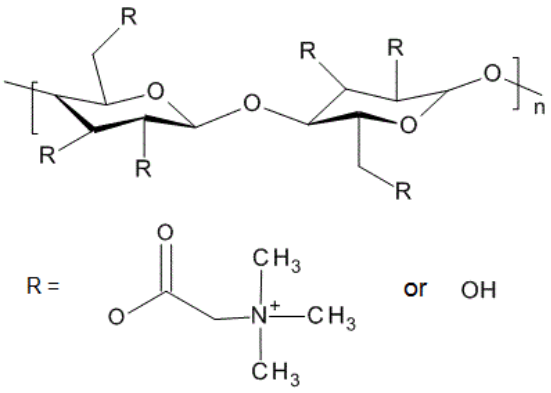

Figure 31. The structure of cellulose betainate

The starting materials for cellulose betainates were dissolving pulps from Domsjö and Borregaard. The cellulose betainate samples were part of a publication by Sievänen, *et al*. (2015). The DS for the cellulose betainates were determined with the elemental analysis and the results were corrected with ^{1}H-NMR results. The DS values of Domsjö cellulose betainate samples were 0.42, 0.59, 1.20 and 1.60. The DS values of Borregaard cellulose betainates were 0.47, 1.05, 1.07 and 1.28.

A sample series of cellulose acetate, which was synthesized from eucalyptus kraft pulp with acetic acid anhydride, was also received from UH. The structure of cellulose acetate is shown in **Figure 32**. The DS of the cellulose acetate was ensured with ^{31}P NMR technique. The DS values of cellulose acetate samples were 0.23, 0.85, 2.76 and 2.90.

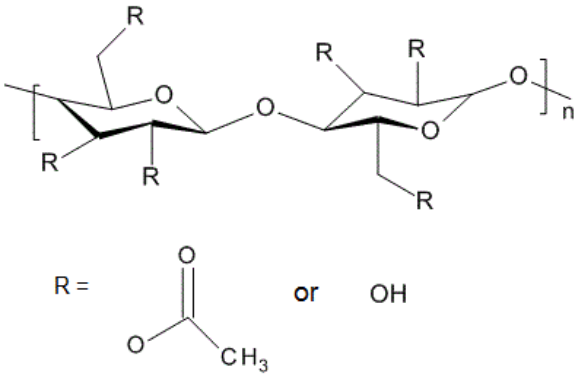

Figure 32. The structure of cellulose acetate.

The raw material in VTT modified pulps was softwood sulfite pulp from Domsjö. The pulp samples were modified by the esterification with palmitic, lauric and acetic acid. The DS of palmitic acid modified pulp samples were 0.2 and 0.8. The DS of acetic and lauric acid esterified pulp samples were 0.7/0.1 and 2.0/0.4. In addition, a commercial grade CMC from CP Kelco with DS 0.8 was used as a reference material in FTIR studies.

The analysis grade acetic anhydride and sodium acetate which were used as a reference for cellulose acetate were purchased from J.T. Baker Chemical Company. The betaine used as a reference for cellulose betainates was purchased from Sigma-Aldrich.

4.2 FTIR analysis

The used FTIR apparatus was Nicolet 6700 FTIR spectrometer equipped with the Smart iTR diamond plate with low pressure ATR bench to ensure the constant pressure of 20 kilobars. The incident angle of the IR beam was 42° and the beam configuration was single bounce. The spectra was analyzed and processed with the Omnic software. 32 scans was collected from the wavenumber area 400-4000 cm^{-1} with the resolution of 4 cm^{-1}. The drying of the samples in desiccator and in oven at 50°C for 24h was tested for the pretreatment.

First step in FTIR analysis was to identify the characteristic frequencies for each samples. From these frequencies the most representative and intense were selected for the peak height ratio measurements. The IR spectra of the modified pulp was also compared to the IR spectra of the applied reagent to determine if the peaks originate from the unreacted reagent or covalently bounded side groups in cellulose.

Five reference samples were recorded from each sample points. The normalization criteria for the good quality spectra was determined so that the highest peak intensity around 1020-1030 cm^{-1} should reach over 0.9 in the absorbance scale. This peak was used as a reference for all samples because it indicates the contact status between sample and ATR crystal. All of the reference spectra were manually baseline corrected with the rubber band method at the wavenumbers 2400, 1800, 1500 1200, 850, 700, 600 and 500 cm^{-1}.

The peak heights were first measured manually, because the increased concentration of the attached group caused the peak wavenumber shifting in some frequencies. Therefore, the automatically determined baseline and peak maximum for the peak height measurement could lead to incorrect results. After the manual peak height determination calibration was done with TQ Analyst software provided by Thermo Scientific. The selected algorithm for the regression was CLS. The frequencies selected for the calibration were those which the peak shifting was found to be minor. The calibration model was compared to manually calculated least squares model. The used software package did not include the PCR or PLS calibration methods which could have been more suitable with the solid samples. The LOD and LOQ was also calculated for the calibration. Some aspects about the determination of the attachment point of the molecule are also discussed. The method development process is summarized in the **Figure 33**.

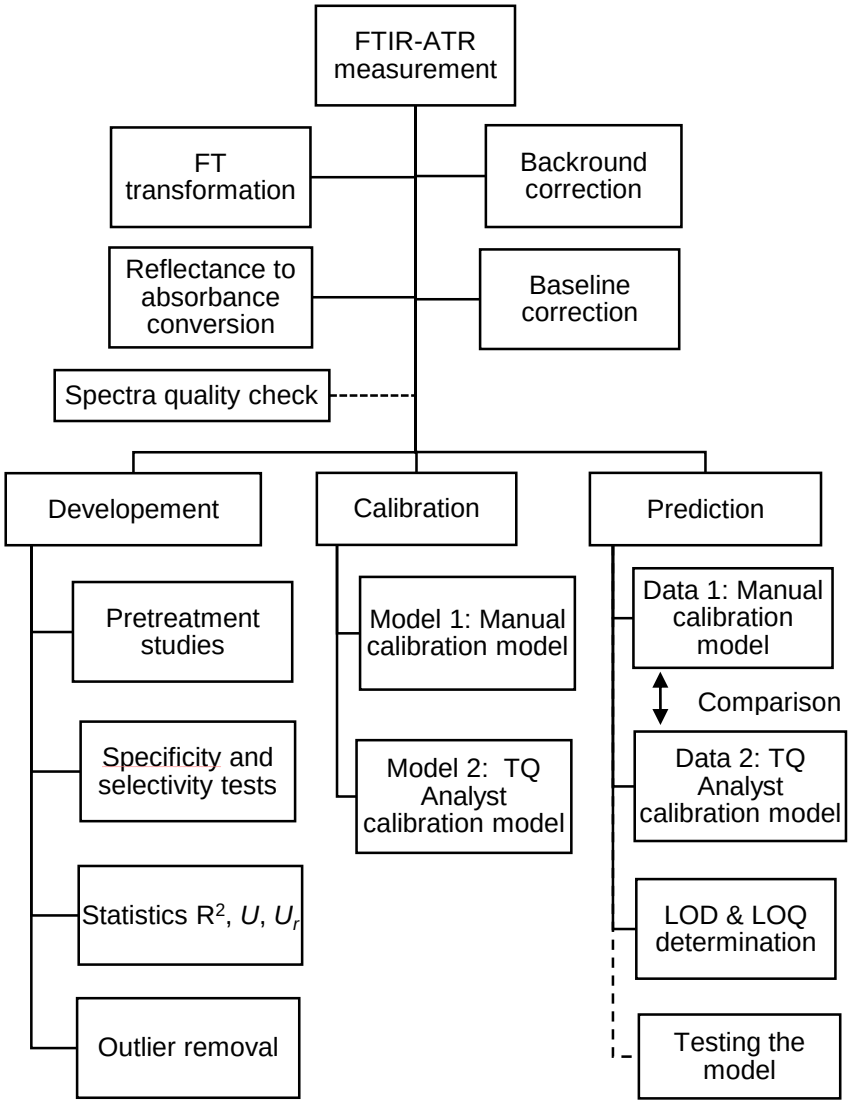

Figure 33. The method development process for FTIR-ATR.

4.3 TG analysis

TGA was performed on the modified pulp samples to examine how different DS effects on the thermal properties of the pulp. The used thermogravimeter was Netzsch TG 209. Approximately 10 milligram of the sample was measured for the TGA. The measurement was conducted by preheating the sample to 50°C and then increasing the temperature 10 °C/min to 600 °C in 20 mL/min N_2 gas flow. The residual sample was burned by increasing the temperature from 600 to 900 °C under 20 mL/min O_2/N_2 gas mixture. The dry solid content of the cellulose betainates were determined from the TGA results at 120 °C.

4.4 Elemental analysis

The CHN and oxygen content of the solid pulp samples were determined with Flash 2000 series elemental analyzer from Thermo Scientific. The determinations were conducted according to ASTM D5291 and D5622 standards and the sampling amount was approximately 2 milligrams. The samples were homogenized in the mortar. Two reference samples were prepared from each sample. From the elemental analysis results of cellulose betainate the DS was calculated from the nitrogen content with **Equation 4.1** by Sievänen, *et al*. (2015):

$$DS = \frac{M(cellulose) * N\%}{M(N) + M(H) * N\% - M(substituent) * N\%} \quad (4.1)$$

Where M Molecular weight of specified molecule

$N\%$ Nitrogen content of sample in mass percentage

The results from the elemental analysis were compared to UH result to examine if there is a significant difference between two elemental analyzers.

4.5 Microscopic analysis

The modified pulp samples were visualized with Zeiss Axio Imager M2m optical light microscope. A small amount of the pulp sample was first stained with Graff C color and then applied evenly on the preparation disc with the preparation needles. The water preparation was also used for phase contras images. 100x and 400x magnifications were used for the visual imaging. The purpose of microscopic study was to find out is it possible to visualize how the attached compound is divided along the fiber surface and does the modification have an effect on the fiber structure. The palmitic acid modified pulp fibers from VTT and cellulose acetate samples from UH were used for this study.

5 RESULTS AND DISCUSSION

5.1 FTIR results

This chapter summarizes the method development process for modified pulp analysis with FTIR-ATR equipment. The major steps were pretreatment studies for the sample, test of selectivity of the method by peak identification from the FTIR spectrum, peak height ratio measurements and determination of LOD and LOQ. In addition, the calibration was demonstrated with TQ Analyst software and LOD and LOQ values were determined from the calibration curve.

5.1.1 Pretreatment studies

The main difficulty in FTIR-ATR analysis was to achieve good contact status between the sample and the ATR crystal. The fibrous material such as dried pulp has porous structure and the contact depends much on the sample thickness and the sample area. This problem could be partially overcome by pressing a small amount of the sample alone in the hydraulic press to produce thin and less porous sample plate with higher density. This pretreatment method was used for all modified and unmodified pulp samples. The compression of samples was conducted for one minute under 10 kiloton pressure.

The effect of different drying methods to the modified pulp samples were studied in the desiccator and in 50 °C oven for 24. The effect of the drying of VTT reference pulp sample is demonstrated in the **Figure 34**. The most significant changes in the spectra can be noticed in the OH stretching area around 3335 cm^{-1} and in OH bending area near 1640 cm^{-1}. Otherwise the spectra remains unchanged.

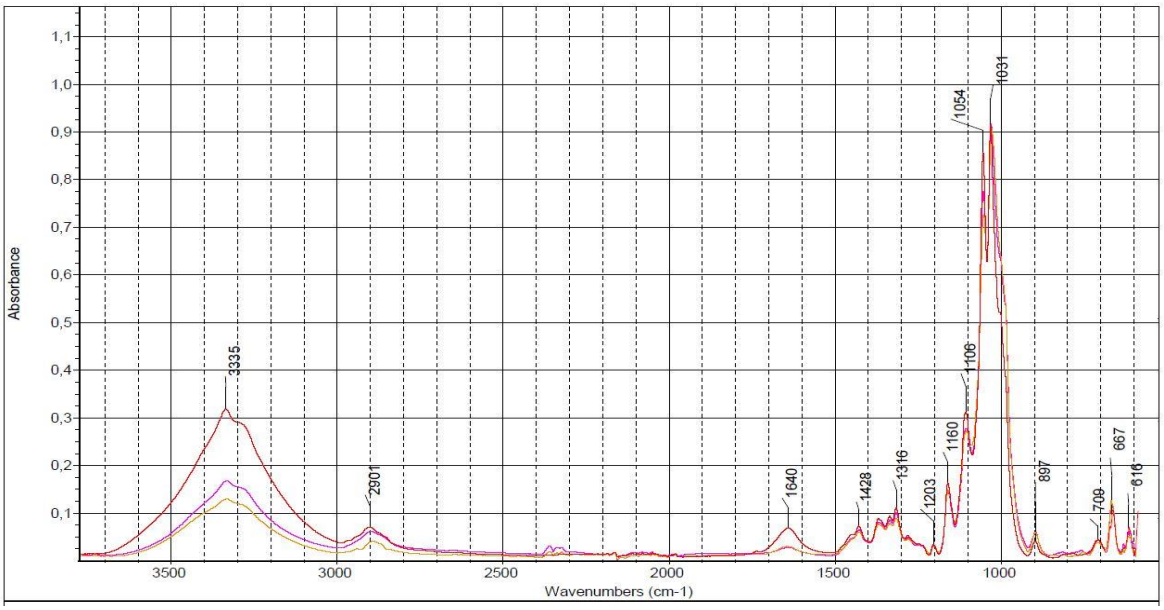

Figure 34. The Effect of different drying methods on VTT reference pulp samples. The IR spectra of undried (red), 24h desiccator dried (violet) and 24h oven dried in 50 °C (yellow).

Too long drying in oven caused chemical change in some modified pulp samples. For example cellulose betainate showed significant change in the chemical structure after 4 days drying in 50 °C oven. The results in IR spectra are shown in **Figure 35.**

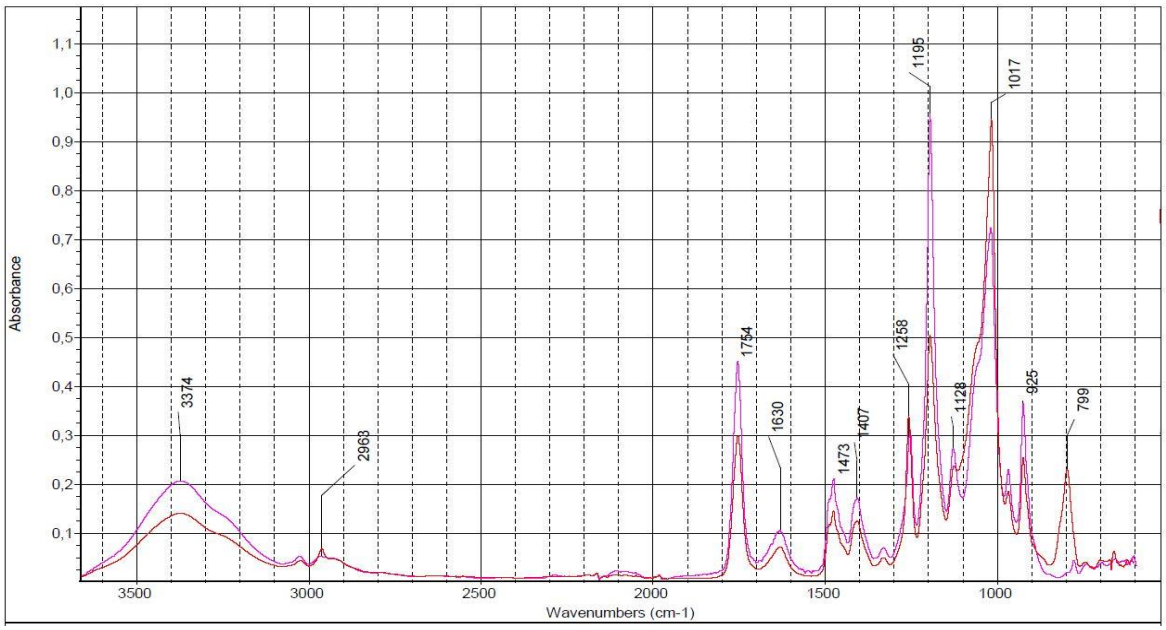

Figure 35. The effect of oven drying on Borregaard cellulose betainate. The spectra of undried cellulose betainate DS 1.28 (violet) and 4 day oven dried in 50 °C (red).

The figure shows significant loss of intensity in various wavenumbers: 1754, 1473, 1407 and 1195 cm^{-1}. These wavenumbers are all associated to betainate side group. The only increase could be seen at 799 cm^{-1} which origin could not be identified.

For the practical point of view, the minimal drying of modified pulp samples seemed to be the best pretreatment method. If the water seems to distract the analysis, the desiccator drying should be the most suitable drying method because it did not cause any detectable chemical change in the samples.

5.1.2 Peak identification and testing of selectivity

The identification of the characteristic peaks were started from unmodified pulp samples. The IR spectra of UPM commercial kraft pulp grades Betula, Betula TCF, Conifer and Euca are shown in **Figure 36**.

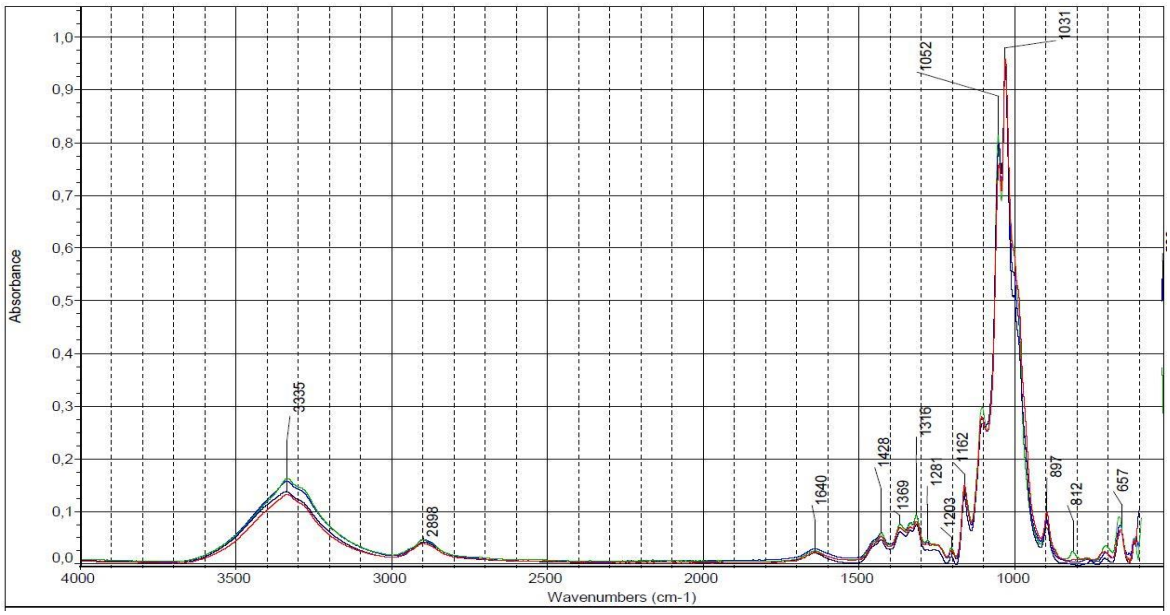

Figure 36. The IR spectra of some UPM commercial pulp grades: UPM Conifer (green), UPM Betula TCF (red), UPM Betula (violet) and UPM Euca (blue).

The figure shows that from the IR spectra no remarkable differences could be detected between different wood species derived kraft pulps. The characteristic group frequencies of cellulose have been listed in the Table 3. Even ECF and TCF bleached pulps does not show any difference for example in region 1700 cm^{-1} where no carbonyl peak could be detected due to oxidized hydroxyl groups.

In addition, the **Figure 37** shows the comparison of Borregaard dissolving grade softwood sulfite pulp and UPM Euca kraft pulp IR spectra. The remarkable finding was that pulping process and different raw material seems to have only very minor effect on the processed pulp IR spectra. This can be explained by the removal of major part of the hemicelluloses and lignin present in raw material during the cooking and bleaching processes and therefore the cellulose in both cases is the major component that effects on the IR spectra.

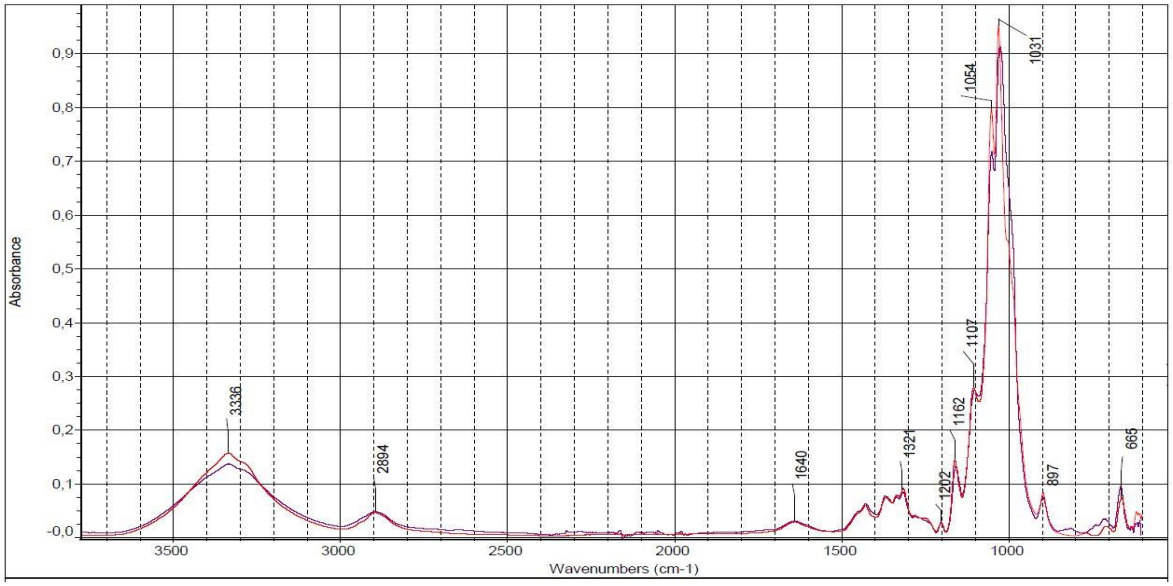

Figure 37. The comparison of IR spectra of UPM Euca kraft pulp (red) and Borregaard softwood sulphite dissolving grade pulp (violet).

The characteristic groups in cellulose betainate can be identified from the **Figure 38**. The new peaks compared to original cellulose can be identify as follows: the weak peak around 3030 cm^{-1} is caused due to N-CH_3 vibration, the medium peaks around 1476 cm^{-1} and 1407cm^{-1} due to asymmetric and symmetric deformation vibration of N-(CH_3)+. The medium and strong peaks at 1253 cm^{-1} and 1198 cm^{-1} are associated to the C-N vibration in CH_2-N-$(CH3)_2$. It was deduced that these two frequencies will apply also for CH_2-N-$(CH_3)_3$ in betainate. In addition, new peak in 968cm^{-1} could be detected due to N-CH_3 asymmetric deformation vibration and quaternary nitrogen stretch. (Socrates, 2001; Ma, *et al*. 2014)

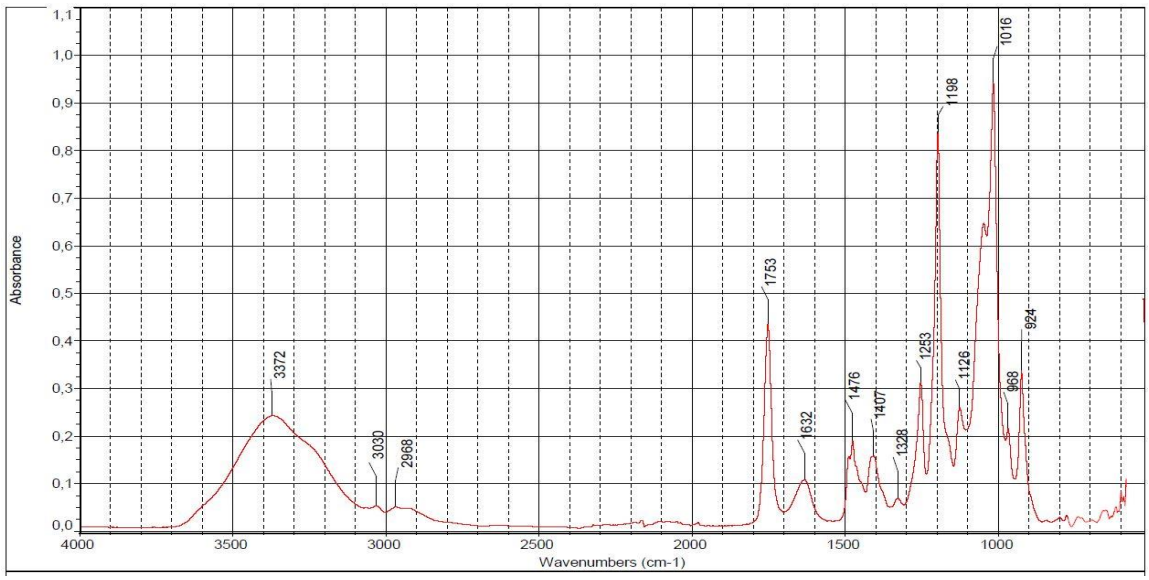

Figure 38. The IR spectra of Domsjö cellulose betainate DS 1.20.

For cellulose betainate the most promising frequencies for the peak height ratio measurements were carbonyl peak around 1750cm^{-1} and two peaks caused by C-N stretch

in 1198 cm^{-1} and 1253 cm^{-1} because they represented the attached compound and had good intensities.

The IR spectra of cellulose betainates was compared to the IR spectra of the pure betainate reagent to exclude the possibility that the certain peaks could be caused by unbounded betainate. The IR spectra of Borregaard reference pulp was also measured in 0.5M betaine solution to find out if the reagent would form hydrogen bonds with cellulose. The comparison is shown in the **Figure 39.**

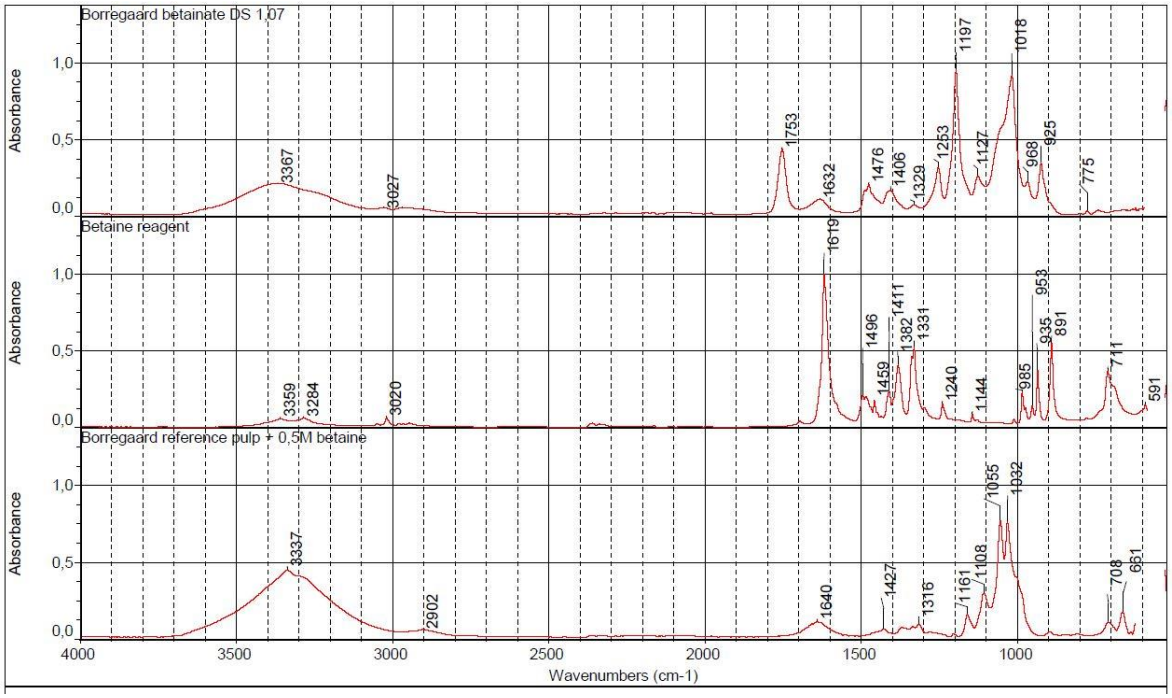

Figure 39. The IR spectra comparison of Borregaard betainate with DS 1.07 pure betaine and Borregaard pulp in 0.5M betaine solution.

The comparison showed that C-N vibration peaks around 1200, 1254 and carbonyl peak around 1750 cm^{-1} are caused by bounded betainate, not by the reagent, while betaine showed no peaks at those frequencies. In addition, the 0.5M water solution of betaine did not show any evidence of formed hydrogen bonds at these wavenumbers. Therefore, these wavenumbers are selected for quantitative studies for DS determination.

The characteristic groups in cellulose acetate could be identified from the **Figure 40**. New peaks could be detected in 1736 cm^{-1} due to the carbonyl stretch, the medium peak around 1370 cm^{-1} caused by the methyl group vibration in acetate, the intense peak around 1230 cm^{-1} due to the C-O stretching in C-(C=O)-CH_3 and the medium peak around 620-580 cm^{-1} due to the acetate C=O wagging vibration. (Socrates, 2001; Sun, *et al*. 2004)

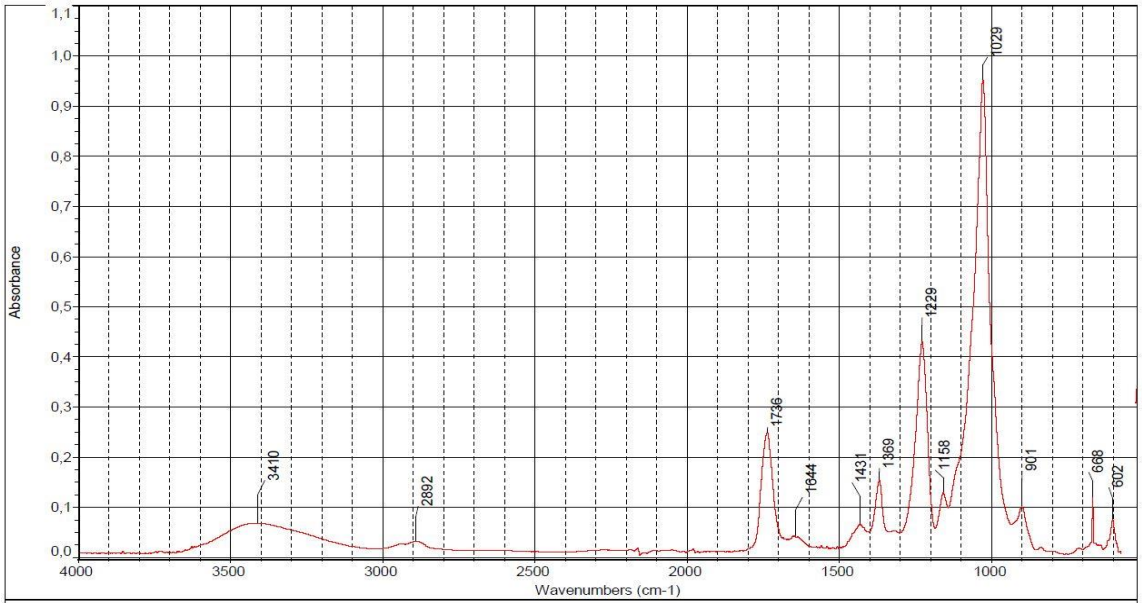

Figure 40. The IR spectra of acetic anhydride acetylated cellulose acetate DS 2.76.

The IR spectra of cellulose acetate was compared to the IR spectra of acetic anhydride and sodium acetate to exclude the possibility that the certain peaks could be caused by the unbounded acetate group or reagent. In addition, the IR spectra of acetic acid and lauric acid modified cellulose from VTT was used to study is it possible to detect impurities with FTIR. The comparison is shown in the **Figure 41.**

The comparison revealed that the carbonyl vibration peak around 1750 cm^{-1} and intensive C-O single bond stretching peak around 1230 cm^{-1} turned out to be the most suitable for the peak height measurements. The dual peak in acetic anhydride spectra at 1822 cm^{-1} and 1752 cm^{-1} is caused by two carbonyl groups in the structure. In cellulose acetate only one carbonyl peak at 1738 cm^{-1} can be detected due to formed ester bond between acetate and cellulose. The C-O single bond stretching peak have shifted to lower frequency from 1224 cm^{-1} to 1215 cm^{-1} which confirms the covalent bonding into cellulose due to increased molecular weight which reduces the absorption frequency.

The methyl group vibration peak at 1370 cm^{-1} appeared at the same wavenumber in cellulose acetate and acetic anhydride IR spectra. It is uncertain whether the peak is caused by the methyl group in unbounded acetic anhydride or the methyl group in cellulose acetate. Therefore, this wavenumber should be used with precautions in the peak height measurement studies.

The comparison of cellulose acetate and cellulose acetate/laurate showed relatively similar spectra. Only some minor shifts could be detected from most of the peaks. The C-O single bond stretch at 1214 cm^{-1} in cellulose acetate had shifted to 1231 cm^{-1} in cellulose acetate/laurate IR spectra.

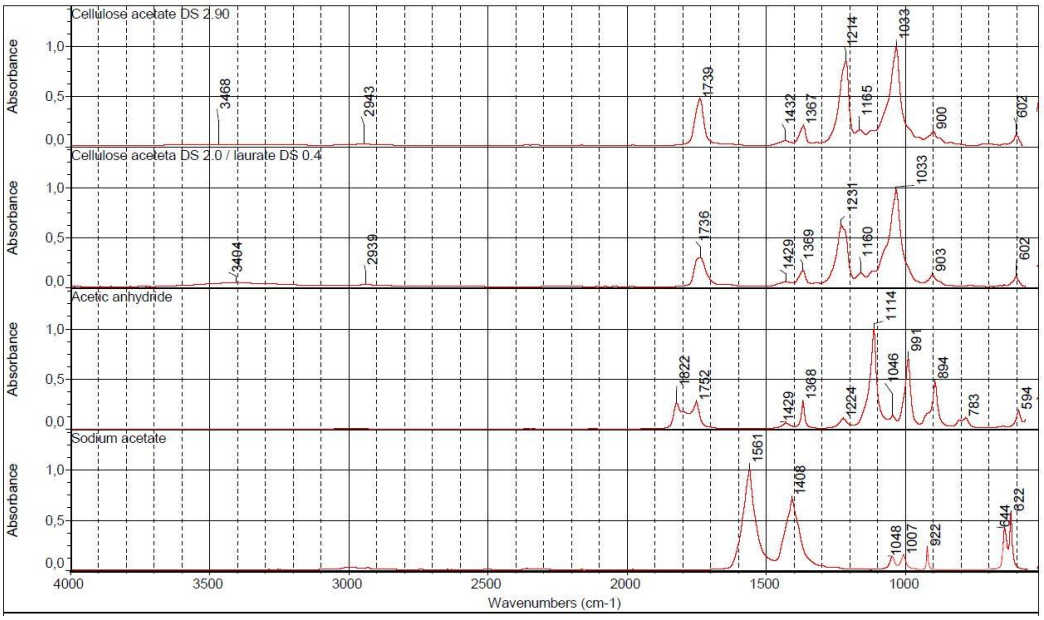

Figure 41. The IR spectra comparison of cellulose acetate DS 2.90, cellulose acetate/laurate DS 2.0/0.4 and acetic anhydride and sodium acetate.

An interesting finding was that no significant signal from CH_2 symmetric and asymmetric stretching caused by lauric acid side group could be detected at the region 2800-3000 cm^{-1} of the spectra. This example showed that one weakness of the FTIR method can be unknown impurities which might not be easily detected from the spectra.

5.1.3 Peak height ratio measurements

The peak height ratio measurements were first conducted manually because increased DS could cause shifting in the measured peak wavenumbers. Therefore, the baseline and peak maximum was determined separately for each DS. The shifting is caused by the attached side groups that increases the molecular mass of cellulose which causes the modified cellulose absorbs IR light at the different frequency as the original cellulose. The applied baselines and the peak maximum frequencies of the cellulose betainate and acetate are listed in the **Table 4** and **5**, respectively.

Table 4. The baselines and peak wavenumbers used in the cellulose betainate peak maximum height measurements. The baselines were determined manually and therefore the given wavenumbers are approximations.

DS	Baselines (approx.)				Peak shift			
	1750 cm^{-1}	1254 cm^{-1}	1200 cm^{-1}	1030 cm^{-1}	1750 cm^{-1}	1254 cm^{-1}	1200 cm^{-1}	1030 cm^{-1}
Borregaard								
0.00	-	-	-	-	-	-	-	1030
0.47	1816-1550	1300-1234	1234-1180	1178-943	1751	1254	1200	1019
1.07	1812-1556	1307-1234	1234-1147	1147-946	1753	1253	1197	1018
1.28	1816-1556	1310-1234	1234-1148	1148-945	1754	1253	1195	1018
Domsjö								
0.00	-	-	-	-	-	-	-	1030
0.42	1814-1563	1300-1234	1234-1177	1177-943	1752	1254	1201	1018
0.59	1816-1556	1298-1235	1235-1178	1178-943	1752	1254	1201	1018
1.20	1812-1558	1307-1234	1234-1146	1146-947	1753	1253	1198	1016
1.60	1820-1560	1310-1234	1234-1147	1147-944	1754	1253	1196	1017

Table 5. The baselines and peak maximum wavenumbers used in the cellulose acetate peak height measurements. The baselines were determined manually and therefore the given wavenumbers are approximations.

DS	Baselines (approx.)				Peak shift			
	1750 cm-1	1370 cm-1	1230 cm-1	1030 cm-1	1750 cm-1	1370 cm-1	1230 cm-1	1030 cm-1
0.00	-	1393-1348	-	1742-856	-	1368	-	1028
0.23	1788-1543	1397-1343	1283-1212	1781-859	1732	1369	1242	1019
0.85	1814-1539	1401-1338	1294-1186	1810-855	1736	1369	1232	1023
2.90	1871-1576	1401-1338	1301-1182	1897-855	1738	1367	1214	1033

The peak ratio calculations from reference samples are shown in the **Appendix V**. The expanded uncertainties and the relative expanded uncertainties calculated from Eq. 3.4 and 3.5 for cellulose betainates are listed in the **Table 6**.

Table 6. The summary of the peak height ratio average, standard deviation, expanded uncertainty and the relative expanded uncertainties of the reference samples of Borregaard and Domsjö cellulose betainates for different DS when the *n* = 5.

DS	$\overline{n}$ (-)	σ (-)	U (±) (-)	U_r (%)
1750/1030 Borregaard				
0.00	0.000	0.000	0.000	0.0
0.47	0.210	0.013	0.011	5.5
1.05	0.355	0.011	0.010	2.8
1.07	0.549	0.022	0.020	3.7
1.28	0.751	0.029	0.026	3.5
1750/1030 Domsjö				
0.00	0.000	0.000	0.000	0.0
0.42	0.224	0.004	0.004	1.8
0.59	0.237	0.010	0.009	3.9
1.20	0.490	0.013	0.011	2.3
1.60	0.684	0.040	0.036	5.3
1200/1030 Borregaard				
0.00	0.000	0.000	0.000	0.0
0.47	0.208	0.036	0.007	15.6
1.05	0.384	0.032	0.008	7.5
1.07	1.010	0.078	0.009	6.9
1.28	1.455	0.050	0.010	3.1
1200/1030 Domsjö				
0.00	0.000	0.000	0.000	0.0
0.42	0.258	0.019	0.017	6.7
0.59	0.214	0.008	0.007	3.4
1.20	0.814	0.039	0.035	4.3
1.60	1.354	0.086	0.077	5.7
1254/1030 Borregaard				
0.00	0.000	0.000	0.000	0.0
0.47	0.092	0.008	0.007	7.5
1.05	0.171	0.009	0.008	4.6
1.07	0.272	0.010	0.009	3.2
1.28	0.364	0.012	0.010	2.8
1254/1030 Domsjö				
0.00	0.000	0.000	0.000	0.0
0.42	0.109	0.003	0.003	2.7
0.59	0.108	0.003	0.003	2.8
1.20	0.246	0.006	0.006	2.3
1.60	0.343	0.018	0.016	4.8

The results from the cellulose acetate peak height measurements are shown in the **Table 7**. The sample series included unmodified pulp sample and cellulose acetate with four different DS values.

Table 7. The summary of peak height ratio average, standard deviation, expanded uncertainty and the relative expanded uncertainties of cellulose acetate reference samples with different DS when n = 5.

DS	$\bar{n}$ (-)	σ (-)	U (±) (-)	U_r (%)
1370/1030				
0.00	0.022	0.002	0.002	7.8
0.23	0.027	0.002	0.001	5.2
0.85	0.067	0.004	0.004	5.5
2.76	0.119	0.006	0.006	4.8
2.90	0.186	0.004	0.003	1.9
1700/1030				
0.00	0.000	0.000	0.000	0.0
0.23	0.025	0.004	0.003	11.8
0.85	0.139	0.011	0.010	7.2
2.76	0.279	0.021	0.019	6.7
2.90	0.496	0.013	0.012	2.4
1230/1030				
0.00	0.000	0.000	0.000	0.0
0.23	0.031	0.003	0.003	8.4
0.85	0.193	0.019	0.017	8.8
2.76	0.432	0.040	0.036	8.3
2.90	0.795	0.021	0.019	2.4

The standard deviation of the cellulose betainate reference samples were relatively low, which caused the relative expanded uncertainty to be in most cases under 5 %. The exception was peak height ratio 1200/1030 cm^{-1} which showed higher relative expanded uncertainties. The standard deviation of cellulose acetate reference samples were a bit higher, but the relative expanded uncertainties remained still mainly under 9 %.

The linear correlation between the DS and selected peak height ratios for cellulose betainates are shown in the **Figures 42-47**.

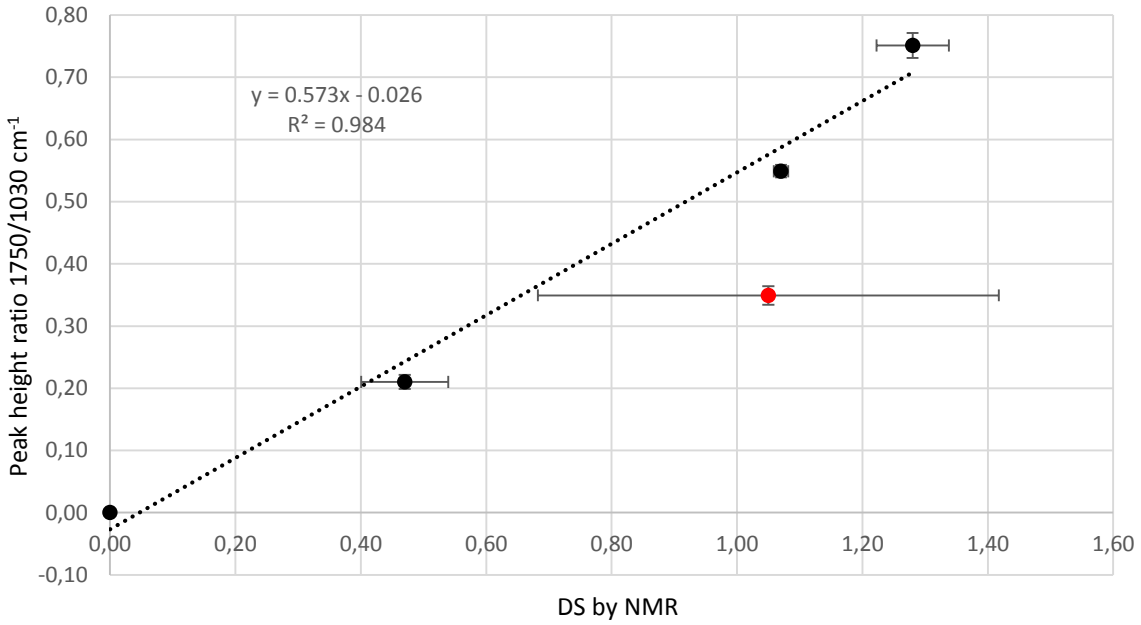

Figure 42. The peak height ratio of 1750/1030 cm^{-1} versus DS of the Borregaard cellulose betainate with 95% confidence interval.

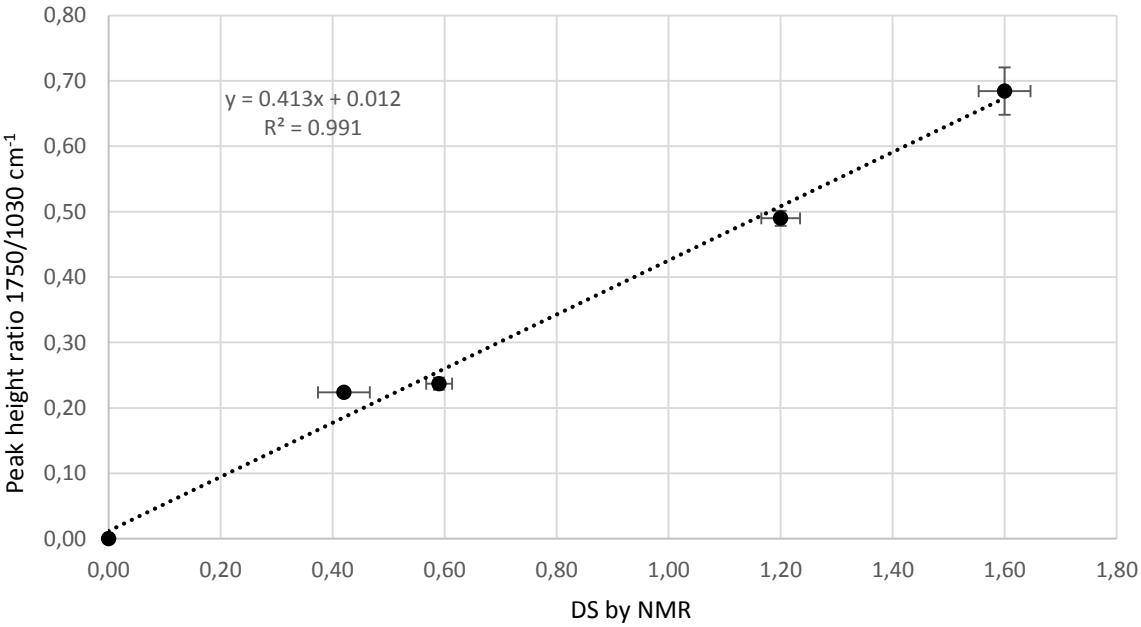

Figure 43. The correlation between peak height ratio of 1750/1030 cm^{-1} and DS of the Domsjö cellulose betainate with 95% confidence interval.

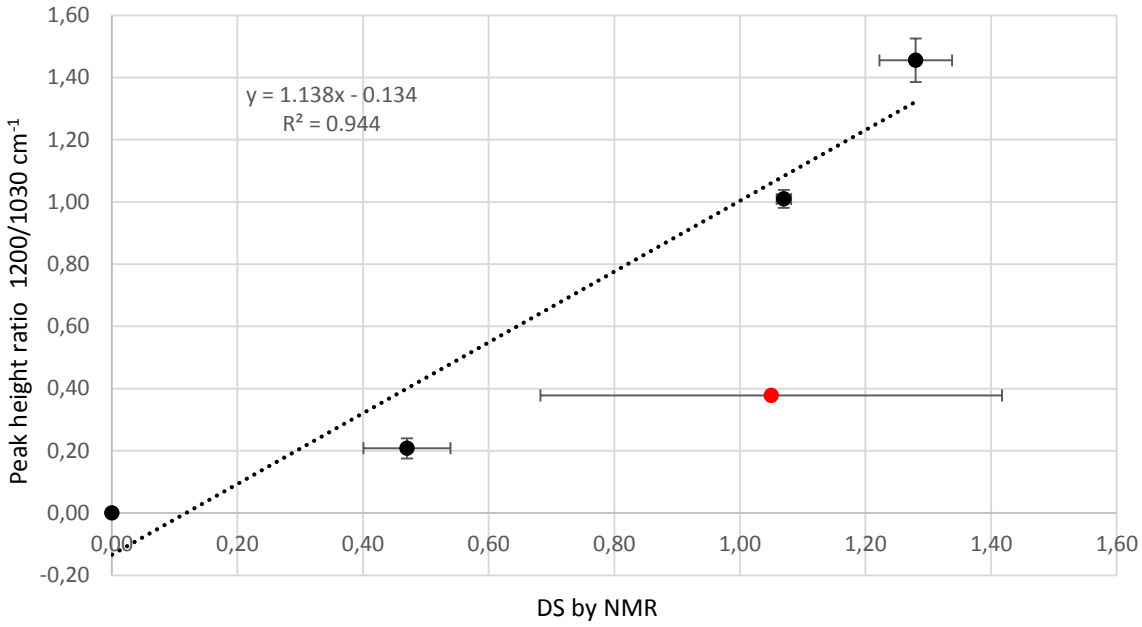

Figure 44. The correlation between peak height ratio of 1200/1030 cm^{-1} and DS of the Borregaard cellulose betainate with 95% confidence interval.

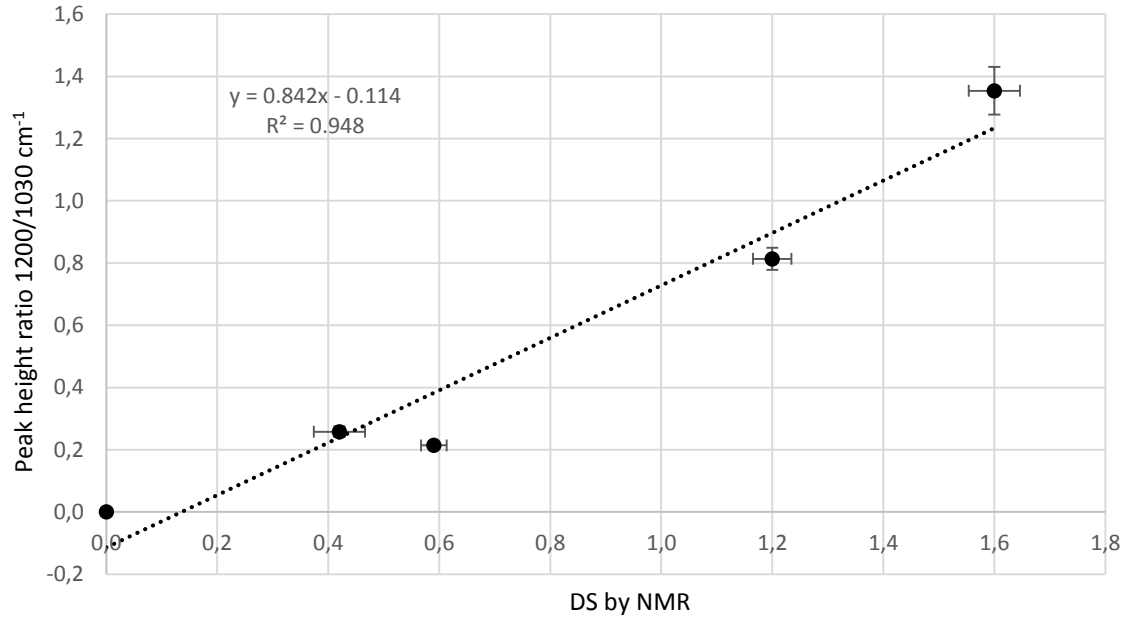

Figure 45. The correlation between peak height ratio of 1200/1030 cm^{-1} and DS of the Domsjö cellulose betainate with 95% confidence interval.

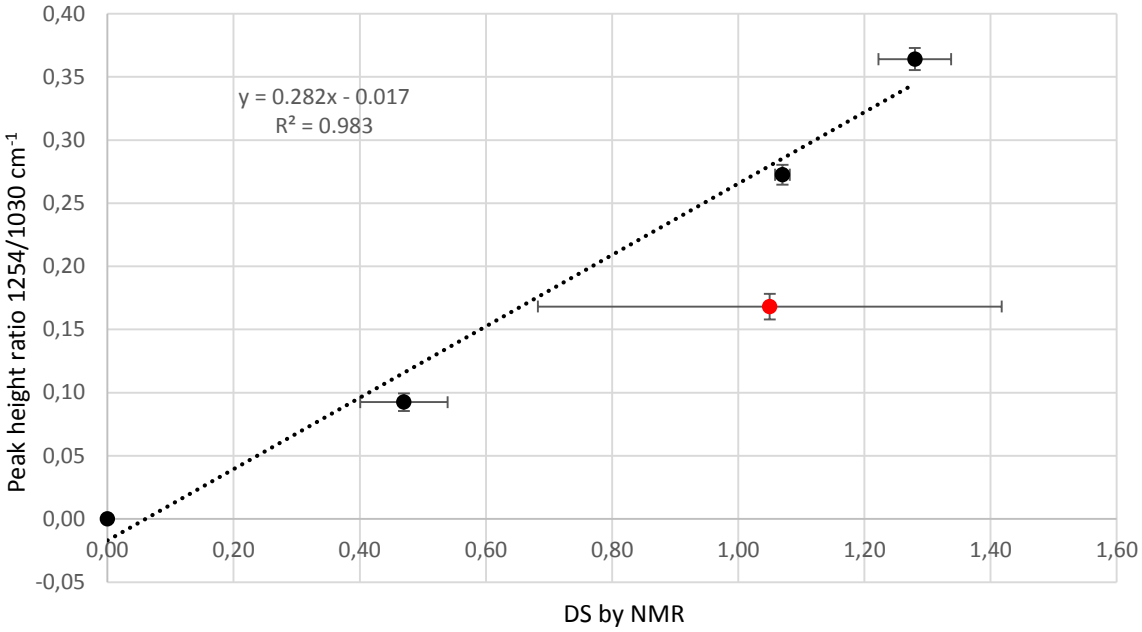

Figure 46. The correlation between peak height ratio of 1254/1030 cm^{-1} and DS of the Borregaard cellulose betainate with 95% confidence interval.

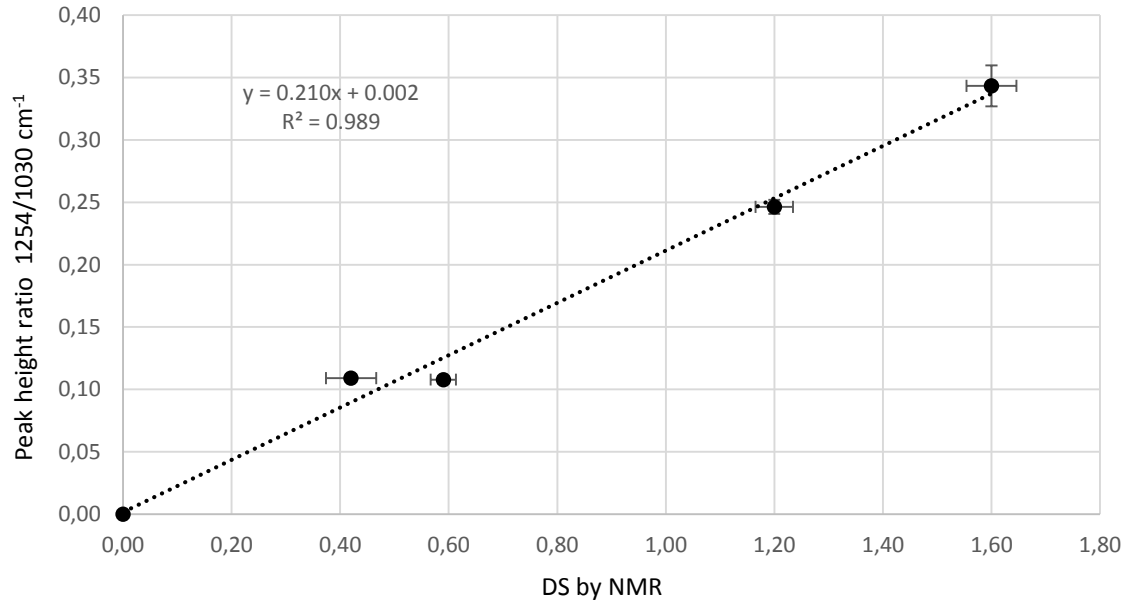

Figure 47. The correlation between peak height ratio of 1254/1030 cm^{-1} and DS of the Domsjö cellulose betainate with 95% confidence interval.

The regression results between DS and the peak height ratios 1750/1030 cm^{-1} and 1254/1030 cm^{-1} showed over 98 % squared correlation for both cellulose betainates. The ratio 1200/1030 cm^{-1} showed instead a lot weaker squared correlation to DS. One explanation for this may be the high intensity of the band 1200 cm^{-1} especially with higher DS where it grows higher than the reference peak at 1030 cm^{-1} as shown in the **Appendix IV**. Due to inaccuracy of this peak height ratio it is leaved out for further studies.

The clear exception in the Borregaard betainate sample series was found out at DS 1.05. This sample point showed very high error in x-axis direction. This is caused by the high standard deviation in elemental analysis described in the article by Sievänen *et al.* (2015). Because of this, the sample point was left out from the study as an outlier.

The error in x–axis direction can be explained with the uncertainty in the elemental analysis and the error in y-axis direction is most likely caused by inhomogeneous distribution of betaine side groups among the pulp. This causes variation in peak heights between the reference samples in IR measurements which increases the error.

The peak height ratio of the selected wavenumbers and DS had also a good correlation with cellulose acetate samples which can be seen from the **Figures 48-50**.

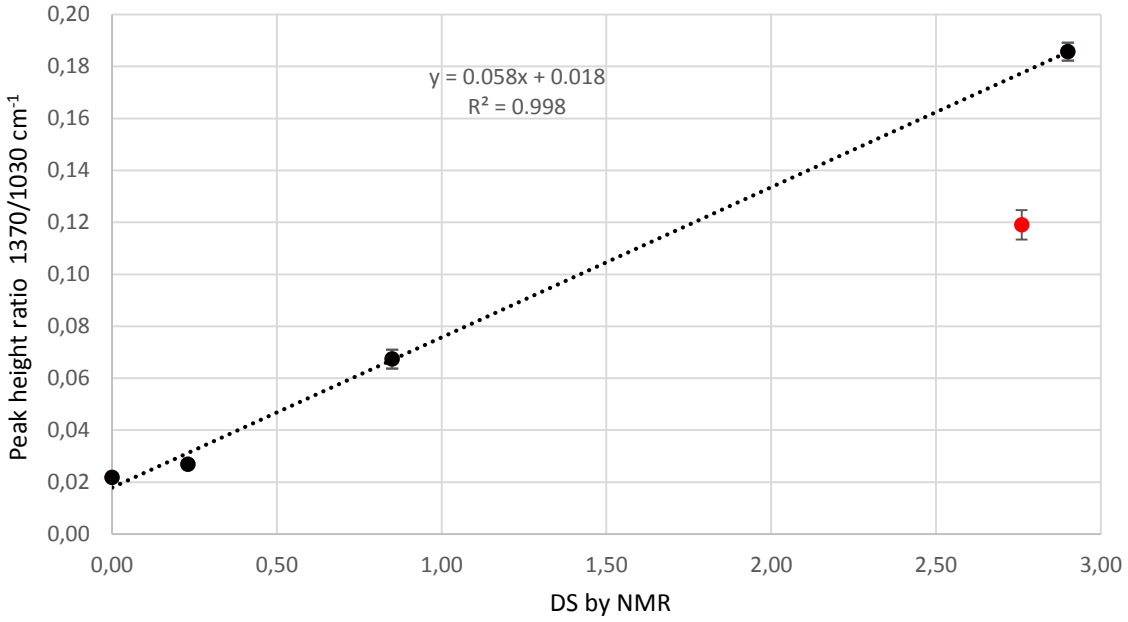

Figure 48. The correlation between peak height ratio of 1370/1030 cm^{-1} and DS of the cellulose acetate with 95% confidence interval.

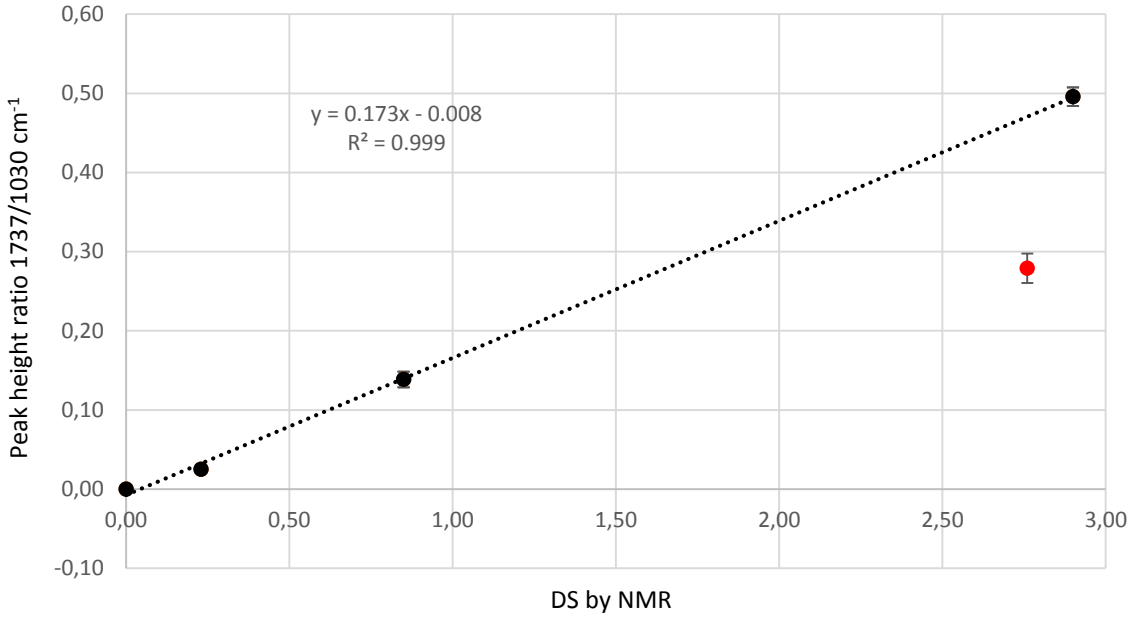

Figure 49. The correlation between peak height ratio of 1737/1030 cm^{-1} and DS of the cellulose acetate with 95% confidence interval.

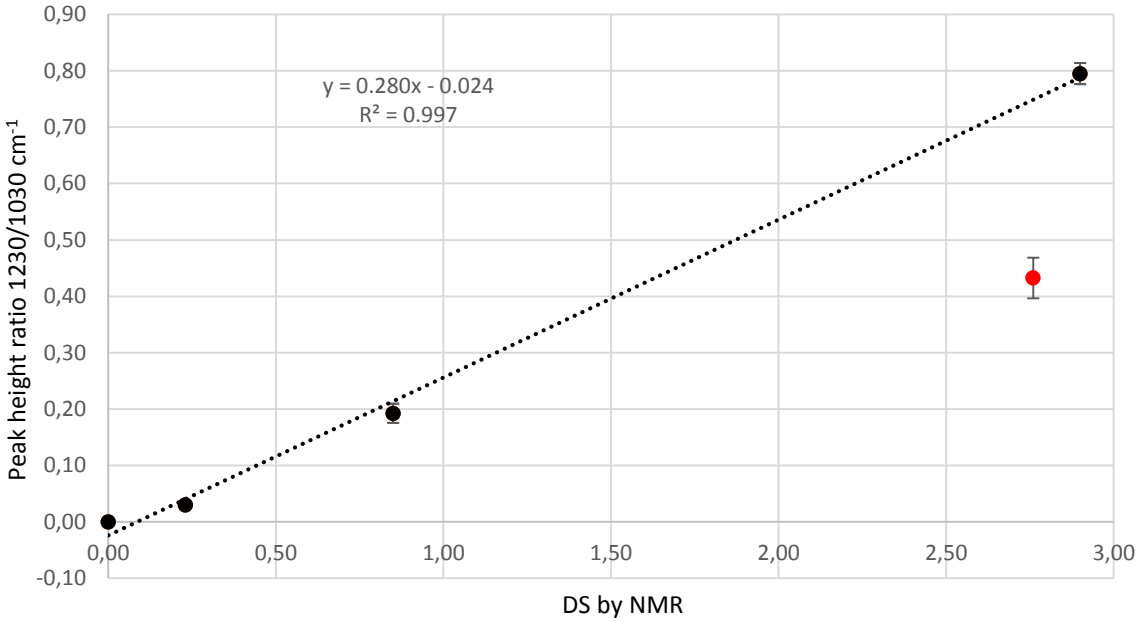

Figure 50. The correlation between peak height ratio of 1230/1030 cm^{-1} and DS of the cellulose acetate with 95% confidence interval.

All of the selected frequencies seems to have relatively good linear correlation with DS. Only clear exception in the sample series was the sample point at DS 2.76 as can be seen from the Figures 42-44. One possible reason for the exception could be unsuccessful ^{31}P-NMR analysis due to the incomplete dissolution of the sample during the sample preparation. Therefore, this point was leaved out from the study as an outlier.

However, the sample series of cellulose acetate had only few sample points and there were no samples from the DS region 1-2.5. Therefore, reliable conclusions about the linear correlation throughout the whole region could not be done based on the available data.

5.1.4 Demonstration of calibration

The calibration was demonstrated on Domsjö cellulose betainate with the manually calculated regression model and with TQ Analyst software. Domsjö cellulose betainate was selected for demonstration because the sample points covered wide DS area. The calibration example was done for the peak height ratios of 1750/1030 cm^{-1} from the same spectra that were used in the manual peak height measurements. The LOD and LOQ values were also determined from the manually calculated regression model.

The calibration was manually determined with Excel by comparing the DS values from NMR analysis and the DS estimations calculated with the regression line equation from the Fig. 43. The squared correlation and RMESC was received from the regression analysis. The manually determined regression model for all reference samples and average values is shown in the **Figure 51**.

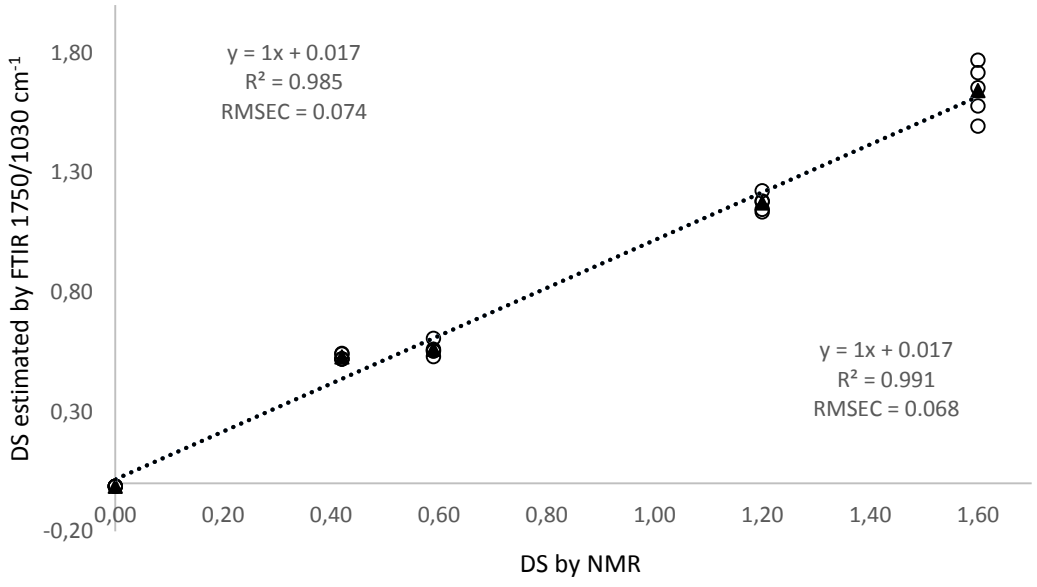

Figure 51. The correlation and RMSEC of the manually determined calibration model for the peak height ratio 1750/1030 cm^{-1} of Domsjö cellulose betainate. The open squares (upper equation) for the reference samples and filled triangle (lower equation) for the average values are shown.

The LOD and LOQ were determined with the method based on the regression line. The LOD and LOQ were calculated for the regression model based on the average values of the reference samples of Domsjö cellulose betainate shown in Figure 51 with Eq. 3.7. The

standard deviation of the y-intercept and slope of the regression line was obtained from the regression analysis conducted with Excel data analysis tool. The results from the regression analysis is shown in the **Appendix VI**.

The calculated LOD value was 0.169 and LOQ value 0.512 which are visualized in the **Figure 52**. The calculated LOD values are below the smallest DS value sample point which was in this case 0.42. LOD value could be tested with sample which DS is close to calculated LOD value. If the signal response in IR spectra would be clearly detectable the LOD value could be validated. However, this could not be conducted due to lack of suitable samples.

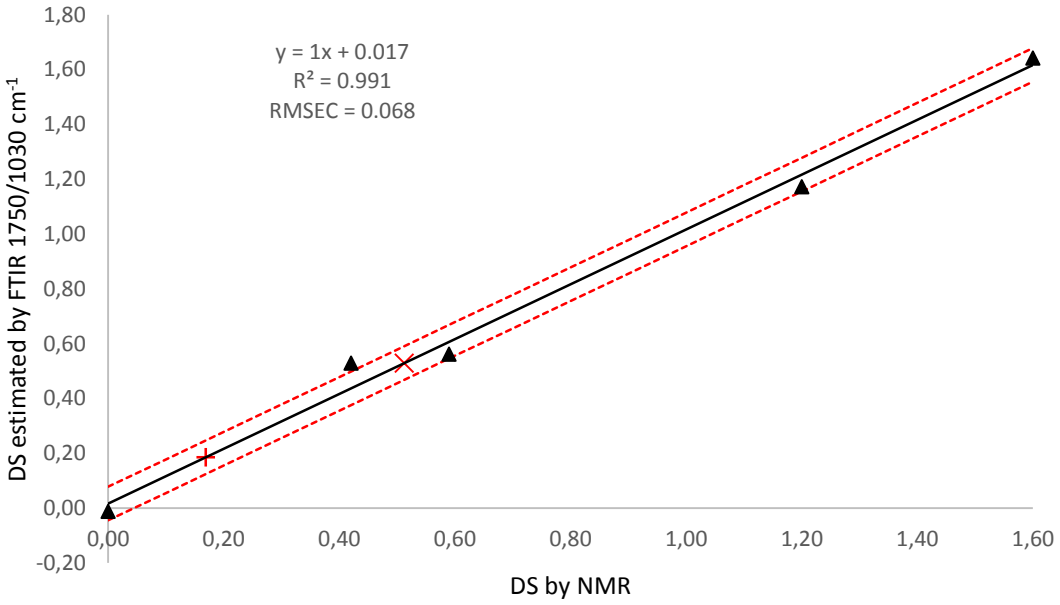

Figure 52. The LOD and LOQ values of manually calculated regression model for peak height ratio 1750/1030 cm^{-1} of Domsjö cellulose betainate. Used values are averages of the measured. (-) = 95 % confidence interval, (+) = LOD and (×) = LOQ

The visual estimation from the Figure 52 shows that the DS values exceeding the LOQ value seems to behave linearly. Due to small number of calibration samples the determination of linear working area remains uncertain. In some cases the constant F used for LOQ in the Equation 3.7 is 6, which would result lower LOQ value to betainate. The additional samples would be essential to confirm empirically the linearity of the working area or reliability of LOQ value.

The calibration was also demonstrated with TQ Analyst software. The used peak maximum values were 1017 cm^{-1} for the reference and 1753 cm^{-1} for the carbonyl peak. The corresponding baselines were 1234-944 cm^{-1} and 1846-1548 cm^{-1}.

The quality of the calibration model TQ Analyst program could be estimated by the correlation coefficient and root mean squared error of calibration (RMSEC) which is the

standard error of the regression model. The calibration model from TQ Analyst is shown in the **Figure 53**.

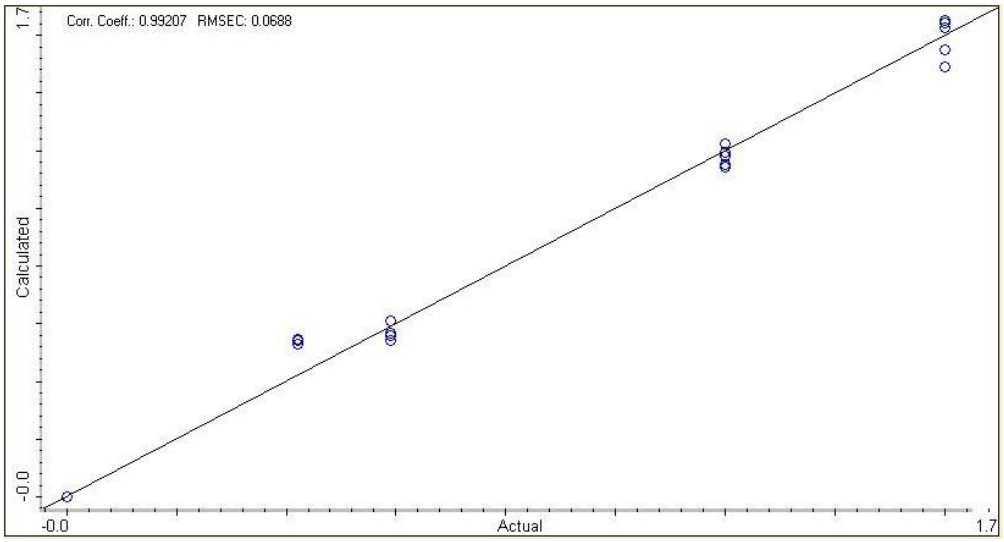

Figure 53. The correlation and RMSEC of calibration model created with TQ Analyst software for 1750/1030 cm^{-1} of Domsjö cellulose betainate.

The calibration model obtained by TG Analyst showed a bit higher correlation and slightly lower RMSEC values than manually calculated regression model in Figure 50. Almost the same correlation and RMSEC values could be achieved by using the average values of the reference samples as shown also in Fig. 51**.** However, the correlation alone does not provide reliable evidence about the accuracy of the calibration model. Both model reveal similar lack of fit at the lowest DS values. For the repetitive analysis the software based calibration would be better choice due to its ease of use.

5.1.5 Visual estimation of the point of attachment

As discussed in the Chapter 3.1.1 the hydrogen bonds formed by the differently oriented hydroxyl groups in cellulose gives the IR signal in the frequency region of 3600-3000 cm^{-1}. The hydrogen bonds formed by the hydroxyl groups at C6, C3 and C2 gives the IR response at 3230-3310, 3340-3375 and 3410-3460 cm^{-1} respectively. The modification of cellulose causes degreasing of these peaks, because of the attachment of certain functional group to hydroxyl group breaks the hydrogen bond associated to this certain hydroxyl group. This wavenumber region is nonetheless inaccurate because of the response peaks are broad and many compounds such as water affects at the same area. However, some visual estimation of the point of attachment based on the peak shape was done with ester bonded cellulose acetate and ether bonded CMC shown in the **Figure 54**.

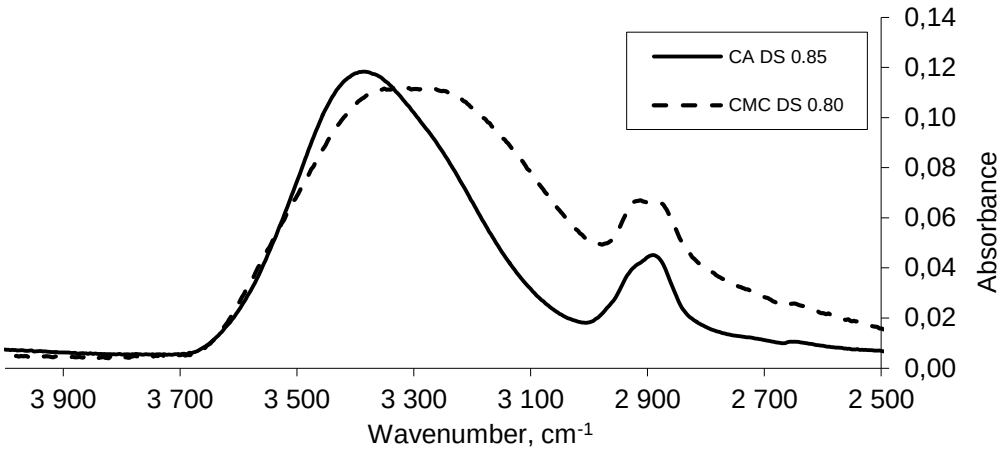

Figure 54. The comparison of OH peaks of cellulose acetate DS 0.85 and CMC DS 0.80

The comparison shows that ester bonded cellulose acetate produces substantially narrower peak at 3230-3310 cm^{-1} which indicates the attachment of acetate group mainly at C6. This supports the fact that ester bond is formed more likely to primary than secondary alcohol. The ether bonds in CMC are more likely formed with OH groups at C2 and C3 and the OH peak at corresponding frequencies have decreased more than in the case of the esterification. The **Figure 55** shows the decreasing OH peak with increasing DS.

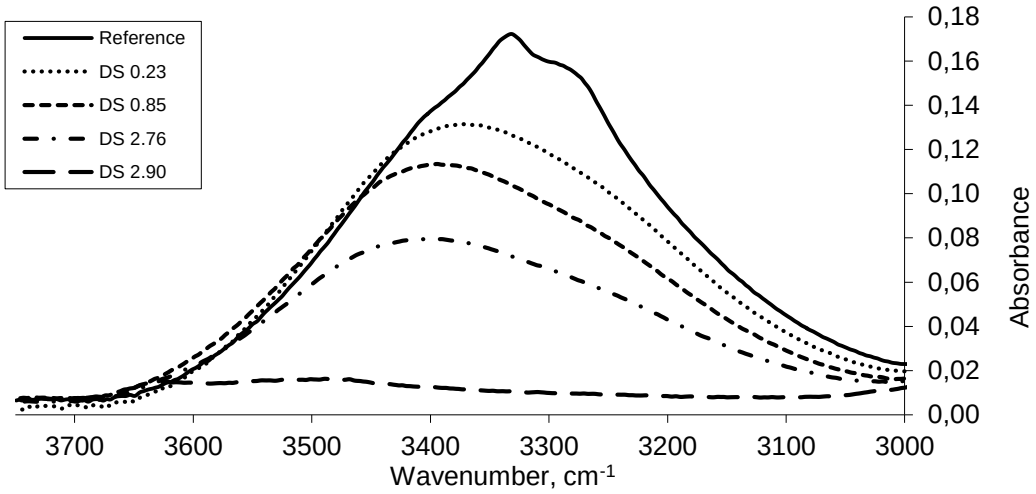

Figure 55. The OH peak of reference eucalyptus pulp and cellulose acetate with different DS.

The peak shifting on the higher wavenumber direction of cellulose acetate supports also the fact that esterification reaction with cellulose happens preferably on the primary alcohol at C6. The visual examination of wavenumber region 3000-3700 cm^{-1} of the modified fibers with different DS might give the general information about the attachment point in cellulose. However, the method is only a rough estimation and any accurate conclusions based on the visual examination may not be done.

5.2 TGA results

The degradation of the selected modified pulp samples was studied with TGA. The aim of the study was to examine how different modifications with the different DS effect on the thermal behavior of the pulp. The TGA curve of palmitic acid modified sulfite dissolving pulp is shown in the **Figure 56.**

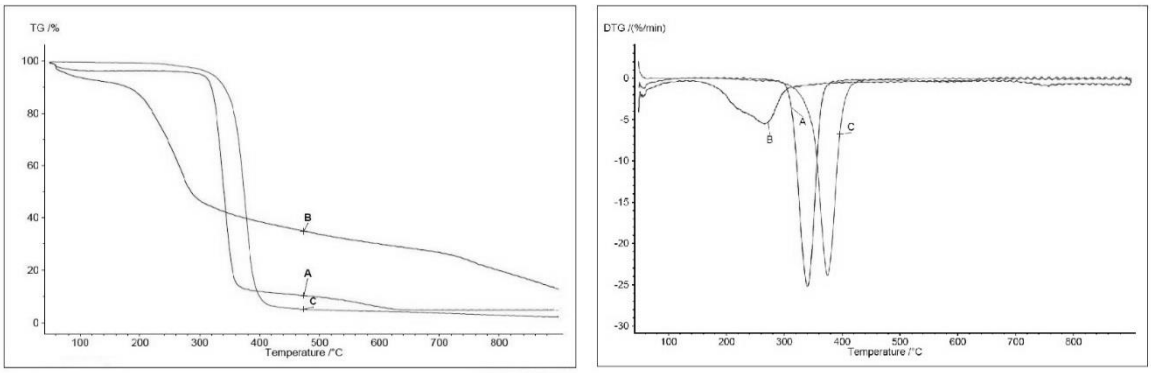

Figure 56. TGA and DTG results of palmitic acid modified sulphite pulp. A) Unmodified pulp fibre, B) palmitic acid modified pulp DS 0.2, C) palmitic acid modified pulp DS 0.8. The samples are preheated in 50 °C and temperature is increased 10 °C/min in nitrogen atmosphere to 600 °C. After 600 °C the oxygen is added and the residual sample is heated to 900 °C under 20 mL/min O_2/N_2 gas mixture flow.

The thermogravimetric analysis gave interesting results for palmitic acid modified pulp. The modified pulp with DS 0.2 started to degrade about 150 °C lower temperature than original pulp. The higher DS increased the degradation temperature of the modified pulp fibre compared to the unmodified pulp. The thermal properties of the modified pulp showed the great variance with increasing DS. Therefore, the characterization of the degradation products based on the TGA curve was found to be difficult. TGA results of lauric and acetic acid modified pulp is shown the **Figure 57**.

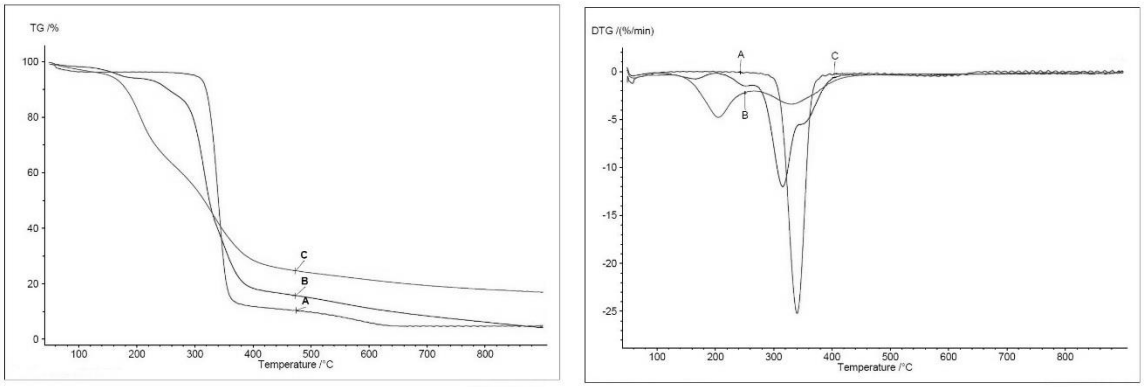

Figure 57. TGA and DTG results of lauric and acetic acid modified sulphite pulp. A) Unmodified pulp fibre, B) lauric/acetic acid modified pulp DS 0.1/0.7, C) lauric/acetic acid modified pulp DS 0.4/2.0. The samples are preheated in 50 °C and temperature is increased 10 °C/min in nitrogen atmosphere to 600 °C. After 600 °C the oxygen is added and the residual sample is heated to 900 °C under 20 mL/min O_2/N_2 gas mixture flow.

The TGA and DTG results showed that clear degradation of the fibre structure could not be detected with higher DS. The degradation of cellulose fibre takes place around 350 °C which could be detected from the TGA curve of the original pulp in the Fig.57. The increasing DS interferes the hydrogen bond network in cellulose molecules while less OH groups are available to form hydrogen bonds. It is possible that this causes cellulose molecules to degrade with a wider temperature region. The characterization of the attached acetic and lauric group based on the TGA results turned out to be really challenging.

The TGA and DTG results of the Domsjö cellulose betainate with different DS is shown in the **Figure 58**. The degradation of cellulose betainates seems to behave relatively similar with increasing DS. The results showed that the major degradation takes place around 200 °C. The interesting finding is that the residual mass after heating remains relatively high, around 20 % with all betainate modified fibres. As in the previous cases, the accurate characterization based on the TGA results was also found out to be difficult.

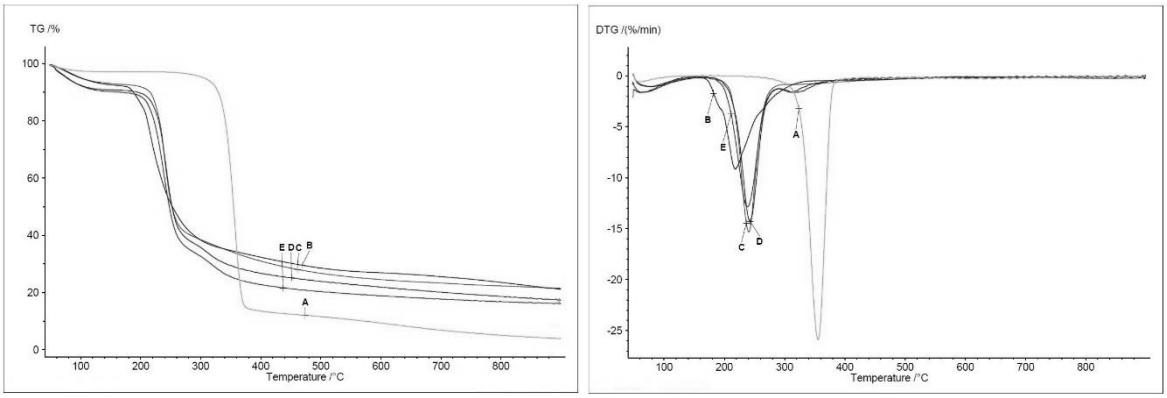

Figure 58. TGA and DTG results of Domsjö cellulose betainate. A) Unmodified pulp fibre, B) DS 0.42, C) DS 0.59, D) DS 1.20, E) 1.60. The samples are preheated in 50 °C and temperature is increased 10 °C/min in nitrogen atmosphere to 600 °C. After 600 °C the oxygen is added and the residual sample is heated to 900 °C under 20 mL/min O_2/N_2 gas mixture flow.

The TGA results of cellulose betainates were also used to determine dry matter content of the fibres. The dry solid content was determined from the TGA curve at the temperature 120 °C. These results were used for correction of DS calculation from elemental analysis. The dry matter contents are listed in the **Table 8**.

Table 8. The dry solid contents of cellulose betainates with different DS. Values are determined from the TGA results at 120 °C.

Origin	DS by NMR (-)	Dry weight (w-%)
Domsjö	0.42	93.70
	0.59	93.87
	1.20	91.30
	1.60	91.01
Borregaard	0.47	95.14
	1.05	95.00
	1.07	92.27
	1.28	92.27

5.3 Elemental analysis results

The nitrogen content (w-%) of cellulose betainates were studied with the elemental analyzer in UPM research center. The obtained results were compared elemental analysis results from UH. UPM results are shown in the **Table 9** and UH results are shown in the **Table 10**.

Table 9. The results from nitrogen analysis of cellulose betainate by UPM. The nitrogen content is average from two replicates. [1]Ensured DS from [1]H-NMR results by UH. The results are calculated with [2]Eq. 4.1, [3]Eq. 3.4 and [4]Eq. 3.5.

Origin	DS by NMR[1] (-)	N % (w-%)	DS calculated[2] (-)	σ (w-%)	$U(\pm)$[3] (w-%)	U_r [4] (%)
Domsjö	0.42	3.61	0.65	0.030	0.042	6.55
	0.59	3.30	0.57	0.050	0.071	12.51
	1.20	4.96	1.12	0.080	0.113	10.11
	1.60	5.52	1.40	0.100	0.141	10.13
Borregaard	0.47	3.15	0.53	0.040	0.057	10.72
	1.05	4.55	0.95	0.020	0.028	2.97
	1.07	5.10	1.18	0.010	0.014	1.20
	1.28	5.40	1.33	0.030	0.042	3.19

Table 10. The results from nitrogen analysis of cellulose betainate by UH and comparison with UPM results. The nitrogen content is average from three replicates. [1]Ensured DS from [1]H-NMR results by UH. The results are calculated with [2]Eq. 4.1, [3]Eq. 3.4 and [4]Eq. 3.5.

Origin	DS by NMR[1] (-)	N % (w-%)	DS calculated[2] (-)	σ (w-%)	$U(\pm)$[3] (w-%)	U_r[4] (%)	N % Difference (UPM-UH) (w-%)
Domsjö	0.42	3.57	0.63	0.040	0.046	11.00	0.04
	0.59	3.48	0.61	0.020	0.023	3.91	0.18
	1.20	5.33	1.27	0.030	0.035	2.89	0.37
	1.60	6.01	1.66	0.040	0.046	2.89	0.49
Borregaard	0.47	3.23	0.55	0.060	0.069	14.74	0.08
	1.05	5.10	1.19	0.260	0.368	27.62	0.55
	1.07	5.40	1.31	0.010	0.012	1.08	0.30
	1.28	5.82	1.54	0.050	0.058	4.51	0.42

The comparison of the nitrogen content results of UPM and UH showed that UPM analyzer gave smaller values with most of the samples. The possible reason for this is the absorbed water in the material which decreases the percentual values of nitrogen in the samples. To overcome this, the UPM's measured nitrogen results were corrected by dividing the measured nitrogen content with dry solid contents shown in the Table 8. The corrected values are shown in the **Table 11**.

Table 11. The corrected UPM nitrogen content results.[1]Calculated by dividing the N % with dry solid content.[2]Calculated from Eq.4.1.

Origin	Corrected N % by UPM[1]	Corrected DS by UPM[2]	N % Difference (UPM corrected-UH)
	(w-%)	(-)	(w-%)
Domsjö	3.85	0.72	0.28
	3.52	0.62	0.04
	5.43	1.35	0.10
	6.07	1.74	0.06
Borregaard	3.31	0.57	0.08
	4.79	1.05	0.31
	5.53	1.40	0.13
	5.85	1.59	0.03

The corrected N % values showed a lot smaller difference with the UH results. However, the dry solid content or pretreatment of the UH samples were not available and therefore the results are not completely comparable. Other possible reasons for the difference could be caused by the difference between the analyzer devices or the calibrations. The heterogeneous nature of the samples and possible residuals of the reagent also affects highly on the outcome of the elemental analysis, especially with small sample amounts. Another less likely reason could be the conversion of the samples due to long storage times. Only two replicates were made with UPM elemental analyzer which partially explains a high expanded uncertainties for the samples.

5.4 Results from microscopic studies

The visual examination of the modification distribution amongst the pulp fiber was studied with the light microscope. The unmodified dissolving pulp fibers used in palmitic acid modification are shown in the **Figure 59**.

Figure 59. The light microscope images of Graff C stained unmodified dissolving pulp fibres with 100x magnification.

The Graff C stained pulp fibres showed red colour which is typical for relatively pure cellulose components such as dissolving pulp or cotton. Some blue coloured regions are caused by the chemical pulping process. The palmitic acid modified pulp fibres with DS 0.20 are shown in the **Figure 60** and pulp fibres with higher DS 0.80 are shown in the **Figure 61**.

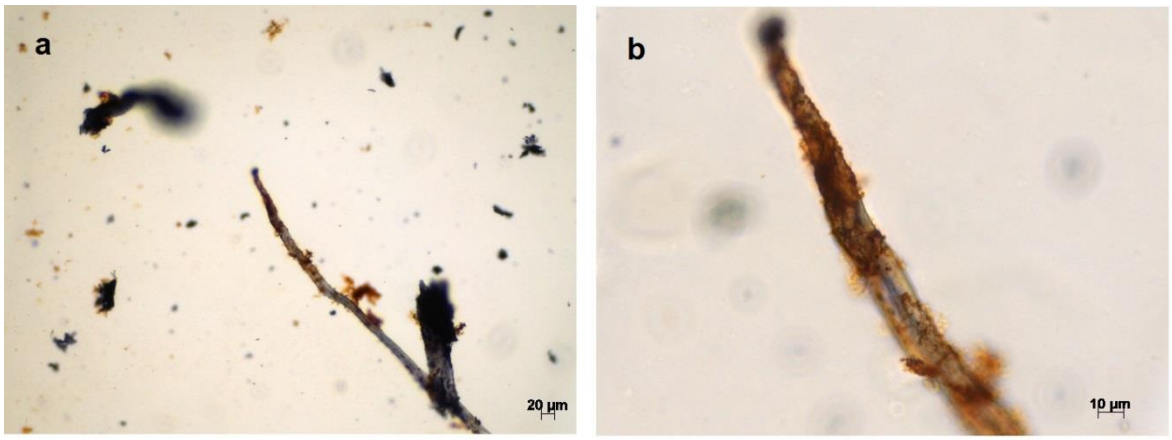

Figure 60. The light microscope images of Graff C stained palmitic acid modified dissolving pulp fibres with DS 0.20 a) 100x magnification and b) 400x magnification.

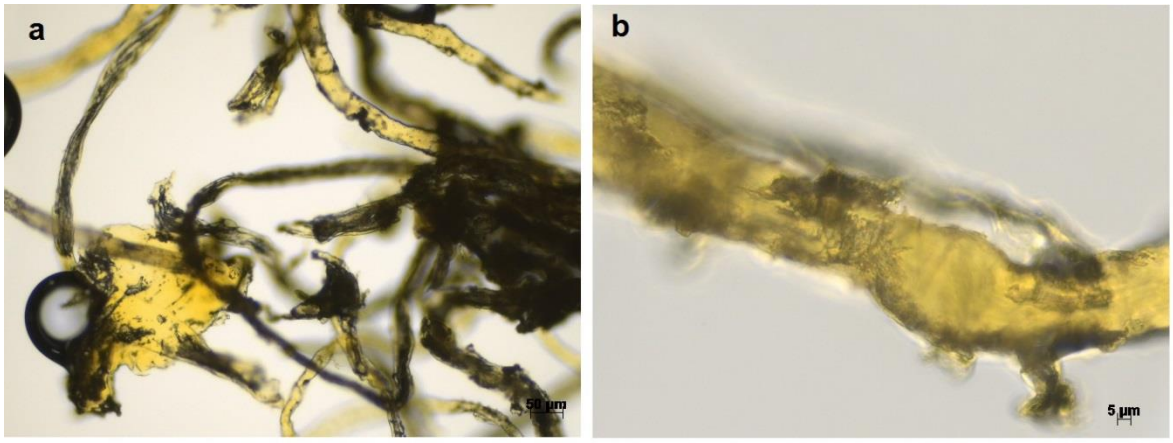

Figure 61. The light microscope images of Graff C stained palmitic acid modified dissolving pulp fibres with DS 0.80 a) 100x magnification and b) 400x magnification.

An interesting colour change between DS 0.2 and 0.8 could be detected from palmitic acid modified pulp samples. The palmitic acid modified pulp with DS 0.2 have changed colour completely blue and fibres with higher DS 0.8 shows bright yellow colour. Some attached palmitic acid can be detected at the surface of the fibres in the Fig 58. A higher DS shows some decomposition of fibre structure in the Fig.59.

The cellulose acetate samples were also analyzed with the light microscope. The reference eucalyptus pulp is shown in the **Figure 62**. The kraft eucalyptus pulp gets clear blue color due to Graff C staining. The typical vessels related to eucalyptus could be detected among the fibers.

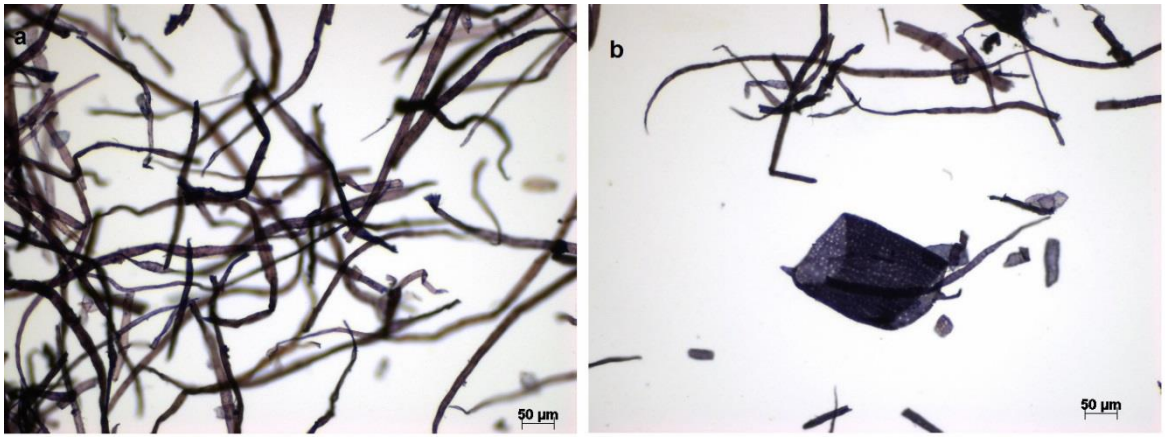

Figure 62. The light microscope images of the reference eucalyptus kraft pulp stained with Graff C colour at 100x magnification. a) Eucalyptus fibres, b) eucalyptus vessel.

The microscopic images of cellulose acetate DS 0.23 are shown in the **Figure 63**. The sample was water prepared and microscopic images were taken with the phase contrast technique while the Graff C staining caused samples to become opaque.

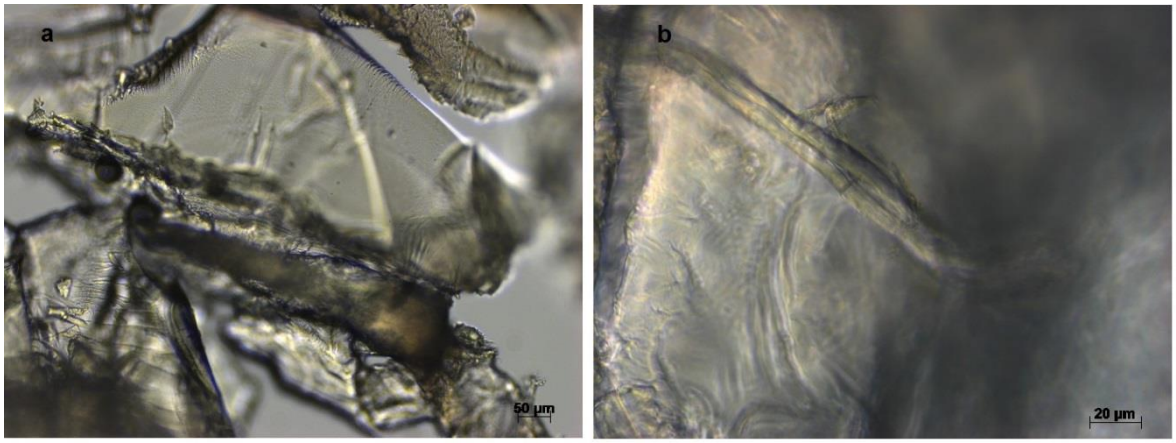

Figure 63. The light microscope phase contrast images of cellulose acetate DS 0.23. a) 100x magnification, b) 400x magnification.

The acetylated samples even with relatively low DS showed formation of crystal-like structure. Only a few fibre structures could be detected from the preparation. The attachment of acetyl groups in the cellulose structure breaks the hydrogen bonds between the cellulose chains which effects on the fibre structure. The microscopic images of the cellulose acetate with higher DS 2.90 are shown in the **Figure 64**.

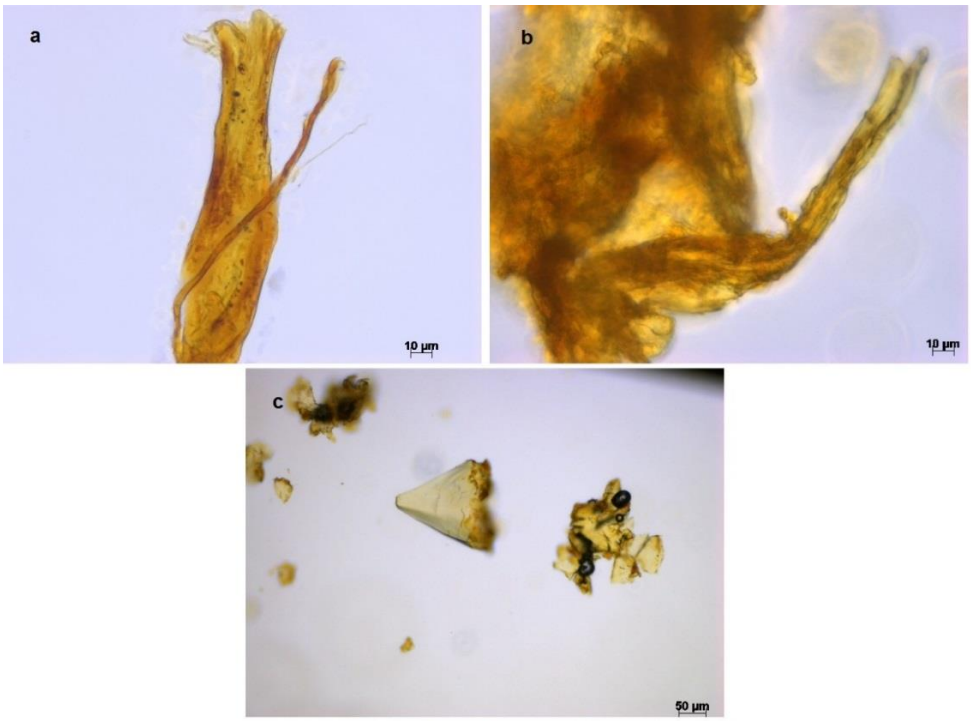

Figure 64. The light microscope images of Graff C stained cellulose acetate DS 2.90. a) 400x magnification and z-stack zoom, b) 400x magnification and c) 100x magnification.

The cellulose acetate sample with DS 2.90 were stained with Graff C. The structure was mostly similar with lower DS and only few partial fiber structures could be detected from the material. An interesting notification was that the fibers had changed they color to yellow from the blue color of the original fibers. This color change is most likely caused by the surface modification but the exact reason would have needed further studies.

6 CONCLUSIONS

The literature review showed a wide variety of different fiber modifications which can be used for kraft pulp fibers. The examined modifications improved the antimicrobial and anti-flammable properties, water absorption and barrier capacity of the pulp derived end products such as tissue papers or non-woven materials. The selection of the suitable analytical method in each case is dependent on how the fiber is modified. The FTIR was found out to be one of the simplest direct analytical method to determine the covalently bonded compounds.

The experiments showed that the quantitative DS determination of the modified pulp fibers with FTIR-ATR technique is possible. It was also found out that FTIR-ATR method seems to be suitable for both modified kraft and sulfite pulp fibers. However, FTIR-ATR technique needs calibration samples which DS needs to be verified with some other analytical method such as NMR. The developed method is suitable for the samples where only one certain compound is attached to the pulp fibers. The detection of two or more different attached compounds was found out to be difficult. Another challenge with the FTIR-ATR method was the heterogeneity of the samples, which caused variation between the parallel measurements.

The other tested analytical methods, elemental analysis, TGA and light microscope were found out to be useful ways to produce assistant information about the modification. The DS determination is possible in some case with elemental analysis alone. However, the elemental analysis alone does not give information whether the compound is attached to fiber or not. The characterization of modified fibers with TGA turned out to be difficult. Nevertheless, the results from TGA showed that even a small amount of attached compound changed the thermal behavior of the fiber. The physical changes and in some cases the distribution of the attached compound among the fiber surface could be detected by light microscope.

The further studies would be needed for the testing the developed method. Due to lack of the calibration samples the calibration model do not cover the whole DS region. The shortage of suitable samples prevented also the testing of the calibration model with the samples with the unknown DS. The FTIR study, where the modified fibers would have been dissolved into the suitable solvent and analyzed with FTIR, would be an interesting topic for further studies. This method could partially overcome the heterogeneity problem which occurred in the current method.

REFERENCES

Abdel-Halim, E. S. et al., 2010. Incorporation of chlorohexidin diacetate into cotton fabrics grafted with glycidyl methacrylate and cyclodextrin. *Carbohydrate Polymers,* Volume 79, pp. 47-53.

Buder, P., 2012. *Paper product with disinfecting properties.* United States of America, Patent No. US8211454 B2.

Casey, J. P., 1979. *Pulp and Paper Chemistry and Chemical Technology.* 2nd ed. s.l.:John Wiley & Sons, inc..

Catel-Ferreira, M. et al., 2015. Antiviral effects of polyphenols - Development of bio-based cleaningwipes and filters. *Journal of virological methods,* Volume 212, pp. 1-7.

Chang, L.-M. & Cheng, L.-Q., 2002. Water-soluble grafted polysaccharides containing sulfobetaine groups - Synthesis and characterization of graft copolymers of hydroxyethyl cellulose with 3-dimethyl(methacryloyloxyethyl)ammonium propane sulfonate. *Journal of Applied Polymer Science,* Volume 83, pp. 2755-2761.

Charest, M.-H., 2012. *Antimicrobial tissue paper and process to manufacture same.* Canada, Patent No. EP2526227 A1.

Coats, A. W. & Redfern, J. P., 1963. Thermogravimetric analysis - A review. *Analyst,* Volume 88, pp. 906-924.

Cooke, T. F., 2006. Fibers: Superabsorbent. In: M. A., ed. *Concise Encyclopedia of Composite Materials.* s.l.:Elsevier, pp. 391-395.

de Cuadro, P. et al., 2015. Cross-linking of cellulose and poly(ethylene glycol) with citric acid. *Reactive & Functional Polymers,* Volume 90, pp. 21-24.

Debashis, R., Semsarilar, M., Guthrie, J. T. & Perrier, S., 2009. Cellulose modification by polymer grafting - a review. *Chemical Society Reviews,* Volume 38, pp. 2046-2064.

Demitri, C. et al., 2008. Novel superabsorbent cellulose-based hydrogels crosslinked with citric acid. *Journal of Applied Polymer Science,* Volume 110, pp. 2453-2460.

Dorez, G. et al., 2014. Use of Py-GC/MS and PCFC to characterize the surface modification of flax fibers. *Journal of Analytical and Applied Pyrolysis,* Volume 105, pp. 122-130.

Ek, M., Gellersted, G. & Henriksson, G., 2009. Cellulose products and chemicals from wood. In: *Wood chemistry and wood biotechnology.* Berlin: Walter de Gruyter GmbH & Co. KG.

Emam, H. E. et al., 2014. Copper(I)oxide surface modified cellulose fibers—Synthesis, characterization and antimicrobial properties. *Surface & Coatings Technology,* Volume 254, pp. 344-351.

Evtuguin, D. & Pascoal Neto, C., 2007. *Recent advances in eucalyptus wood chemistry - Structural features through the prism of technological response.* Belo Horizonte, s.n.

Fan, M., Dai, D. & Huang, B., 2012. Fourier Transform Infrared Spectroscopy for Natural Fibres. In: S. Salih, ed. *Fourier Transform-Material Analysis.* s.l.:InTech, pp. 45-68.

Fras, L., Ristic, T. & Tkavc, T., 2012. Adsorption and antibacterial activity of soluble and precipitated chitosan on cellulose viscose fibers. *Journal of Engineered Fibers and Fabrics,* 7(1), pp. 50-57.

Gremlich, H.-U., 2012. Infrared and Raman spectroscopy. In: *Ullmann's Encyclopedia of Industrial Chemistry.* Weinheim: Wiley-VHC Verlag GmbH & Co.KGaA, pp. 177-220.

Guan, Y., Xiao, H., Sullivan, H. & Zheng, A., 2007. Antimicrobial-modified sulfite pulps prepared by in situ copolymerization. *Carbohydrate Polymers,* Volume 69, pp. 688-696.

Gürdag, G. & Sarmad, S., 2013. Cellulose graft copolymers - synthesis, properties and applications. In: S. Kalia & M. W. Sabaa, eds. *Polysaccharide based graft polymers.* Berlin: Springer-Verlag, pp. 15-57.

Haaland, D. M. & Thomas, E., 1988. Partial least-squares methods for spectral analyses. 1. Relation to other quantitative calibration methods and the extraction of qualitative information. *Analytical Chemistry ,* Volume 60, pp. 1193-1202.

Haber, F. & Weiss, J., 1934. The catalytic decomposition of hydrogen peroxide by iron salts. *The Royal Society,* 147(861), pp. 332-351.

Hinterstoisser, B. & Salmén, L., 2000. Application of dynamic 2D FTIR to cellulose. *Vibrational Spectroscopy,* Volume 22, pp. 111-118.

Hou, A., Zhou, M. & Wang, X., 2009. Preparation and characterization of durable antibacterial cellulose biomaterials modified with triazine derivatives. *Carbonhydrate polymers,* Volume 75, pp. 328-332.

Kallavus, U., Kärner, K., Kärner, K. & Elomaa, M., 2015. Rapid semi-quantitative determination of aspen lignin in lignocellulosic products. *Proceedings of the Estonian Academy of Sciences,* Volume 64, pp. 105-112.

Katovic, D., Grgac, S. F., Bichof-Vukusic, S. & Katovic, A., 2012. Formaldehyde free binding system for flame retardant finishing of cotton fabrics. *Fibers & Textiles in Eastern Europe,* Volume 20, pp. 94-98.

Kiiskinen, H., Asikainen, J. & Turkka, H., 2012. *Pehmopaperit - Tutkimuskartta,* Jyväskylä: VTT.

Klimsch, H. M., Kohl, G. S. & Sabourin, J. M., 1987. A quantitative diffuse reflectance method using Fourier transform infrared spectroscopy for determining siloxane deposition on keratin surfaces. *Journal of Cosmetic Science,* Volume 38, pp. 247-261.

Kondo, T., 1997. The assignment of IR absorption bands due to free hydroxyl groups in cellulose. *Cellulose,* Volume 4, pp. 281-292.

Korpela, A., 2008. *Crosslinking of birch kraft pulp for bulky paper and board,* s.l.: Keskuslaboratorio oy.

Kou, L. et al., 2006. Antimicrobial cellulose - preparation and application of 5-methyl-5-aminomethylhydantoin. *Research Journal of Textiles and Apparel,* Volume 10, pp. 1-21.

Kringstad, K. P. & Lindström, K., 1984. Spent liquors from pulp bleaching. *Environmental Science and Technology,* Volume 18, pp. 236-248.

Le Blan, T., Vouters, M., Magniez, C. & Normand, X., 2007. The development of non-wovens. In: *Multifunctional barriers for flexible structure.* s.l.:Springer Science, pp. 139-150.

Leclerc, D. F., 2000. Fourier transform infrared spectroscopy in the pulp and paper industry. In: R. A. Meyers, ed. *Encyclopedia of analytical chemistry.* Chinchester: John Wiley & Sons Ltd, pp. 8361-8388.

Lund, K. et al., 2011. Diepoxide treatment of softwood kraft pulp-influence on absorption properties of fibre networks. *Cellulose,* Volume 18, pp. 1365-1375.

Luo, J., Lv, W., Deng, Y. & Sun, Y., 2013. Cellulose - ethylenediaminetetraacetic acid conjugates protect mammalian cells from bacterial cells. *Biomacromolecules,* Volume 14, pp. 1054-1062.

Ma, W., Yan, S., Meng, M. & Zhang, S., 2014. Preparation of betaine-modified cationic cellulose and its application in the treatment of reactive dye wastewater. *Journal of Applied Polymer Science,* Volume 131, p. 40522.

Miletzky, A. et al., 2015. Modifying cellulose fibers by adsorption/precipitation of xylan. *Cellulose,* Volume 22, pp. 189-201.

Missoun, K., Belgacem, M. N. & Bras, J., 2013. Nanofibrillated cellulose surface modification - a review. *Materials,* Volume 6, pp. 1745-1766.

Murphy, D. B., 2001. *Fundamentals of light microscopy and electronic imaging.* s.l.:Wiley-Liss Inc..

Nakashima, T., Sakagami, Y., Ito, H. & Matsuo, M., 2001. Antibacterial activity of cellulose fabrics modified with metallic salts. *Textile Research Journal,* Volume 71, pp. 688-694.

Neira, A., Tarraga, M. & Catalan, R., 2008. Degradation of acrylic acid-grafted cellulose in aqueous medium with radical initiators. *Journal of the Chilean Chemical Society,* 53(1), pp. 1410-1414.

Noureddine, A., Hequet, E. & Cabrales, L., 2011. Applications of Fourier transform infrared spectroscopy to study cotton fibers. In: P. G. Nikolic, ed. *Fourier Transforms - New Analytical Approaches and FTIR Strategies.* s.l.:InTech, pp. 89-114.

O'Connor, R. T., DuPré, E. F. & McCall, E. R., 1957. Infrared spectrophotometric procedure for analysis of cellulose and modified cellulose. *Analytical Chemistry,* Volume 29, pp. 998-1005.

Owen, T., 1996. *Fundamentals of UV-Visible spectroscopy : A Primer.* s.l.:Hewlett-Packard.

Peng, X.-w., Ren, J.-l. & Sun, R.-c., 2010. Homogeneous esterification of xylan-rich hemicelluloses with maleic anhydride in ionic liquid. *Biomacromolecules,* Volume 11, pp. 3519-3524.

Ristic, T. et al., 2011. Antimicrobial efficiency of functionalized cellulose fibres as potential medical textiles. In: A. Mendez-Vilas, ed. *Science against microbial pathogens: communicating current research and technological advances.* s.l.:Formatex Research Center, pp. 36-51.

Rodionova, G., Lenes, M., Eriksen, Ø. & Gregersen, Ø., 2011. Surface chemical modification of microfibrillated cellulose improvement of barrier properties for packaging applications. *Cellulose,* Volume 18, pp. 127-134.

Romi, R. et al., 2005. Bioengineering of a cellulosic fabric for insecticide delivery via grafted cyclodextrin. *Biotechnology Progress,* Volume 21, pp. 1724-1730.

Roy, D., Semsarilar, M., Guthrie, J. T. & Perrier, S., 2009. Cellulose modification by polymer grafting: a review. *Chemical Society Reviews,* Volume 38, pp. 2046-2064.

Sannino, A., Demitri, C. & Madaghiele, M., 2009. Biodegradable cellulose-based hydrogels - design and applications. *Materials,* Volume 2, pp. 353-373.

Sannino, A. et al., 2005. Crosslinking of cellulose derivatives and hyaluronic acid with water-soluble carbodiimide. *Polymer,* Volume 46, pp. 11206-11212.

Schaller, J. & Heinze, T., 2005. Studies on the synthesis of 2,3-O-hydroxyalkyl ethers of cellulose. *Macromolecular bioscience,* Volume 5, pp. 58-63.

Seong, H.-S., Kim, J.-P. & Ko, S.-W., 1999. Preparing chito-oligosaccharides as antimicrobial agents for cotton. *Textile Research Journal,* pp. 483-488.

Shimadzu corporation, 2015. *Fundamentals of FTIR analysis: ATR Precautions.* [Online] Available at: http://www.shimadzu.com/an/ftir/support/ftirtalk/letter2/atr2.html [Accessed 28 September 2015].

Shirazi, M., van de Ven, T. G. M. & Garnier, G., 2003. Adsorption of modified starches on pulp fibers. *Langmuir,* Volume 19, pp. 10835-10842.

Shrivastava, A. & Gupta, V., 2011. Methods for the determination of limit of detection and limit of quantitation of the analytical methods. *Chronicle of young scientists,* 2(1), pp. 21-25.

Sievänen, K. et al., 2015. Cationic cellulose betainate for wastewater treatment. *Cellulose,* Volume 22, pp. 1861-1872.

Silva, T. C. F. et al., 2010. Adsorption of chemically modified xylans on eucalyptus pulp and its effect on the pulp physical properties. *Industrial & Engineering Chemistry Research,* Volume 50, pp. 1138-1145.

Simoncic, B. & Klemcic, D., 2015. Preparation and performance of silver as an antimicrobial agent for textiles: A review. *Textile Research Journal.*

Sjöström, E., 1993. *Wood chemistry funtamentals and applications.* 2nd ed. San Diego: Academic Press.

Sjöström, E. & Westermark, U., 1999. Chemical composition of wood and pulps. In: *Analytical methods in wood chemistry, pulping and papermaking.* I ed. Berlin: Springer-Verlag Berlin Heidelberg, pp. 1-19.

Socrates, G., 2001. *Infrared and Raman characteristic group frequencies tables and charts.* 3rd ed. s.l.:John Wiley & Sons.

Stenius, P. & Vuorinen, T., 1999. Direct characterization of chemical properties of fibers. In: E. Sjöström & R. Alén, eds. *Analytical methods in wood chemistry, pulping and papermaking.* s.l.:Springer, pp. 149-192.

Stinchfield, R. L., 1929. *Soluble cellulose esters containing phthalic groups and process of making the same.* United States of America, Patent No. US 1704306 A.

Stuart, B. H., 2004. Spectral analysis. In: *Infrared spectroscopy: fundamentals and applications.* s.l.:John Wiley & Sons, pp. 45-70.

Sun, G. & Worley, S., 2006. Halamine chemistry and its applications in biocidal textiles and polymers. In: J. V. Edwards, ed. *Modified fibers with medical and specialty applications.* s.l.:Springer, pp. 81-89.

Sun, R.-c., Fang, J. & Tomkinson, J., 2000. Characterization and esterification of hemicelluloses from rye straw. *Journal of agricultural and food chemistry,* Volume 48, pp. 1247-1252.

Sun, X. F., Sun, R. S. & Sun, J. X., 2004. Acetylation of sugarcane bagasse using NBS as a catalyst under mild reaction conditions for the production of oil sorptive materials. *Bioresource technology,* Volume 95, pp. 343-350.

Talába, P., Skroková, P., Hodul, P. & Ebringerová, A., 1996. New procedure for the preparation of cellulose esters with aromatic carboxylic acids. *Chemical Papers,* 50(6), pp. 365-368.

Thompson, M., Ellison, S. L. & Wood, R., 2002. Harmonized guidelines for single laboratory validation of methods of analysis. *Pure applied Chemistry,* Volume 74, pp. 835-855.

Tkacheva, N. I. et al., 2013. Modification of cellulose as a promising direction in the design of new materials. *Polymer Science,* Volume 55, pp. 409-429.

Torres, F. G., Troncoso, O. P., Torres, C. & Grande, C. J., 2013. Cellulose based blends, composites and nanocomposites. In: *Advances in natural polymers - composites and nanocomposites.* Berlin: Springer, pp. 21-54.

Vaca-Garcia, C., Thiebaud, S., Borredon, M. & Gozzelino, G., 1998. Cellulose esterification with fatty acids and acetic anhydride in lithium chloride/N,N-dimethylacetamide medium. *Journal of the American Oil Chemists' Society,* Volume 75, pp. 315-319.

Vartiainen, J., Vähä-Nissi, M. & Harlin, A., 2014. Biopolymer films and coatings in packaging applications—a review of recent developments. *Materials Sciences and Applications,* Volume 5, pp. 708-718.

Vasiljevic, J. et al., 2014. Novel multifunctional water- and oil-repellent, antibacterial and flame-retardant cellulose fibers created by the sol-gel process. *Cellulose,* Volume 21, pp. 2611-2623.

Weil, E. D. & Levchik, S. V., 2008. Flame retardants in commercial use or development for textiles. *Journal of Fire Science,* Volume 26, pp. 243-281.

Wu, T., Du, Y., Yan, N. & Farnood, R., 2015. Cellulose fiber networks reinforced with glutaraldehyde–chitosan complexes. *Journal of Applied Polymer Science,* p. 42375.

Xhanari, K. et al., 2011. Reduction of water wettability of nanofibrillated cellulose by adsorption of cationic surfactants. *Cellulose,* Volume 18, pp. 257-270.

Yang, C. Q., Xu, Y. & Wang, D., 1996. FT-IR spectroscopy study of the polycarboxylic acids used for paper wet strength improvement. *Industrial & Engineering Chemistry Research,* Volume 35, pp. 4037-4042.

Zheng, Y. et al., 2015. Preparation and flame retardancy of 3-(hydroxyphenylphosphinyl)-propanoic acid esters of cellulose. *Cellulose,* Volume 22, pp. 229-244.

Zohuurian-Mehr, M. J. & Kabiri, K., 2008. Superabsorbent polymer materials - a review. *Iranian Polymer Journal,* Volume 17, pp. 451-477.

Appendix I The characteristic frequencies of different compounds in FTIR

Table I. The characteristic frequencies of certain functional groups (Segneanu *et al*. 2012)

Class	Group	Wavenumber (cm^{-1})
Hydrocarbons		
Alkane	C-H	2850-3000
	C-C	800-1000
Aromatic	C-H	3000-3100
	C=C	1450-1600
Alkene	C-H	3080-3140
	C=C	1630-1670
Alkyne	C-H	3300-3320
	C-C	2100-2140
Oxygen Compounds		
Alcohol	O-H	3300-3600
	C-O	1050-1200
Ether	C-O	1070-1150
Aldehyde	C=O	1720-1740
	C-H	2700 -2900
	C=O	1700-1725
Carboxylic Acids	O-H	2500-3300
	C-O	1100-1300
Ester	C=O	1735-1750
	C-O	1000-1300 (2 bands)
Ketone	C=O	1700-1725
Acyl halides	C=O	1785-1815
Anhydrides	C=O	1750;1820 (2 bands)
	O-C	1040-1100
Amides	C=O	1630-1695
	N-H	1500-1560
Isocyanates,Isothiocyanates, Diimides, Azides, Ketenes	-N=C=O, -N=C=S -N=C=N-, -N3, C=C=O	2100-2270
Nitrogen compounds		
	N-H	3300-3500
Amines	C-N	1000-1250
	NH2	1550-1650
	NH2 & N-H	660-900
Nitriles	C≡N	2240-2260

Oxidized Nitrogen Functions		
	O-H	3550–3600
Oxime (=NOH)	C=N	1665± 15
	N-O	945± 15
Amine oxide (N-O)	aliphatic	960± 20
	aromatic	1250± 50
N=O	nitroso	1550± 50
	nitro	1530± 20;1350± 30
Alkyl bromide	C-H	667
Sulfur compounds		
Thiols	S-H	2550-2600
Esters	S-OR	700-900
Disulfide	S-S	500-540
Thiocarbonyl	C=S	1050-1200
Sulfoxide	S=O	1030-1060
Sulfone	S=O	1325± 25; 1140± 20
Sulfonic Acid	S=O	1345
Sulfonyl chloride	S=O	1365± 5;1180± 10
Sulfate	S=O	1350-1450
Phosphorous compounds		
Phosphine	P-H	2280-2440
		950-1250
Phosphonic acid	(O=)PO-H	2550-2700
Esters	P-OR	900–1050
Phosphine oxide	P=O	1100-1200
Phosphonate	P=O	1230-1260
Phosphate	P=O	1100-1200
Phosphoramide	P=O	1200-1275
Silicon compounds		
	Si-H	2100-2360
Silane	Si-OR	1000-1110
	Si-CH3	1250±10

Appendix II The IR spectra of cellulose acetate references

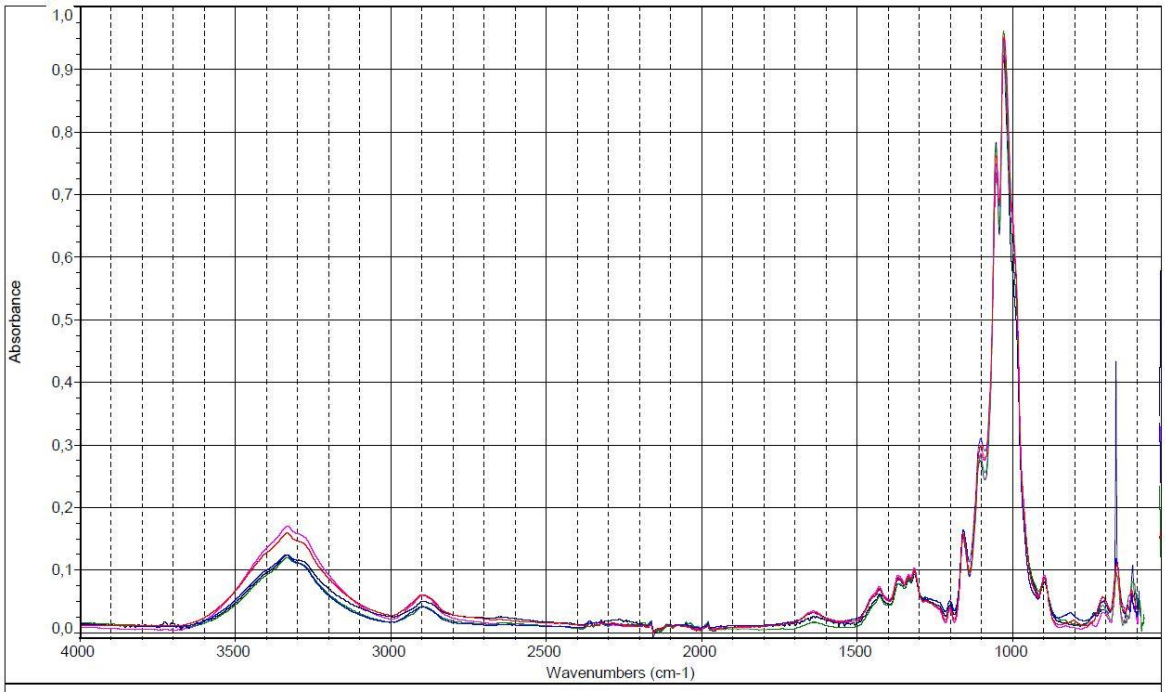

Figure 65. The reference spectra of eucalyptus kraft pulp used as base material for cellulose acetate.

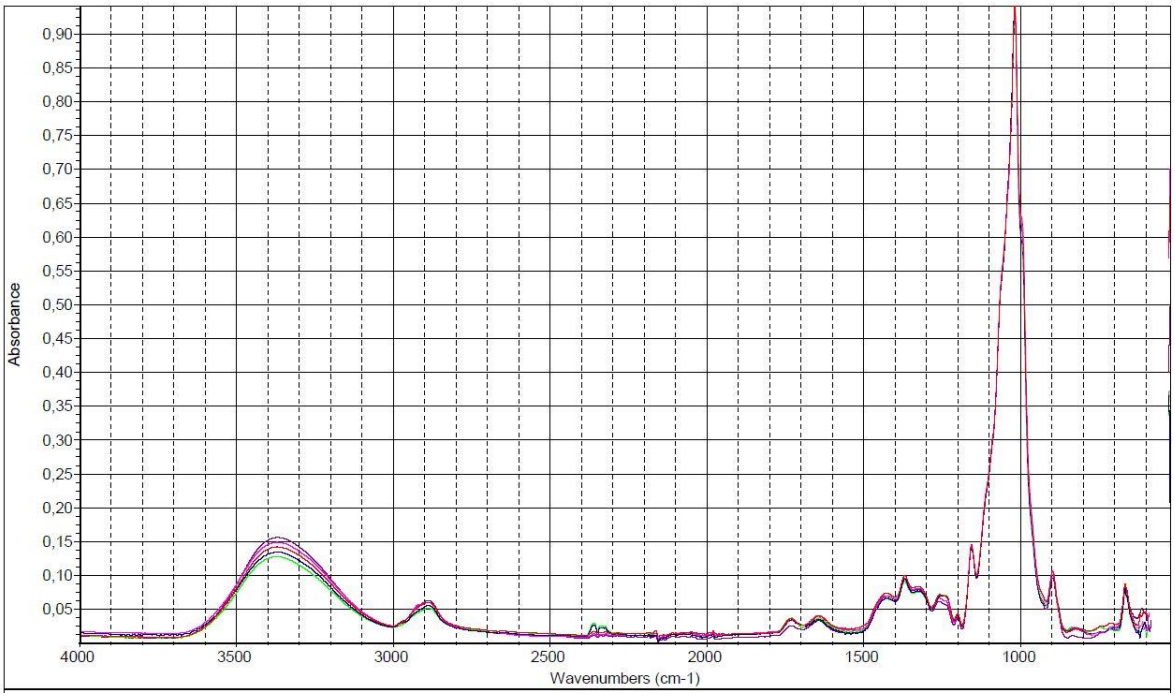

Figure 66. The reference spectra of cellulose acetate DS 0.23.

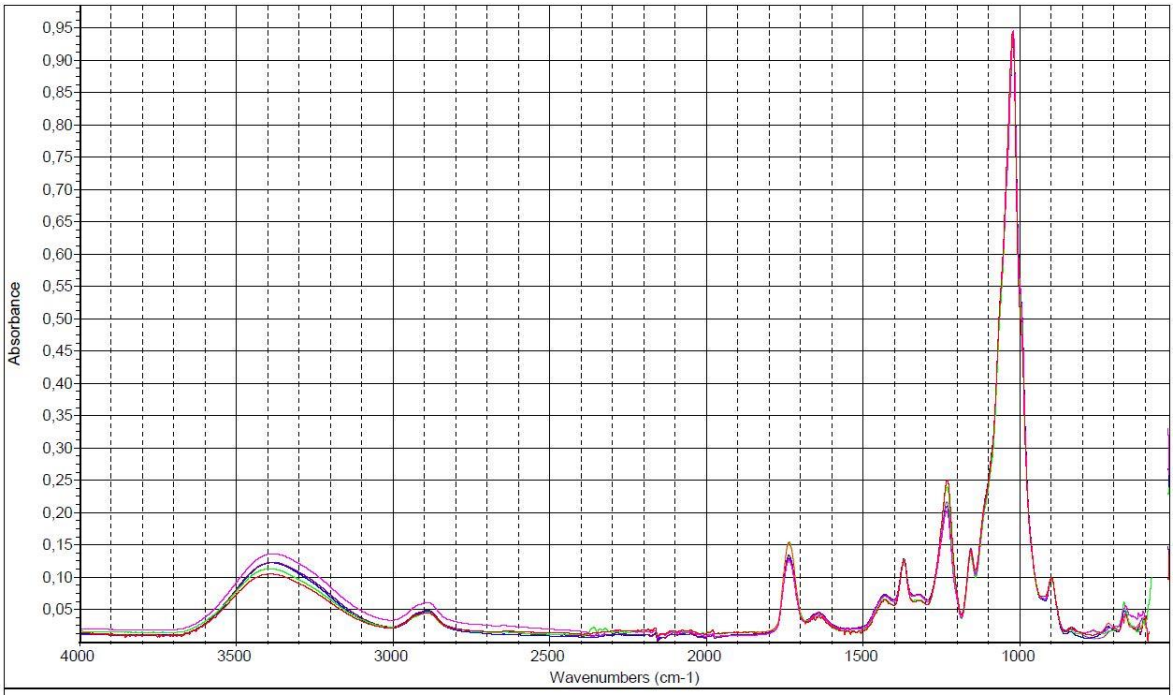

Figure 67. The reference spectra of cellulose acetate DS 0.85.

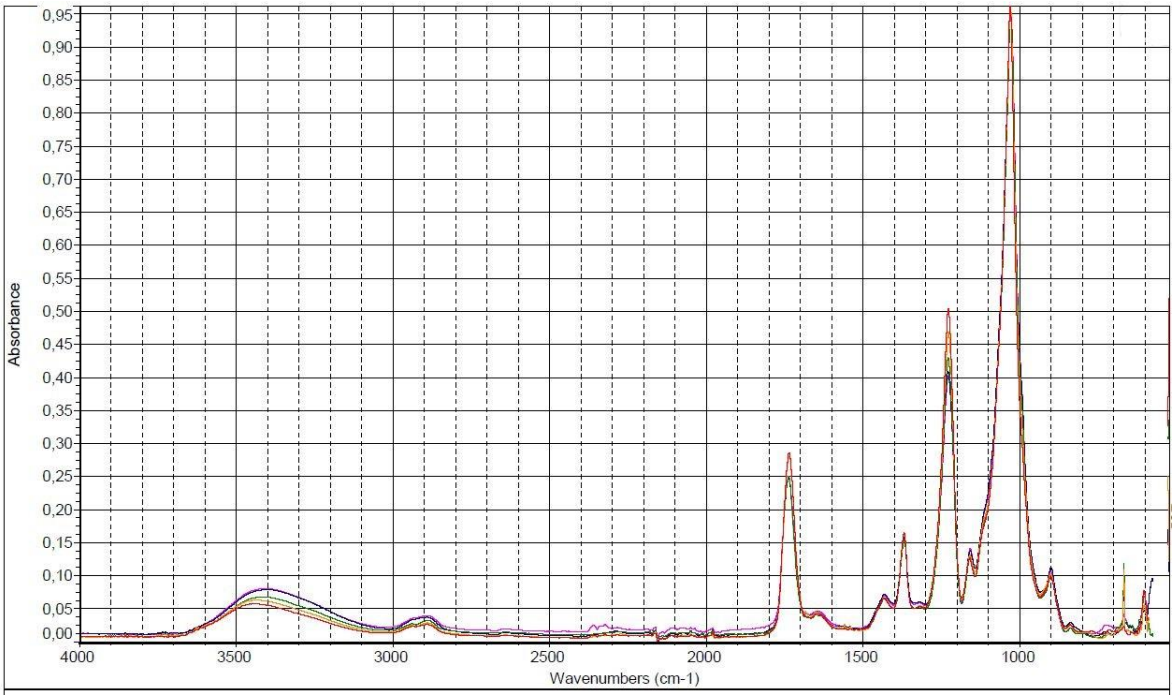

Figure 68. The reference spectra of cellulose acetate DS 2.76.

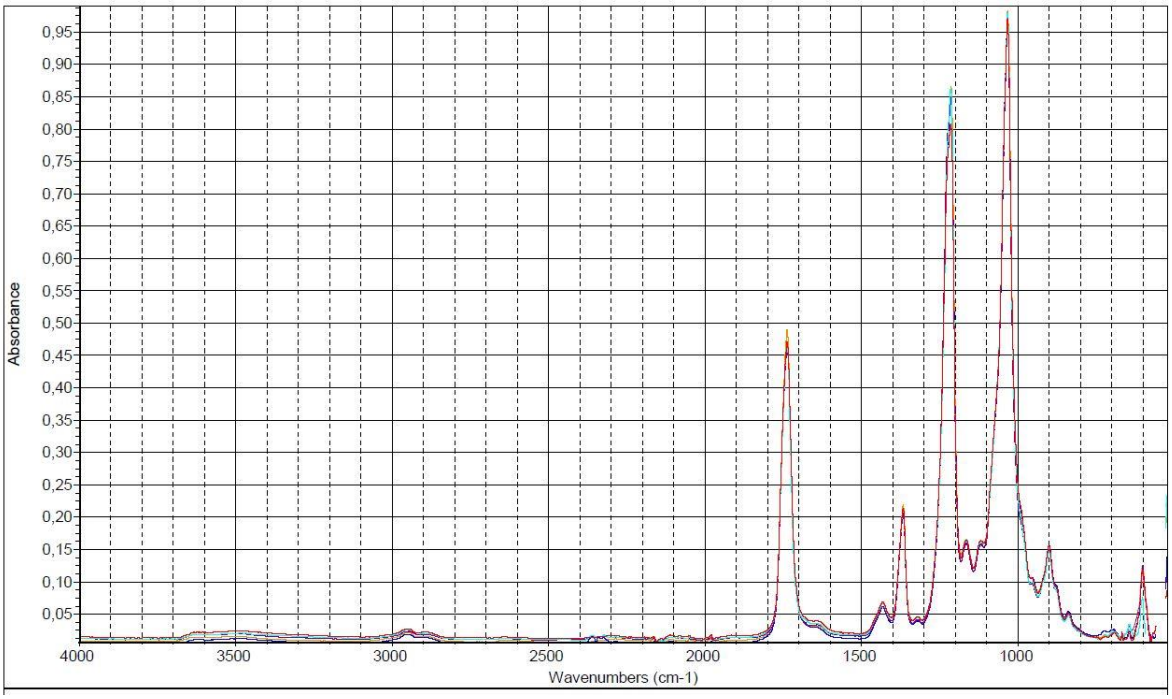

Figure 69. The reference spectra of cellulose acetate DS 2.90.

Appendix III The IR spectra of Borregaard cellulose betainate references

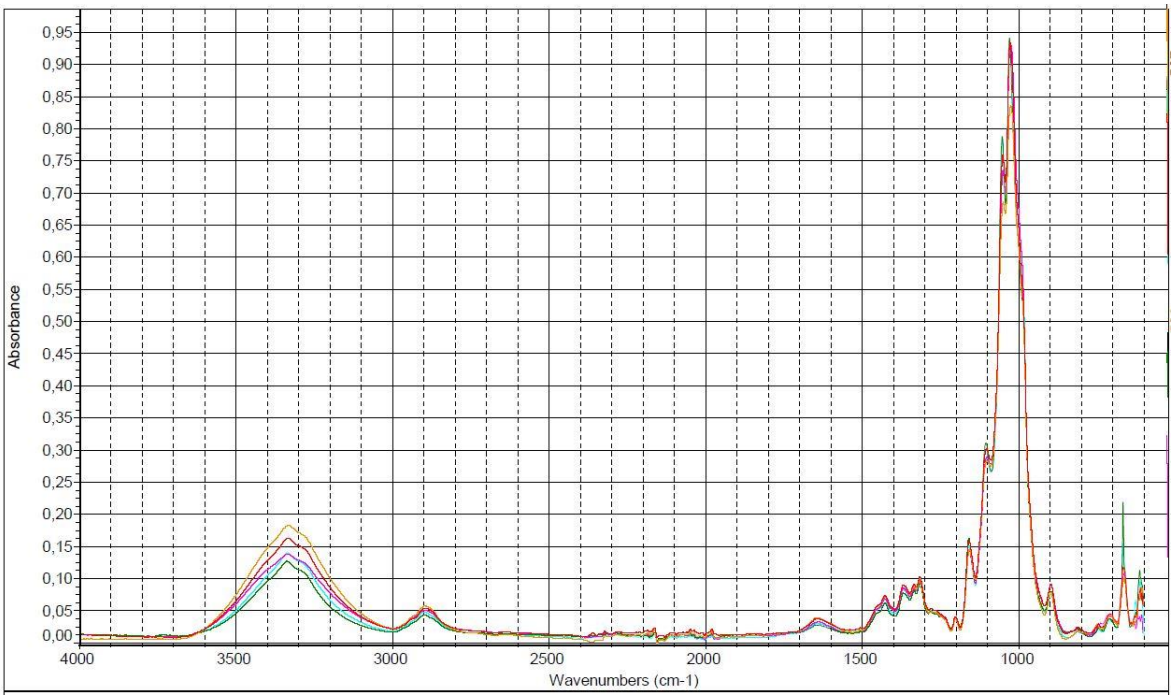

Figure 70. The reference spectra of Borregaard dissolving pulp used as a raw material for cellulose betainate.

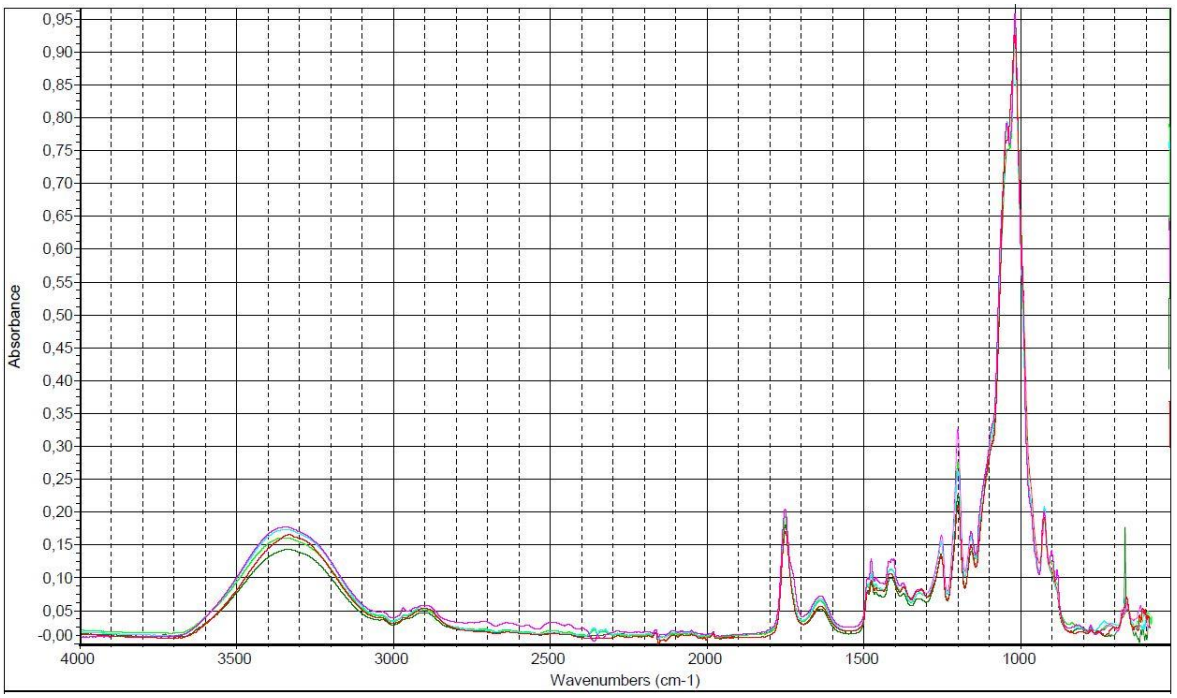

Figure 71. The reference spectra of Borregaard cellulose betainate DS 0.47

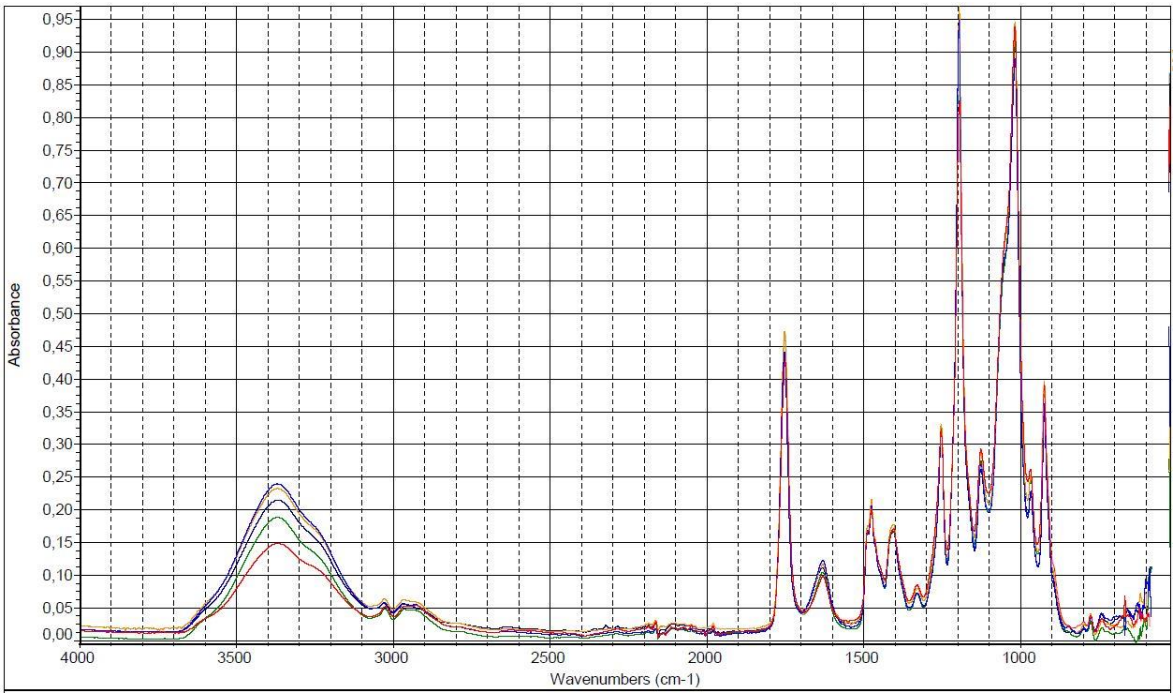

Figure 72. The reference spectra of Borregaard cellulose betainate DS 1.07

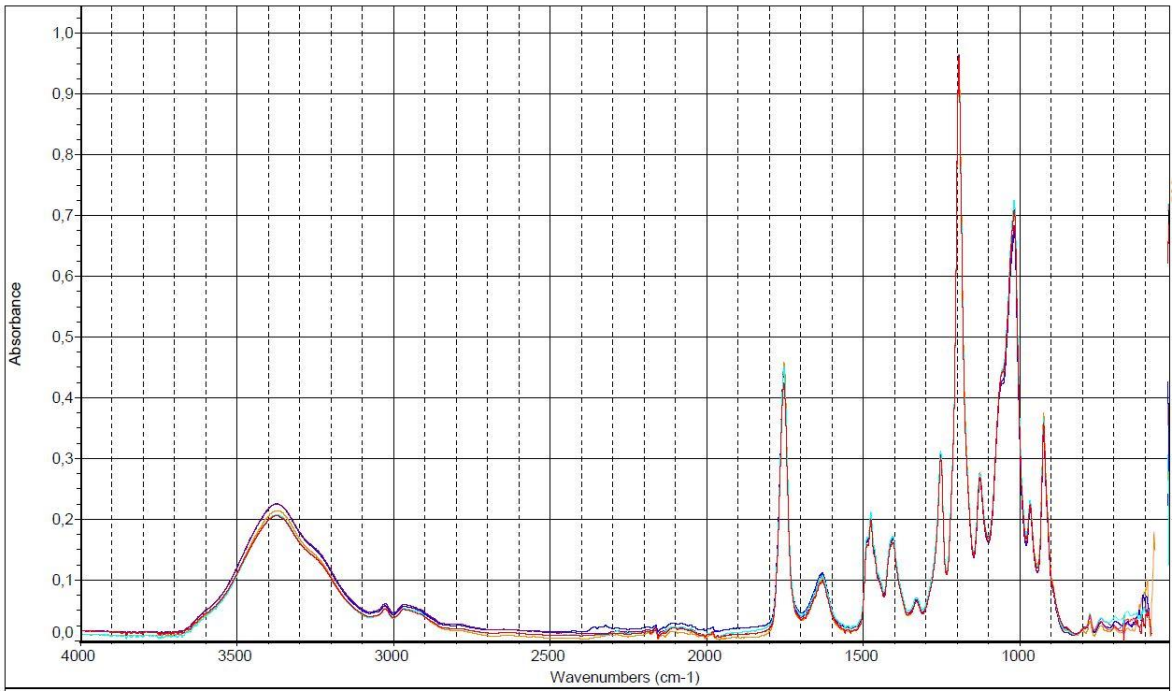

Figure 73. The reference spectra of Borregaard cellulose betainate DS 1.28

Appendix IV The IR spectra of Domsjö cellulose betainate references

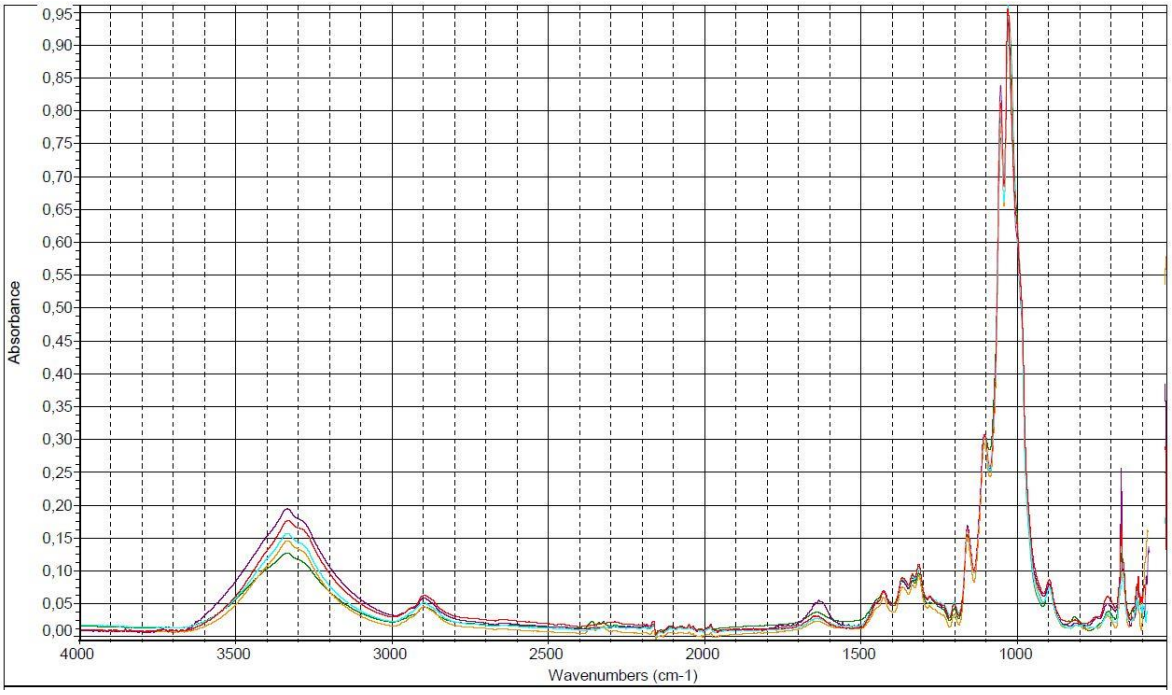

Figure 74. The reference spectra of Domsjö dissolving pulp used as a raw material for cellulose betainate.

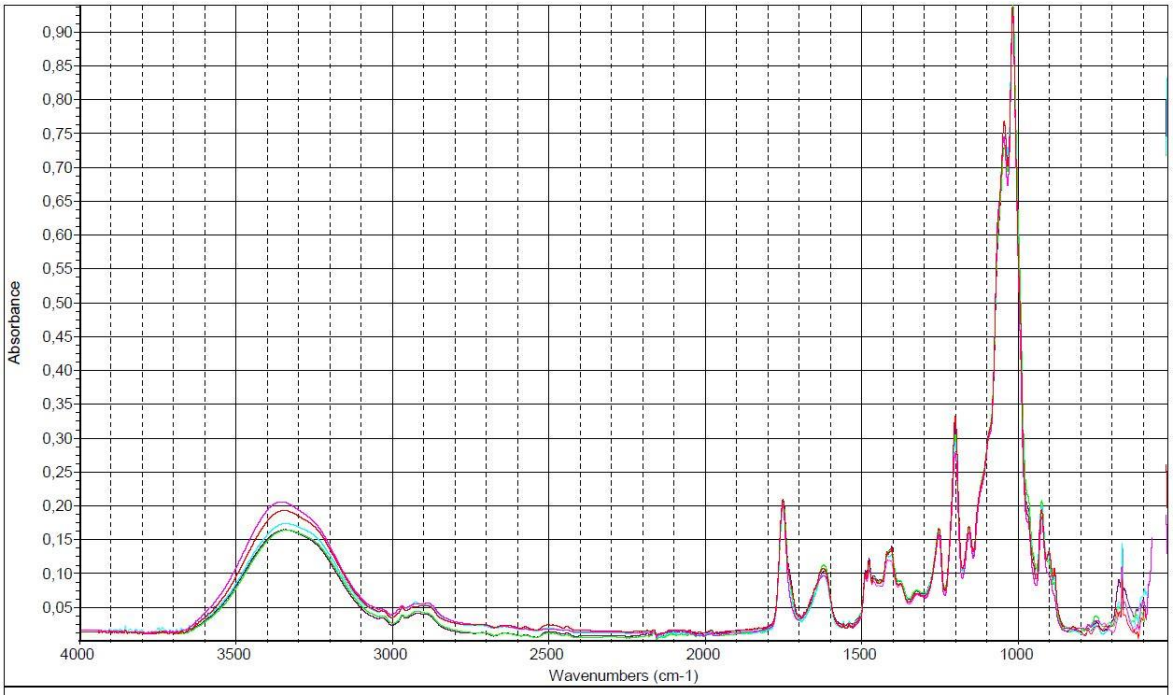

Figure 75. The reference spectra of Domsjö cellulose betainate DS 0.42

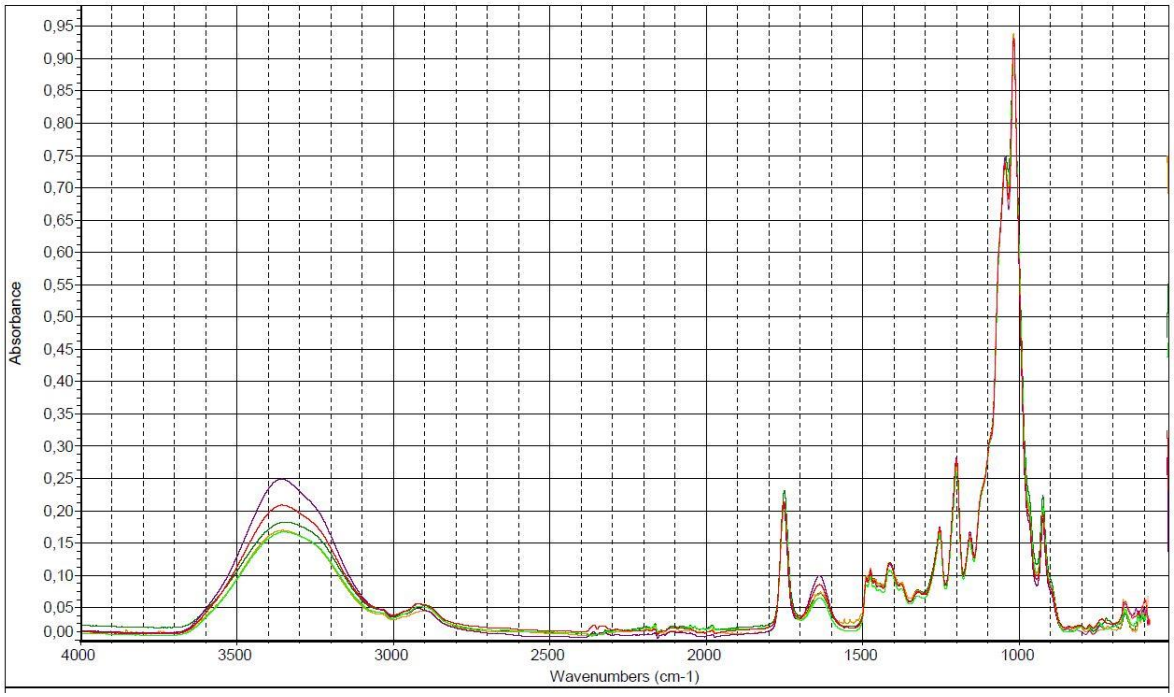

Figure 76. The reference spectra of Domsjö cellulose betainate DS 0.59

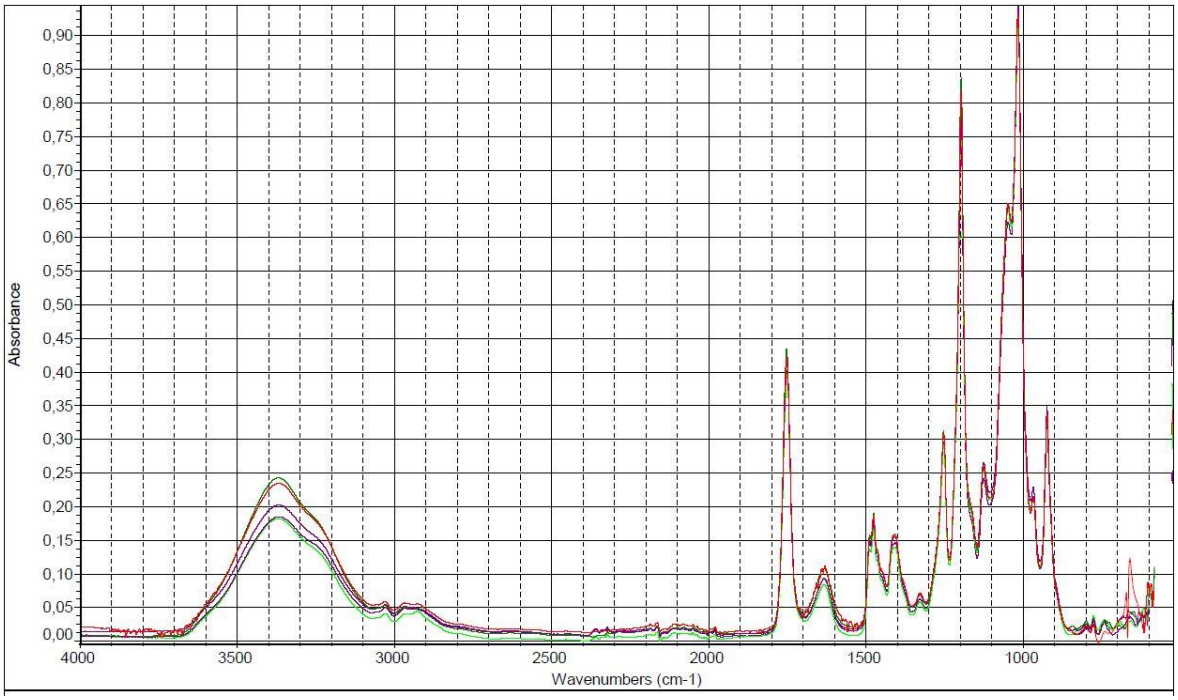

Figure 77. The reference spectra of Domsjö cellulose betainate DS 1.20

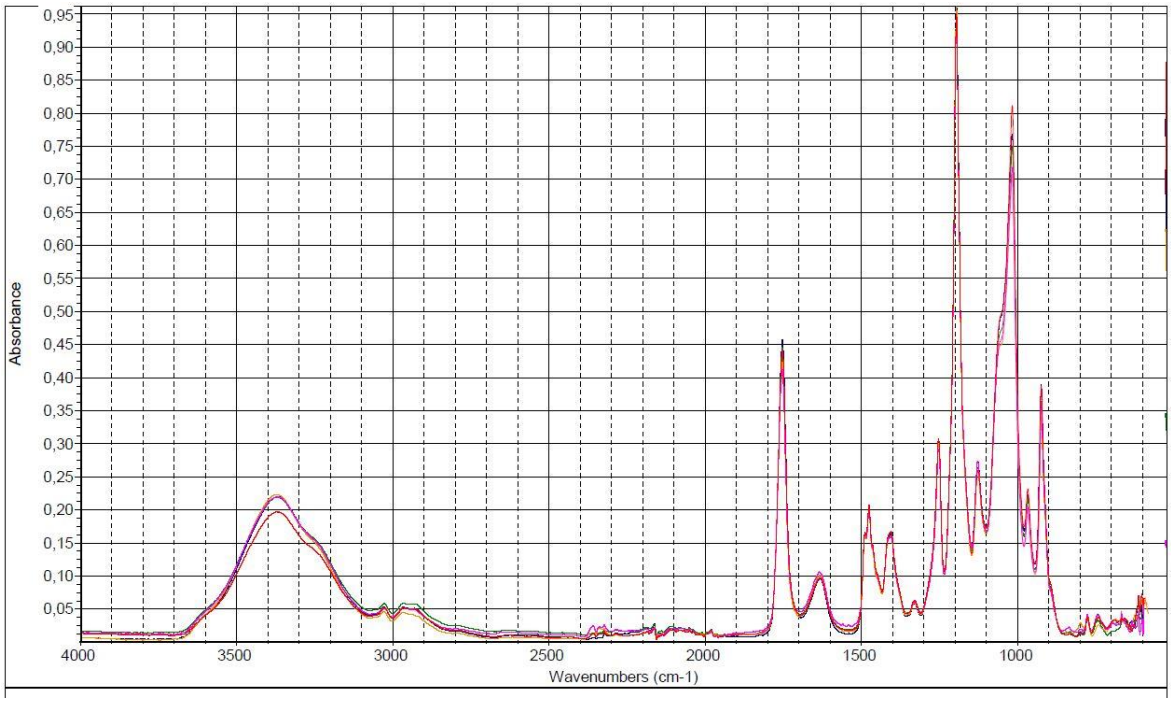

Figure 78. The reference spectra of Domsjö cellulose betainate DS 1.60

Appendix V The calculated peak height ratios of reference samples

Table II. The peak height ratios 1750 cm^{-1}/1030 cm^{-1} of Borregaard cellulose betainate for each reference sample.

Peak height ratio			**DS**		
1750 cm^{-1}/1030 cm^{-1}	0.00	0.47	1.05	1.07	1.28
Ref 1	0.000	0.198	0.375	0.581	0.784
Ref 2	0.000	0.192	0.351	0.558	0.761
Ref 3	0.000	0.214	0.345	0.557	0.775
Ref 4	0.000	0.227	0.360	0.519	0.707
Ref 5	0.000	0.218	0.346	0.528	0.727
Average	**0.000**	**0.210**	**0.355**	**0.549**	**0.751**
Stdev.	**0.000**	**0.012**	**0.011**	**0.022**	**0.029**

Table III. The peak height ratios 1750 cm^{-1}/1030 cm^{-1} of Domsjö cellulose betainate for each reference sample.

Peak height ratio			**DS**		
1750 cm^{-1}/1030 cm^{-1}	0.00	0.42	0.59	1.20	1.60
Ref 1	0.000	0.229	0.256	0.479	0.715
Ref 2	0.000	0.230	0.224	0.492	0.737
Ref 3	0.000	0.221	0.234	0.511	0.689
Ref 4	0.000	0.220	0.235	0.493	0.623
Ref 5	0.000	0.221	0.237	0.474	0.658
Average	**0.000**	**0.224**	**0.237**	**0.490**	**0.684**
Stdev.	**0.000**	**0.004**	**0.010**	**0.013**	**0.040**

Table IV. The peak height ratios 1200 cm^{-1}/1030 cm^{-1} of Borregaard cellulose betainate for each reference sample.

Peak height ratio			**DS**		
1200cm^{-1}/1030cm^{-1}	0.00	0.47	1.05	1.07	1.28
Ref 1	0.000	0.180	0.444	1.046	1.437
Ref 2	0.000	0.163	0.352	1.034	1.524
Ref 3	0.000	0.221	0.363	1.069	1.499
Ref 4	0.000	0.208	0.384	0.855	1.434
Ref 5	0.000	0.268	0.375	1.044	1.382
Average	**0.000**	**0.208**	**0.384**	**1.010**	**1.455**
Stdev.	**0.000**	**0.036**	**0.032**	**0.078**	**0.050**

Table V. The peak height ratios 1200 cm^{-1}/1030 cm^{-1} of Domsjö cellulose betainate for each reference sample.

Peak height ratio			**DS**		
1200cm^{-1}/1030cm^{-1}	0.00	0.42	0.59	1.20	1.60
Ref 1	0.000	0.254	0.214	0.804	1.344
Ref 2	0.000	0.277	0.206	0.852	1.438
Ref 3	0.000	0.234	0.219	0.865	1.422
Ref 4	0.000	0.283	0.227	0.787	1.197
Ref 5	0.000	0.242	0.205	0.760	1.369
Average	**0.000**	**0.258**	**0.214**	**0.814**	**1.354**
Stdev.	**0.000**	**0.019**	**0.008**	**0.039**	**0.086**

Table VI. The peak height ratios 1254 cm^{-1}/1030 cm^{-1} of Borregaard cellulose betainate for each reference sample.

Peak height ratio			**DS**		
1254 cm^{-1}/1030 cm^{-1}	0.00	0.47	1.05	1.07	1.28
Ref 1	0.000	0.088	0.188	0.273	0.354
Ref 2	0.000	0.080	0.165	0.274	0.384
Ref 3	0.000	0.096	0.166	0.285	0.371
Ref 4	0.000	0.100	0.171	0.255	0.355
Ref 5	0.000	0.100	0.165	0.275	0.357
Average	**0.000**	**0.092**	**0.171**	**0.272**	**0.364**
Stdev.	**0.000**	**0.008**	**0.009**	**0.010**	**0.012**

Table VII. The peak height ratios 1254 cm^{-1}/1030 cm^{-1} of Domsjö cellulose betainate for each reference sample.

Peak height ratio			**DS**		
1254 cm^{-1}/1030 cm^{-1}	0.00	0.42	0.59	1.20	1.60
Ref 1	0.000	0.110	0.109	0.244	0.342
Ref 2	0.000	0.113	0.104	0.252	0.364
Ref 3	0.000	0.107	0.109	0.255	0.358
Ref 4	0.000	0.112	0.113	0.240	0.311
Ref 5	0.000	0.104	0.105	0.240	0.341
Average	**0.000**	**0.109**	**0.108**	**0.246**	**0.343**
Stdev.	**0.000**	**0.003**	**0.003**	**0.006**	**0.018**

Table VIII. The peak height ratios 1734 cm^{-1}/1030 cm^{-1} of cellulose acetate for each reference sample.

Peak height ratio			**DS**		
1734 cm^{-1}/1023 cm^{-1}	0.00	0.23	0.85	2.76	2.90
Ref 1	0.000	0.023	0.143	0.263	0.495
Ref 2	0.000	0.022	0.150	0.262	0.484
Ref 3	0.000	0.022	0.123	0.304	0.495
Ref 4	0.000	0.028	0.128	0.305	0.485
Ref 5	0.000	0.031	0.149	0.261	0.520
Average	**0.000**	**0.025**	**0.139**	**0.279**	**0.496**
Stdev.	**0.000**	**0.004**	**0.011**	**0.021**	**0.013**

Table IX. The peak height ratios 1370 cm^{-1}/1030 cm^{-1} of cellulose acetate for each reference sample.

Peak height ratio			**DS**		
1370 cm^{-1}/1023 cm^{-1}	0.00	0.23	0.85	2.76	2.90
Ref 1	0.021	0.025	0.065	0.114	0.192
Ref 2	0.020	0.027	0.072	0.116	0.186
Ref 3	0.020	0.029	0.063	0.126	0.180
Ref 4	0.025	0.027	0.065	0.127	0.187
Ref 5	0.023	0.025	0.072	0.113	0.183
Average	**0.022**	**0.027**	**0.067**	**0.119**	**0.186**
Stdev.	**0.002**	**0.002**	**0.004**	**0.006**	**0.004**

Table X. The peak height ratios 1230 cm^{-1}/1030 cm^{-1} of cellulose acetate for each reference sample.

Peak height ratio			**DS**		
1230 cm^{-1}/1023 cm^{-1}	0.00	0.23	0.85	2.76	2.90
Ref 1	0.000	0.034	0.189	0.394	0.817
Ref 2	0.000	0.032	0.210	0.422	0.785
Ref 3	0.000	0.033	0.167	0.460	0.809
Ref 4	0.000	0.028	0.179	0.495	0.759
Ref 5	0.000	0.026	0.218	0.389	0.805
Average	**0.000**	**0.031**	**0.193**	**0.432**	**0.795**
Stdev.	**0.000**	**0.003**	**0.019**	**0.040**	**0.021**

Appendix VI The results from the regression analysis

Regression Analysis

OVERALL FIT	
Multiple R	0.995
R Square	0.991
Adjusted R Square	0.988
Standard Error	0.068
Observations	5

ANOVA				Alpha	0.05	
	df	*SS*	*MS*	*F*	*p-value*	*sig*
Regression	1	1.621	1.621	344.986	0.0003	yes
Residual	3	0.014	0.004			
Total	4	1.635				

	coeff	*std err*	*t stat*	*p-value*	*lower*	*upper*
Intercept	0.016	0.051	0.327	0.764	-0.146	0.179
Group 1	0.999	0.053	18.573	0.0003	0.828	1.171

Obs	*X1*	*Y*	*Pred Y*
1	1	-0.011	0.016
2	1	0.529	0.436
3	1	0.561	0.606
4	1	1.172	1.216
5	1	1.642	1.616